Modeling and Simulation of the Thermo-Acoustic Instabilities of Low-Emission Gas Turbines

Ayoub ben Amor Hmaidi

I hereby declare that I have written this thesis on my own and used no other than the stated sources and aids.

Acknowledgements

Contents

Part I

Introduction

Due to environmental and economical reasons, the development and the improvement of gas turbines by increasing the efficiency and reducing fuel consumption and pollutant formation has become more essential than ever before. In order to meet the stringent emission requirements, modern gas turbines are more and more operated in the lean premixed regime since lean premixed combustion offers the potential of significantly reducing NOx emissions.

Yet, a major drawback of the lean premixed regime is that it is highly susceptible to thermoacoustic oscillations and favors the developement of self-excited oscillations of pressure and temperature. The self-excited oscillations increase the amplitude of the flame motion and heat release which in turn leads to high variations in the pressure field. Many systems with lean premixed flames have experienced structural damage caused by these large pressure fluctuations resulting from the interaction between sound waves and combustion. In extreme cases of resonance the thermo-acoustic instabilities may lead to the destruction of the whole gas turbine. Consequently there is an important need to better understand combustion instabilities and to be able to assess the dynamical behavior of modern low-emission gas turbines already at the design stage. The numerical simulation of reactive flows in the combustion chamber is an important step towards reaching these goals in modern power plants.

In this work we focus on the equations which describe the different oscillatory phenomena taking place in the thermoacoustic system. The wave equation describing the pressure fluctuations and their interaction with the unsteady heat release is of particular interest. Furthermore we are interested in the chemical composition of the flow as well as the emission levels. Hence we provide the equations describing the evolution of species concentrations. This enables us to predict the heat release variation.

One further aim of this work is to develop a model describing the thermo-acoustic feedback loop. We are interested in a model that couples the pressure and velocity fluctuations to the unsteady heat release and describes how the interaction takes place. Most models used sofar rely on empirical assumptions and use model parameters which need to be adjusted from one application to the other. We will focus on developing a model without any empirical assumptions or parameters and which could be used for various configurations and combustion mechanisms. Moreover such a model would enable us to identify the variables of interest that trigger the thermo-acoustic instabilities. In a next step we would like to use this model to perform an analysis of the reactive flow properties in the frequency domain. This analysis includes the determination of the acoustic eigenmodes of pressure and temperature as well as the assessment of the combustion effects on the thermo-acoustic system.

Einführung

Die alarmierende Umweltsituation erfordert eine Minimierung aller aus Verbrennungsprozessen resultierenden Schadstoffe. In dem letzten Jahrzehnten wurden viele internationale Abkommen zur Minderung der Emissionen getroffen und die Forderungen an den Energieunternehmen werden immer strenger. Besondere Bedeutung kommt den Stickoxiden (NOx) zu, die in der Troposphäre die Bildung des Ozons und des photochemischen Smogs begünstigen. Stickoxiden tragen auch zum Abbau des stratosphrischen Ozons bei, was die ultraviolette Bestrahlung der Erdoberfläche erhöht.

Heutzutage beruhen etwa 90% der weltweiten Energieversorgung auf Verbrennung, so dass auch kleine Verbesserungen zur erheblichen Reduzierung der Umweltbelastung beitragen sowie zu riesigen Kosten- und Energieeinsparungen führen können.

Der Bedarf, Verbrennungsprozesse in Gasturbinen genauer zu untersuchen und besser zu verstehen, gewinnt aufgrund der alarmierenden Umweltlage zunehmend an Bedeutung. Zudem fordert der verstärkte Wettbewerb zwischen den Energieunternehmen eine Antwort auf noch ungelösten technischen Fragestellungen.

Um diese strengen Forderungen zu treffen, wurden magere vorgemischte Verbrennungssysteme in den modernen Gaskraftwerken eingeführt. Diese ermöglichen eine hohe Effizienz sowie eine Reduzierung der Schadstoffen, neigen jedoch zu thermo-akustischen Instabilitäten, welche die ganze Anlage gefährden und enorme Schaden einrichten können. Um diese Oszillationen vorherzusagen und zu vermeiden, ist es vonnöten, den Entstehungsmechanismus der thermo-akustischen Instabilitäten zu verstehen.

Leider sind experimentelle Untersuchungen von Gasturbinen extrem teuer und sehr begrenzt. Größtenteils des Entwicklungspotentiales von modernen Gasturbinen steckt daher in der numerischen Simulation der verschiedenen Vorgänge, die in der Brennkammer stattfinden. Die Simulation dieser Vorgänge umfasst das Zusammenspiel verschiedener Bereichen, u.a. Thermodynamik, Strömungsmechanik, Reaktionskinetik und Numerische Mathematik.

Ziel der Dissertation ist die Entwicklung numerischer Methoden zur Simulation der turbulenten Verbrennung in Brennkammern von Gasturbinen. Dazu soll ein mathematisches Modell entwickelt werden, das die Kopplung zwischen den chemischen Prozessen und der thermo-akustischen Instabilitäten beschreibt. Zudem soll die numerische Simulation im Frequenzbereich eine Vorhersage der Eigenmoden des Systems liefern. Die Fluktuationen von dem Druck, der Temperatur und der chemischen Zusammensetzung sind vom besonderen Interesse.

1 Problem description

1.1 Gas turbines and power generation

A gas turbine is an internal combustion engine that operates with rotary motion. It consists of three main components :

1. an upstream air compressor

2. a combustion chamber

3. a downstream turbine

The upstream compressor and the downstream turbine are mechanically coupled and the combustion chamber lies in between. The gas turbine extracts energy from the hot gas flow produced by combustion of fuel in a stream of compressed air.
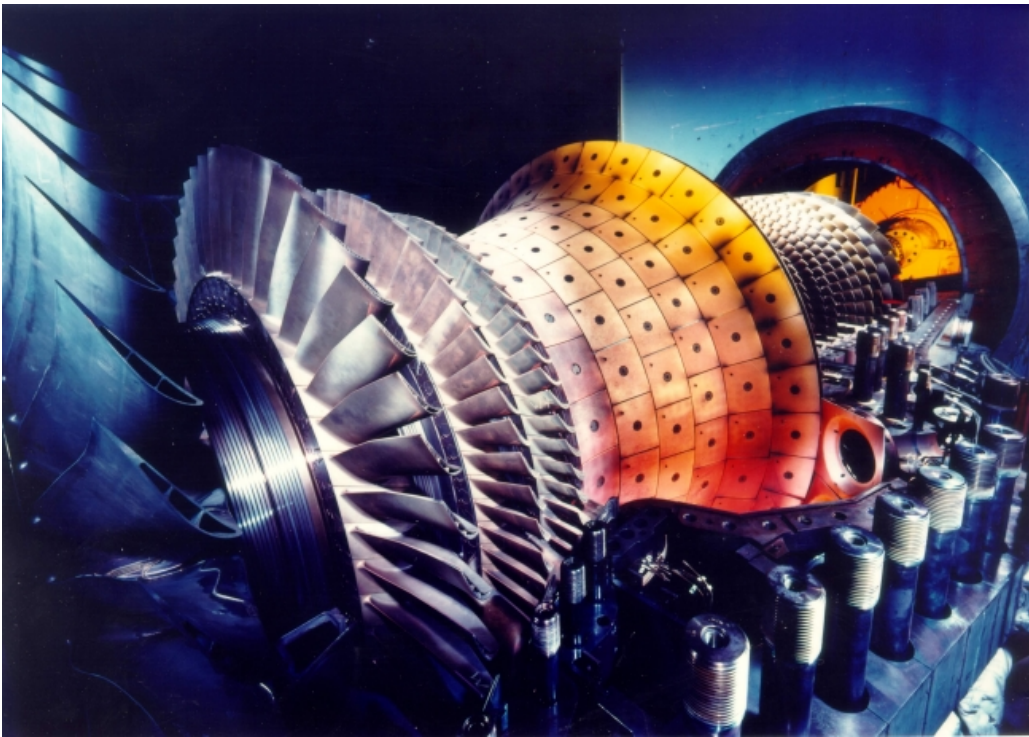
Figure 1: Gas Turbine

The compressor draws in ambient air and compresses it by a pressure ratio of up to 30 times ambient pressure. After being compressed, the air is then directed to the combustor section and gets mixed with fuel and ignited in the combustion chamber, where highly exothermic chemical reactions induce a large temperature increase. In fact flame temperatures in the combustor can reach $2000°C$. The hot combustion gases are then diluted with additional cool air from the compressor section and directed

over the turbine's blades, spinning the turbine and resulting in work output [29].

Energy is recovered in the turbine section in the form of shaft horsepower. A substantial part of the output (typically about 60%) is required to drive the internal compressor section and is hence not available as useful work output. Through the combination of gas and steam turbines it is possible to achieve a better efficiency such as in the Siemens GuD turbines [2] where around 58% of the work output is transformed in electrical energy.

Gas turbines are characterized by a high horsepower-to-size ratio which allows efficient space utilization and a short time from order placement to on-site operation. Furthermore, because of their high reliability, cost-effectiveness and suitability for remote operation, gas turbines are very attractive power sources.

1.1.1   Different types of compressors and turbines

The compressor and turbine sections can each be a single fan-like wheel assembly but are usually made up of a series of stages. There are mainly three kinds of configurations : *single-shaft*, *two-shaft* and *three-shaft*.

In a *single-shaft* gas turbine all compressor and turbine stages are fixed to a single, continuous shaft and operate at the same speed. A single-shaft gas turbine is typically used to drive electric generators where there is little speed variation.

In the two-shaft gas turbine, the turbine section is divided into a high-pressure and low-pressure arrangement, where the high-pressure turbine is mechanically tied to the compressor section by one shaft, while the low-pressure turbine has its own shaft and is connected to the external load unit. This configuration allows the high-pressure turbine/compressor shaft assembly to operate at or near optimum design speeds, while the power turbine rotor speed can vary over as wide a range as is required by most external-load units in mechanical drive applications (i.e., compressors and pumps). A third configuration is a *three-shaft* gas turbine : the compressor section is divided into a low-pressure and high-pressure configuration. The low-pressure compressor stages are mechanically tied to the low-pressure turbine stages, and the high-pressure compressor stages are similarly connected to the high-pressure turbine stages. These low-pressure and high-pressure rotors operate at optimum design speeds independent of each other. The low-pressure turbine stages are mounted on a third independent shaft and form the power turbine rotor, the speed of which can vary over as wide a range as is necessary for mechanical drive applications.

1.1.2   Different types of combustors

We distinguish between three types of combustors: *silo*, *annular* and *can-annular* [28].

1. the *silo* combustor type is one or more chambers mounted external to the gas turbine body.

2. the *annular* combustor is a single continuous chamber roughly in the shape of a torus that rings the turbine in a plane perpendicular to the air flow.

3. the *can-annular* type uses a similar configuration but is a series of can-shaped chambers rather than a single continuous chamber.

No matter which type of combustor is used, an inherent problem to combustion consists in the exhaust products and emissions [36, 46]. Some of these combustion products, in particular nitrogen oxides and carbon monoxides, represent a major concern in the design of modern power plants. The next section describes the formation principles of NOx emissions in gas turbines [7].

1.2   NOx emissions and causes of concern

Nitrogen oxides, or NOx, is the generic term for a group of highly reactive gases, all of which contain nitrogen and oxygen in varying amounts. Many of the nitrogen oxides are colorless and odorless. Chief causes of concern are that NOx reacts to form toxic chemicals which cause serious respiratory problems (such as acid aerosols, NO_2 as well as ground-level ozone) and that it contributes to formation of acid rain and to global warming. Also since NOx pollutants can be transported over long distances, NOx-associated problems are of global consequences and not just confined to areas where NOx are emitted. Nitrogen oxides form when fuel is burned at high temperatures, as in combustion processes. The primary sources of NOx are motor vehicles (around 50%), electric utilities, and other industrial, commercial, and residential sources that burn fuels [46].
The next section presents the principles of NOx formation, the types of NOx emitted (i.e. thermal NOx , prompt NOx , and fuel NOx), and how they are generated in a gas turbine combustion process.

1.2.1   Principles of NOx formation in gas turbines

Nitrogen oxides form in the gas turbine combustion process as a result of the dissociation of nitrogen (N_2) and oxygen (O_2) into N and O, respectively. Reactions following this dissociation result in seven known oxides of nitrogen: NO, NO_2 , NO_3 , N_2O, N_2O_3 , N_2O_4 , and N_2O_5. Nitric oxide (NO) and nitrogen dioxide (NO_2) are formed in sufficient quantities to be significant in atmospheric pollution. We will use NOx to refer to either or both of these gaseous oxides of nitrogen.
There are two mechanisms by which NOx is formed in turbine combustors :

1. the oxidation of atmospheric nitrogen found in the combustion air (thermal and prompt NOx)

2. the conversion of nitrogen chemically bound in the fuel (fuel NOx).

The mechanisms leading to the formation of thermal, prompt and fuel NOx are presented below.

1.2.2   Formation of thermal NOx

Thermal NOx is formed by a series of chemical reactions in which oxygen and nitrogen present in the combustion air dissociate and subsequently react to form oxides of nitrogen. The major contributing chemical reactions are known as the Zeldovich mechanism and take place in the high temperature area

of the gas turbine combustor, i.e. in the burnt gas region behind the flame front.

$$\begin{aligned}
N_2 + O &\rightleftharpoons NO + N \\
N + O_2 &\rightleftharpoons NO + O \\
N + OH &\rightleftharpoons NO + H
\end{aligned}$$
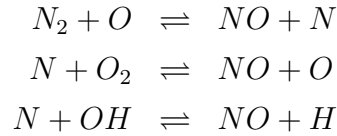
Although the Zeldovich mechanism has been one of the most investigated reaction mechanism, there is still no agreement on the choice of the rate constants of each reaction. Simply stated, the Zeldovich mechanism postulates that thermal NOx formation increases exponentially with increases in temperature and linearly with increases in residence time. Hence, the introduction of cooling air into the combustor as well as design parameters controlling equivalence ratios and residence time strongly influence thermal NOx formation.

1.2.3   Formation of prompt NOx

Prompt NOx is formed in the proximity of the flame front as intermediate combustion products such as HCN, N and NH are oxidized to form NOx as shown in the following equations:

$$\begin{aligned}
CH + N_2 &\rightleftharpoons HCN + N \\
CH_2 + N_2 &\rightleftharpoons HCN + NH \\
HCN, N, NH + Ox &\rightleftharpoons NOx + ...
\end{aligned}$$
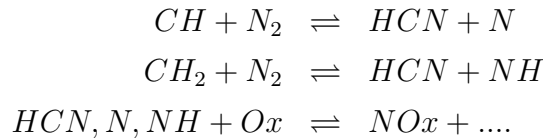
Prompt NOx is formed in both fuel-rich flame zones and fuel-lean premixed combustion zones. The contribution of prompt NOx to overall NOx emissions is relatively small in conventional near-stoichiometric combustors, but this contribution increases with decreases in the equivalence ratio (fuel-lean mixtures). For this reason, prompt NOx becomes an important consideration for the low-NOx combustor designs and establishes a minimum NOx level attainable in lean mixtures.

1.2.4   Formation of fuel NOx

Fuel NOx (also known as organic NOx) is formed when fuels containing nitrogen are burned. Molecular nitrogen, present as N_2 in some natural gas, does not contribute significantly to fuel NOx formation. However, nitrogen compounds are present in coal and petroleum fuels. When these fuels are burned, the nitrogen bonds break and some of the resulting free nitrogen oxidizes to form NOx. With excess air, the degree of fuel NOx formation is primarily a function of the nitrogen content in the fuel.
Most gas turbines that operate in a continuous duty cycle are fueled by natural gas that typically contains little or no fuel-bound nitrogen. As a result, when compared to thermal NOx , fuel NOx is not currently a major contributor to overall NOx emissions from stationary gas turbines.

1.3   Thermo-acoustic instabilities

Many solutions have been proposed to reduce NOx emissions. One of the very promising methods to reduce NOx is the *lean premixed combustion*. This technology has been introduced in order to limit pollutant emissions (especially NOx), and thus comply with the stringent environment norms. In a conventional turbine combustor, the air and fuel are introduced at an approximately stoichiometric ratio and air/fuel mixing occurs simultaneously with combustion. Conversely, a lean premixed combustor design premixes the fuel and air prior to combustion. Premixing results in a homogeneous air/fuel mixture, which minimizes localized fuel-rich pockets that produce elevated combustion temperatures and higher NOx emissions [7].

Development of this technology is very active and modern low-NOx gas turbines are now widely operated in lean premixed regime. Nevertheless, the use of lean premixed combustion presents a major drawback. In fact, it decreases significantly the stability margin of the flames and makes gas turbines more prone to thermoacoustic instabilities. Indeed, combustion instabilities have become a major problem of concern in the conception of modern low-emission gas turbine. In the following section, we will provide a physical description of this phenomenon and try to understand why and how combustion instabilities occur.

1.3.1   Historical background and first observations

It has been known for scientists and engineers since a long time that the coupling between acoustic waves and flames can lead to generation of sound and in some cases to high-amplitude instabilities.

Historically, the first documented observation of combustion oscillation was done by Higgins in the late 18th Century through his experiments with the "*singing flame*". Several researchers investigated this phenomenon and described that it is possible to produce high levels of sound by placing a flame (fixed on a small-diameter fuel tube) in a tube of a larger diameter. They noticed that the presence of the flame excited the fundamental mode or one of the harmonics of the larger tube.

Later on in 1858, another very interesting phenomenon was observed by Le Conte in quite fortuitous circumstances. He observed that the flame pulsed synchronous with the beats of a music instrument. This phenomenon was called the "*dancing flame*". Le Conte quoted :

It was exceedingly interesting to observe how perfectly even the trills of the musical instrument were reflected on the sheet of the flame. A deaf man might have seen the harmony !

On the other side of the Atlantic, in 1859, Rijke discovered a way of using heat to generate a sound in a vertical tube open at both ends. He used a cylindrical glass tube and placed a metal gauze in its lower half. While keeping the tube in the vertical position, he heated the gauze with a flame until it became glowing red hot. Upon removing the flame, he could hear a loud sound from the tube until the gauze cooled down. In a following experiment, he heated the gauze electrically and hence managed to get a continuous heat supply. The generated sound became also continuous. Furthermore, Rijke noted that the sound was heard only when the heating element was placed in the lower half of the vertical tube.

In 1878, Rayleigh observed the interaction between unsteady heat release and sound generation [42]. He stated a necessary condition for the instabilities to occur based on a phenomenological description

of the instabiliy. Rayleigh explained that :

If heat be periodically communicated to, and abstracted from, a mass of air vibrating in a cylinder bounded by a piston, the effect produced will depend upon the phase of the vibration at which the transfer of heat takes place. If heat be given to the air at the moment of greatest condensation, or be taken from it at the moment of greatest rarefaction, the vibration is encouraged. On the other hand, if heat be given at the moment of greatest rarefaction, or abstracted at the moment of greatest condesation, the vibration is discouraged.

In the late 1930s and early 1940s, during the development of solid rocket motors [15, 16], combustion instabilities caused numerous failures and led to many interrupted launches or erratic behaviors. Since then, a considerable effort has been spent on the experimental investigation of this phenomenon to understand the underlying mechanisms of these so-called *thermo-acoustic instabilities* . Also, many mathematical models have been developed in order to find ways to reduce the magnitude of these instabilities and mitigate their effects.

1.3.2   Underlying mechanisms

Combustion instability [15, 16] is essentially a self-excited oscillation. It is mainly due to the complex interplay between chemical processes in the flame zone and instationary flow processes in the combustion chamber. It has been long recognized as a problem in continuous combustion systems [17]. As a matter of fact, it is important to note that the thermo-acoustic oscillations are not a menace in all industrial applications. For example, ramjet engines strongly depend on the presence of such sustained oscillations. However, in most technical applications, particularly in gas turbines, these instabilities are highly undesirable. In fact, they are manifested by large pressure variations as well as growing heat release. These can lead to serious mechanical failures, high levels of noise [12]. In some cases, it can lead to uncontrolled burn and heat tranfer possibly resulting in component melting and decrease of efficiency.

In gas turbines the thermoacoustic instabilities are generated by the coupling between the unsteady heat release and the pressure oscillations. Both of these subprocesses are affected by each other, resulting in a tightly closed feedback loop. The interplay acts in both directions : the heat release from the combustion of the reactants produces sound and affects the acoustics of the system by generating instability waves [15, 16]. Due to fluid dynamic effects, these waves amplify and finally break down into small-scale perturbations which affect the heat release dynamics, thus closing the interaction loop.
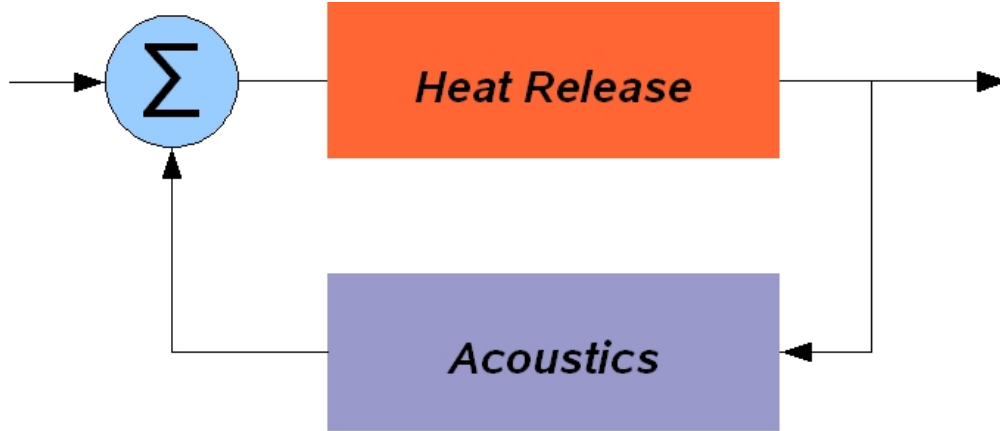
Figure 2: Thermoacoustic system

As described by Rayleigh in 1878, if the heat release is out of phase with the pressure, the system is stable. However, if the heat release is in phase with the pressure, then the closed-loop mechanism becomes unstable and may lead under favorable circumstances to the degradation of the engine performance and the shortening of component life.

In the recent years, the thermoacoustic instability problem has gained importance and is becoming more relevant due to the new restrictions on emissions and the ever-growing high-power requirements. As combustion is very sensitive to the interaction between chemical kinetics and fluid mechanics [18], we need to understand the flow processes that describe the evolution of the physical quantities within the combustion chamber, as well as the chemical processes responsible for the production of energy which eventually maintains or enhances the thermo-acoustic oscillations [17].

In an active combustion chamber, many processes take place, interact and contribute to the global dynamics of the thermo-acoustic system, such as transport and diffusion processes, fluid dynamics [18], acoustics, wave reflections [11], chemical kinetics, flame kinematics [9], heat transfer [5, 6], fuel/air mixing and injection dynamics, as well as atomization and vaporization phenomena [7]. These processes interact in many different ways and take place at very different time and length scales. The complex coupling and the large scale range make an accurate description and a detailed modeling of such a system impossible with the currently available computing ressources.

Hence, we wil be focusing on the two dominant mechanisms that contribute to combustion instabilities, namely heat release dynamics and acoustics [23]. Our objective is to provide a mathematical model for the combustion dynamics in form of a system of partial differential equations that describe the acoustics and gas dynamics [11], as well as the heat release dynamics and chemical kinetics. Using computational methods to solve these equations numerically, it is possible to predict the evolution of the main flow variables such as acoustic pressure and velocity as well as the variables that influence the heat release dynamics.

Part II

Mathematical Modeling

2   Navier-Stokes equations

2.1   Continuity equation

Conservation of mass [31] states that mass can neither be created nor destroyed. It can only be moved from one place to another, that is if mass increases somewhere then it must decrease somewhere else. Let us consider a fluid flowing through a volume Ω during a time interval $[t_1, t_2]$. Then, a statement of conservation of mass for this flow reads

change in total mass in Ω in time interval $[t_1, t_2]$

$=$

net mass passing through boundaries of Ω in time interval $[t_1, t_2]$

Let $\rho(x, t)$ denote the mass per unit volume and $v(x, t)$ the velocity of the flow. If Ω is a one-dimensional pipe, say $[a, b]$, then this statement is written mathematically as

$$\int_a^b [\rho(x, t_2) - \rho(x, t_1)]dx = -\int_{t_1}^{t_2} [\rho(b, t)v(b, t) - \rho(a, t)v(a, t)]dt \tag{1}$$

$\rho(x, t)v(x, t)$ denotes the time rate of mass flow past point x. Thus $\int_a^b \rho(x, t)dx$ is the total mass in $[a, b]$ at time t and $\int_{t_1}^{t_2} \rho(x, t)v(x, t)dt$ is the total mass passing x in time interval $[t_1, t_2]$.

In standard fluid mechanics terminology [18], the mass per unit volume ρ is called *density*, and the timed rate of flow of any property through any surface called *flux*. So ρv is the instantaneous mass flux and $\int_{t_1}^{t_2} \rho(b, t)v(b, t)dt$ represents the total mass flux through the surface $x = b$ during time interval $[t_1, t_2]$.

The arbitrary spatial region $[a, b]$ is called *control volume*. Similarly, the region in the x-t plane defined by $[a, b]$ and $[t_1, t_2]$ is called *space-time control volume*.

We extend this result to the three-dimensional case and consider a finite control volume $\Omega \in \mathbb{R}^3$. At a point of the control surface $\partial\Omega$, the flow velocity is $\mathbf{v}$, the unit normal vector is $\mathbf{n}$ and dS denotes an element surface area. The conservation of mass in Ω in the time interval $[t_1, t_2]$ reads

$$\int_\Omega [\rho(x, t_2) - \rho(x, t_1)]dv = -\int_{t_1}^{t_2} \int_{\partial\Omega} \rho(s, t)(\mathbf{v}(s, t) \bullet \mathbf{n})dSdt \tag{2}$$

Remark : By convention, the unit normal vector $\mathbf{n}$ points out of the control volume. As a result, we have :

- if the scalar product $(\mathbf{v} \bullet \mathbf{n})$ is positive, the mass flow leaves the control volume : we speak of *outflow*.

- if the scalar product $(\mathbf{v} \bullet \mathbf{n})$ is negative, we speak of *inflow*.

2.2   Momentum equation

Conservation of momentum states that only three factors can change momentum, and these consist in redistribution, conversion of momentum to or from energy and force. So, if momentum decreases somewhere, it means that either momentum or an equivalent amount of energy increases somewhere else, or a force is acting. The statement of conservation of momentum [31] reads

change in total momentum in Ω in time interval $[t_1, t_2]$

=

net momentum flow through boundaries of Ω in time interval $[t_1, t_2]$

+

net momentum change due to forces acting on the control volume Ω in time interval $[t_1, t_2]$

We distinguish between two kinds of forces acting on the fluid :

1. **external forces** or **body forces** :
   These forces act directly on the control volume itself such as gravitational, buoyancy, Coriolis, centrifugal or eventually electromagnetic forces.

2. **surface forces** :
   These forces act directly on the surface of the control volume. They are the result of :

   - the *pressure distribution* imposed by the outside fluid surrounding the control volume, or

   - the *shear and normal stress* due to friction between the fluid and the surface of the control volume.

If we sum up all these contributions, the momentum conservation in the pipe $[a, b]$ takes the form

$$
\begin{aligned}
\int_a^b [\rho(x, t_2)v(x, t_2) - \rho(x, t_1)v(x, t_1)]dx \ = \ & -\int_{t_1}^{t_2} [\rho(b, t)v^2(b, t) - \rho(a, t)v^2(a, t)]dt \\
& + \int_{t_1}^{t_2} \int_a^b \rho(x, t)f_e(x, t)dxdt \\
& - \int_{t_1}^{t_2} [p(b, t) - p(a, t)]dt + \int_{t_1}^{t_2} [\tau(b, t) - \tau(a, t)]dt \quad (3)
\end{aligned}
$$

where $\rho(x, t)v(x, t)$ represents momentum per unit volume and $\rho(x, t)v^2(x, t)$ denotes the instantaneous momentum flux. Then $\int_a^b \rho(x, t)v(x, t)dx$ is the total momentum in $[a, b]$ at time t, $\int_{t_1}^{t_2} \rho(x, t)v^2(x, t)dt$ is the total momentum flux past x in time interval $[t_1, t_2]$. $\int_a^b \rho(x, t)f_e(x, t)dx$ is the contribution of the external forces f_e to the momentum conservation. $\int_{t_1}^{t_2} p(x, t)dt$ is the total momentum change at x due to pressure in time interval $[t_1, t_2]$. $\int_{t_1}^{t_2} [\tau(b, t) - \tau(a, t)]dt$ represents the effect of viscous stress

on the boundary.

The extension of this result to the three-dimensional case yields

$$
\int_\Omega [\rho(x,t_2)\mathbf{v}(x,t_2) - \rho(x,t_1)\mathbf{v}(x,t_1)]dx \;=\; -\int_{t_1}^{t_2}\int_{\partial\Omega}[\rho(a,t)\mathbf{v}(s,t)(\mathbf{v}(s,t)\bullet\mathbf{n})]dSdt
$$
$$
+\; \int_{t_1}^{t_2}\int_\Omega \rho(x,t)f_e(x,t)dxdt
$$
$$
-\; \int_{t_1}^{t_2}\int_{\partial\Omega}p(s,t)\mathbf{n}dSdt + \int_{t_1}^{t_2}(\overline{\overline{\tau}}(s,t)\bullet\mathbf{n})dSdt \qquad (4)
$$

$\overline{\overline{\tau}}$ denotes the viscous stress tensor of second order.

Remark : The equation of momentum is the same in reactive and non-reactive flows. Although this equation does not involve explicit combustion terms, the flow is modified by the chemical reactions. In fact, the density ρ as well as the dynamic viscosity change dramatically across the flame front, which leads to a proportional increase of velocity [9]. So even though the momentum equations are exactly the same with and without combustion process, the behaviour of reactive flows is very different.

2.3   Energy equation

Conservation of energy states that energy changes due to one of three factors which are redistribution, conversion of energy to or from momentum, and conversion to or from some other form of energy, heat or work of forces acting on the volume. So, if energy increases in one place, either energy or an equivalent amount of momentum must decrease someplace else, heat is produced or work is done. The conservation of energy can be written as

change in total energy in Ω in time interval $[t_1, t_2]$

=

net energy flow through boundaries of Ω in time interval $[t_1, t_2]$

+

net energy change due to heat or work of forces on Ω in time interval $[t_1, t_2]$

For the mathematical formulation of this statement we introduce some important variables :

- the *specific internal energy e* which denotes the energy per unit mass contained in the microscopic motions of the individual fluid molecules,

- the *specific kinetic energy* $\frac{1}{2}|v|^2$ which denotes the energy per unit mass contained in the macroscopic motion of the whole fluid,

- the *specific total energy E* is the energy per unit mass stored in both microscopic and macroscopic motion and hence total. It is obtained by adding the internal energy per unit mass, e, to the kinetic energy per unit mass $\frac{1}{2}|v|^2$. Thus, the expression for the total energy is

$$
E(x,t) = e(x,t) + \frac{1}{2}|v|^2(x,t) \qquad (5)
$$

The contribution of the heat flux into the volume may take two forms :

1. diffusion of heat due to molecular thermal conduction : the diffusive flux is proportional to the gradient of the internal energy and is equal $\lambda \nabla T$, with λ standing for the *thermal conductivity* and T the absolute static temperature.

2. volumetric heating due to chemical reactions, or due to absorption or emission of radiation. We will denote these heat sources [6]- the time rate of heat transfer per unit mass- as $\dot{Q}$. The volume sources are obtained by the sum of the heat sources to the work done by the body forces that will be denoted by f_e.

In addition to the heat flux, the surface forces also contribute to the energy equation. Their contribution consists in the pressure and shear and normal stresses on the control surface.
We summarize these effects in the equation of conservation of energy [31] which reads

$$
\begin{aligned}
\int_a^b [\rho(x,t)E(x,t)]_{t_1}^{t_2} dx = \quad & - \int_{t_1}^{t_2} [\rho(b,t)v(b,t)E(b,t) - \rho(a,t)v(a,t)E(a,t)]dt \\
& + \int_{t_1}^{t_2} \int_a^b \rho(x,t)f_e(x,t)v(x,t)dxdt \\
& - \int_{t_1}^{t_2} [p(b,t)v(b,t) - p(a,t)v(a,t)]dt + \int_{t_1}^{t_2} [\tau(b,t)v(b,t) - \tau(a,t)v(a,t)]dt \\
& + \int_{t_1}^{t_2} \lambda[\frac{\partial T(b,t)}{\partial x} - \frac{\partial T(a,t)}{\partial x}]dt + \int_{t_1}^{t_2} \int_a^b \dot{Q}(x,t)dxdt
\end{aligned}
$$

$$(6)$$

ρE is the total energy per unit volume, and $\rho v E$ is the instantaneous total energy flux. Then we can interpret the integrals $\int_a^b \rho(x,t)E(x,t)dx$ as the total energy in $[a,b]$ at time t, $\int_{t_1}^{t_2} \rho(x,t)v(x,t)E(x,t)dt$ as the total energy flowing past x in time interval $[t_1,t_2]$, and $\int_{t_1}^{t_2} p(x,t)v(x,t)dt$ as the *pressure work*, i.e. the total energy change at x in time interval $[t_1,t_2]$.
The extension of these results to the three-dimensional case yields

$$
\begin{aligned}
\int_\Omega [\rho(x,t)E(x,t)]_{t_1}^{t_2} dx = \quad & - \int_{t_1}^{t_2} \int_{\partial\Omega} \rho(s,t)E(s,t)(\mathbf{v}(s,t) \bullet \mathbf{n})dSdt \\
& + \int_{t_1}^{t_2} \int_\Omega \rho(x,t)f_e(x,t)\mathbf{v}(x,t)dxdt \\
& - \int_{t_1}^{t_2} \int_{\partial\Omega} p(s,t)(\mathbf{v}(s,t) \bullet \mathbf{n})dSdt + \int_{t_1}^{t_2} \int_{\partial\Omega} (\overline{\overline{\tau}}(s,t) \bullet \mathbf{v}(s,t)) \bullet \mathbf{n})dSdt \\
& + \int_{t_1}^{t_2} \int_{\partial\Omega} \lambda(\nabla T(s,t) \bullet \mathbf{n})dSdt + \int_{t_1}^{t_2} \int_\Omega \dot{Q}(x,t)dxdt
\end{aligned}
$$

$$(7)$$

For a compact version of the previous equation we introduce two new variables :

- the *specific enthalpy* $h = e + \frac{p}{\rho}$ which is the sum of the energy per unit mass found in the microscopic motions of the fluid molecules, e, and the potential energy per unit mass stored by compression, $\frac{p}{\rho}$

- the *specific total enthalpy* $H = h + \frac{v^2}{2}$ which is the total energy per unit mass stored in the microscopic and macroscopic motions of the fluid plus the potential energy per unit mass stored by compression.

Using the total enthalpy, we get an equivalent equation of the conservation of energy

$$
\begin{aligned}
\int_\Omega [\rho(x,t_2)E(x,t_2) - \rho(x,t_1)E(x,t_1)]dx = \ &- \int_{t_1}^{t_2} \int_{\partial\Omega} \rho(s,t)H(s,t)(\mathbf{v}(s,t) \bullet \mathbf{n})dSdt \\
&+ \int_{t_1}^{t_2} \int_\Omega \rho(x,t)f_e(x,t)\mathbf{v}(x,t)dxdt \\
&+ \int_{t_1}^{t_2} \int_{\partial\Omega} (\overline{\overline{\tau}}(s,t) \bullet \mathbf{v}(s,t)) \bullet \mathbf{n})dSdt \\
&+ \int_{t_1}^{t_2} \int_{\partial\Omega} \lambda(\nabla T(s,t) \bullet \mathbf{n})dSdt + \int_{t_1}^{t_2} \int_\Omega \dot{Q}(x,t)dxdt
\end{aligned}
\tag{8}
$$

2.4   Conservation form

In this section we present an other form of the Navier-Stokes equations, which is known as the differential form or the *conservation form*of the Navier-Stokes equations [13]. This form has been used in a lot of simulation programs. It is less general than the integral form since it is assumed that all flow variables are differentiable in time and space. In the presence of discontinuities or shocks, special care is needed to resolve the fronts and one has to consider the integral form of the Navier-Stokes equations.
To show how to deduce the differential form from the integral from of the Navier-Stokes equations, we consider the conservation of mass.
Supposing that $\rho(x,t)$ is differentiable in time, we have then

$$
\rho(x,t_2) - \rho(x,t_1) = \int_{t_1}^{t_2} \frac{\partial \rho}{\partial t}dt
\tag{9}
$$

Similarly if $\rho(x,t)$ and $v(x,t)$ are differentiable in space, we have

$$
\rho(b,t)v(b,t) - \rho(a,t)v(a,t) = \int_a^b \frac{\partial(\rho v)}{\partial x}dx
\tag{10}
$$

Assuming reversibility of space and time integrals, the conservation of mass takes the form

$$\int_{t_1}^{t_2} \int_a^b [\frac{\partial \rho}{\partial t} + \frac{\partial (\rho v)}{\partial x}] dx dt = 0 \tag{11}$$

Since this equation holds for any a,b,t_1,t_2, the integrand must be zero :

$$\frac{\partial \rho}{\partial t} + \frac{\partial (\rho v)}{\partial x} = 0 \tag{12}$$

Similarly we obtain the differential forms of conservation of momentum and of energy.

2.5   Navier-Stokes equations

2.5.1   One-dimensional flows

For essentially one-dimensional flows the conservation of mass, momentum and energy are written as

$$\frac{\partial \rho}{\partial t} + \frac{\partial (\rho u)}{\partial x} = 0 \tag{13}$$

$$\frac{\partial (\rho u)}{\partial t} + \frac{\partial (\rho u^2)}{\partial x} + \frac{\partial p}{\partial x} = \frac{\partial \tau}{\partial x} + \rho F \tag{14}$$

$$\frac{\partial (\rho E)}{\partial t} + \frac{\partial (\rho u E + up)}{\partial x} = \frac{\partial u \tau}{\partial x} - \frac{\partial q}{\partial x} + \rho u F + Q \tag{15}$$

In some cases, it is more practical to use instead of (15) one of the following two equations. These equations are equivalent : the first one accounts for the conservation of enthalpy

$$\frac{\partial (\rho H)}{\partial t} + \frac{\partial (\rho u H)}{\partial x} - \frac{\partial p}{\partial t} = \frac{\partial u \tau}{\partial x} - \frac{\partial q}{\partial x} + \rho u F + Q \tag{16}$$

whereas the second one represents the temperature equation

$$\frac{\partial (\rho T)}{\partial t} + \frac{\partial (\rho u T)}{\partial x} = \frac{1}{c_p} \left(\frac{Dp}{Dt} + \tau \frac{\partial u}{\partial x} - \frac{\partial q}{\partial x} + \dot{Q} \right) \tag{17}$$

In the one-dimensional version of the Navier-Stokes equations, the stress τ and the flux q are expressed in terms of velocity and temperature gradients as

$$\tau = \frac{4}{3} \mu \frac{\partial u}{\partial x}, \quad q = -\lambda \frac{\partial T}{\partial x} \tag{18}$$

2.5.2   Three-dimensional flows

In the three-dimensional case the stress tensor τ_{ij} and the heat flux q_i have different expressions

$$\tau_{ij} = \mu \left(\frac{\partial u_i}{\partial x_j} + \frac{\partial u_j}{\partial x_i} \right) - \frac{2}{3} \mu \frac{\partial u_k}{\partial x_k} \delta_{ij}, \quad q_i = -\lambda \frac{\partial T}{\partial x_i} \tag{19}$$

To simplify the notations we introduce the scalar m and the vector $\mathbf{M}$ defined by

$$m = \frac{\partial u_i \tau_{ij}}{\partial x_j} = \tau : \nabla \mathbf{u} \quad \text{and} \quad \mathbf{M} = \frac{\partial \tau_{ij}}{\partial x_j} = \nabla \bullet \tau \tag{20}$$

With this short-hand notation, the 3D Navier-Stokes equations take the form

$$\frac{\partial \rho}{\partial t} + \nabla \bullet (\rho \mathbf{u}) \;=\; 0 \tag{21}$$

$$\frac{\partial (\rho \mathbf{u})}{\partial t} + \nabla \bullet (\rho \mathbf{u} \otimes \mathbf{u}) + \nabla p \;=\; \mathbf{M} + \rho \mathbf{F} \tag{22}$$

$$\frac{\partial (\rho E)}{\partial t} + \nabla \bullet ((\rho E + p)\mathbf{u}) \;=\; m - \nabla \bullet \mathbf{q} + \rho \mathbf{u} \bullet \mathbf{F} + Q \tag{23}$$

The equations of conservation of enthalpy and temperature are given by

$$\frac{\partial (\rho H)}{\partial t} + \nabla \bullet (\rho H \mathbf{u}) \;=\; m - \nabla \bullet \mathbf{q} + \rho \mathbf{u} \bullet \mathbf{F} + Q \tag{24}$$

$$\frac{\partial (\rho T)}{\partial t} + \nabla \bullet (\rho T \mathbf{u}) \;=\; \frac{1}{c_p}\left(\frac{Dp}{Dt} + \tau_{ij}\frac{\partial u_i}{\partial x_j} - \nabla \bullet \mathbf{q} + Q\right) \tag{25}$$

2.6   Equation of state

The thermodynamic state of a physical system is well-defined by three thermodynamic properties, such as pressure, mass and internal energy. All other thermodynamic properties can be expressed as functions of these three by means of the equations of state. When using specific quantities, i.e. expressing all quantities per unit mass, we eliminate one variable, namely the mass, since mass per unit mass is always one. Thus the specific thermodynamic state is well-defined by two specific thermodynamic properties -for example, density and specific internal energy. All other specific properties can be determined with the specific equations of state [5].

For ideal gases, the equation of state known as the *ideal gas law* gives a relationship between pressure, density and temperature. The ideal gas law for the species i reads

$$\boxed{p_i = \rho_i \frac{\mathcal{R}}{W_i} T} \tag{26}$$

p_i and ρ_i represents the partial pressure and density of species i, W_i denotes the molecular weight of species i and T the temperature. $\mathcal{R} = 8.314 J.K^{-1}.mol^{-1}$ is the universal gas constant.

In a multicomponent flow, the mixture molecular weight W is obtained from the molecular weight W_i of each of its components and reads

$$\frac{1}{W} = \frac{1}{\rho}\sum_{s=1}^{N_s}\frac{\rho_s}{W_s} = \sum_{s=1}^{N_s}\frac{Y_s}{W_s} \tag{27}$$

Dalton's law states that for ideal gases the pressure of a gas mixture is equal the sum of the partial pressures of the gases of which it is composed. This yields the equation of state of the mixture [26]

$$p = \sum_{s=1}^{N_s} p_s = \rho \frac{\mathcal{R}}{W} T \tag{28}$$

The second equation of state for ideal gases relates the internal energy e to the temperature T

$$de(T) = c_v(T)dT \tag{29}$$

where c_v is called the *constant volume specific heat.* An equivalent expression is given for the internal enthalpy h

$$dh(T) = c_p(T)dT \tag{30}$$

where c_p is called the *constant pressure specific heat.*
The ratio of specific heats is the *adiabatic exponent* γ and is given by

$$\gamma = \frac{c_p}{c_v} \tag{31}$$

The gas constant $\mathcal{R}$, the adiabatic exponent γ and the specific heats c_p, c_v are related in many forms

$$c_p = c_v + \frac{\mathcal{R}}{W} \tag{32}$$

$$c_p = \frac{\gamma}{\gamma - 1}\frac{\mathcal{R}}{W} \tag{33}$$

$$c_v = \frac{1}{\gamma - 1}\frac{\mathcal{R}}{W} \tag{34}$$

Inserting one of these relations in the ideal gas law, we obtain a equation relating the pressure p to the internal energy e

$$p = (\gamma - 1)\rho e \tag{35}$$

Further, we deduce that the total energy E of an ideal gas has the following expression

$$E = \frac{1}{\gamma - 1}\frac{p}{\rho} + \frac{v^2}{2} \tag{36}$$

Yet another important equation is the one defining the *speed of sound.* It is the speed at which small disturbances propagate through the flow measured relative to the movement of the flow. For an isentropic flow, we have

$$c^2 = \left[\frac{\partial p}{\partial \rho}\right]_{S=const} = \frac{\gamma p}{\rho} \tag{37}$$

2.7   Pressure equation

Lemma : If the entropy S is defined through the relation

$$S = c_v \ln(\frac{p}{\rho^\gamma}) \tag{38}$$

then the pressure satisfies the relation

$$\frac{\partial p}{\partial t} + u\frac{\partial p}{\partial x} + \gamma p\frac{\partial u}{\partial x} = (\gamma - 1)\rho T\frac{DS}{Dt} \tag{39}$$

Proof : The two first terms in the pressure relation represent the total derivative of p. In fact, we have

$$\frac{\partial p}{\partial t} + u\frac{\partial p}{\partial x} = \frac{Dp}{Dt} \tag{40}$$

Using the continuity equation, we show that

$$\frac{\partial u}{\partial x} = -\frac{1}{\rho}(\frac{\partial \rho}{\partial t} + u\frac{\partial \rho}{\partial x}) = -\frac{1}{\rho}\frac{D\rho}{Dt} \tag{41}$$

Therefore, the third term is proportional to the total derivative of ρ and we obtain

$$\frac{\partial p}{\partial t} + u\frac{\partial p}{\partial x} + \gamma p\frac{\partial u}{\partial x} = \frac{Dp}{Dt} - \frac{\gamma p}{\rho}\frac{D\rho}{Dt} \tag{42}$$

Using the identity provided by the ideal gas law and the definition of the heat capacity c_v

$$p = (\gamma - 1)\rho c_v T \tag{43}$$

the right-hand side of the previous equation takes the form

$$\frac{\partial p}{\partial t} + u\frac{\partial p}{\partial x} + \gamma p\frac{\partial u}{\partial x} = (\gamma - 1)\rho c_v T(\frac{1}{p}\frac{Dp}{Dt} - \frac{\gamma}{\rho}\frac{D\rho}{Dt}) \tag{44}$$

$$= (\gamma - 1)\rho c_v T(\frac{D\ln(p)}{Dt} - \gamma\frac{D\ln(\rho)}{Dt}) \tag{45}$$

$$= (\gamma - 1)\rho T\frac{D}{Dt}\left(c_v \ln(\frac{p}{\rho^\gamma})\right) \tag{46}$$

$$= (\gamma - 1)\rho T\frac{DS}{Dt} \tag{47}$$

∎

Remark : in the one-dimensional case the entropy satisfies the equation

$$\rho T\frac{Ds}{Dt} = \frac{\partial u\tau}{\partial x} - \frac{\partial q}{\partial x} + \rho uF + Q \tag{48}$$

As a consequence of the previous lemma we obtain the following pressure equation

$$\boxed{\frac{Dp}{Dt} + \gamma p\frac{\partial u}{\partial x} = (\gamma - 1)(\frac{\partial u\tau}{\partial x} - \frac{\partial q}{\partial x} + \rho uF + Q)} \tag{49}$$

2.8   Temperature equation

We simplify the right-hand side of the momentum equation

$$\frac{\partial(\rho u)}{\partial t} + \frac{\partial(\rho u^2)}{\partial x} + \frac{\partial p}{\partial x} = \rho\frac{\partial u}{\partial t} + u(\underbrace{\frac{\partial \rho}{\partial t} + \frac{\partial(\rho u)}{\partial x}}_{=0}) + \rho u\frac{\partial u}{\partial x} + \frac{\partial p}{\partial x} \tag{50}$$

$$= \rho\frac{Du}{Dt} + \frac{\partial p}{\partial x} \tag{51}$$

and rewrite the momentum equation in the form

$$\rho \frac{Du}{Dt} + \frac{\partial p}{\partial x} = \frac{\partial \tau}{\partial x} + \rho F \tag{52}$$

As shown in the previous section the internal enthalpy is related to the temperature through $h = c_p T$ therefore it is possible to find a temperature equation equivalent to the enthalpy equation.

Lemma : the temperature satisfies the following equation

$$\rho c_p \frac{DT}{Dt} + \gamma p \frac{\partial u}{\partial x} = \gamma \left(\frac{\partial \tau u}{\partial x} + \rho u F - \frac{\partial q}{\partial x} + Q \right) - u \left(\frac{\partial \tau}{\partial x} + \rho F \right) \tag{53}$$

Proof :

$$\rho c_p \frac{DT}{Dt} - \frac{Dp}{Dt} + \rho u F + u \frac{\partial \tau}{\partial x} = \rho c_p \frac{DT}{Dt} + u \left(-\frac{\partial p}{\partial x} + \frac{\partial \tau}{\partial x} + \rho F \right) - \frac{\partial p}{\partial t} \tag{54}$$

$$= \rho c_p \frac{DT}{Dt} + \rho u \frac{Du}{Dt} - \frac{\partial p}{\partial t} \tag{55}$$

$$= \rho \left(\frac{Dh}{Dt} + \frac{1}{2} \frac{Du^2}{Dt} \right) - \frac{\partial p}{\partial t} \tag{56}$$

$$= \rho \frac{DH}{Dt} - \frac{\partial p}{\partial t} \tag{57}$$

Inserting the continuity equation on the right-hand side of this equation, we obtain

$$\rho c_p \frac{DT}{Dt} - \frac{Dp}{Dt} + \rho u F + u \frac{\partial \tau}{\partial x} = \rho \frac{\partial H}{\partial t} + H \left(\frac{\partial \rho}{\partial t} + \frac{\partial (\rho u)}{\partial x} \right) + \rho u \frac{\partial H}{\partial x} - \frac{\partial p}{\partial t} \tag{58}$$

$$= \frac{\partial (\rho H)}{\partial t} + \frac{\partial (\rho u H)}{\partial x} - \frac{\partial p}{\partial t} \tag{59}$$

The obtained term represents the right-hand side of the enthalpy equation

$$\frac{\partial (\rho H)}{\partial t} + \frac{\partial (\rho u H)}{\partial x} - \frac{\partial p}{\partial t} = \frac{\partial u \tau}{\partial x} - \frac{\partial q}{\partial x} + \rho u F + Q \tag{60}$$

Hence we have

$$\rho c_p \frac{DT}{Dt} - \frac{Dp}{Dt} + \rho u F + u \frac{\partial \tau}{\partial x} = \frac{\partial u \tau}{\partial x} - \frac{\partial q}{\partial x} + \rho u F + Q \tag{61}$$

$$\rho c_p \frac{DT}{Dt} - \frac{Dp}{Dt} = \tau \frac{\partial u}{\partial x} - \frac{\partial q}{\partial x} + Q \tag{62}$$

The pressure equation tells us that

$$\frac{Dp}{Dt} + \gamma p \frac{\partial u}{\partial x} = (\gamma - 1) \left(\frac{\partial u \tau}{\partial x} - \frac{\partial q}{\partial x} + \rho u F + Q \right) \tag{63}$$

This yields the following temperature equation

$$\rho c_p \frac{DT}{Dt} + \gamma p \frac{\partial u}{\partial x} = \gamma \left(\frac{\partial \tau u}{\partial x} + \rho u F - \frac{\partial q}{\partial x} + Q \right) - u \left(\frac{\partial \tau}{\partial x} + \rho F \right) \tag{64}$$

∎

Remark : in the context of gas turbines [10], the impact of body forces is very limited and will be neglected in the following ($F = 0$).

3   Chemistry and reaction kinetics

3.1   Stoichiometry and Flammability Limits

A stoichiometric mixture is the chemically correct air/fuel ratio for complete fuel and oxygen reaction. For most hydrocarbon fuels the stoichiometric air/fuel by mass is in the range $14/1 \sim 15/1$. If the air/fuel ratio is greater than 15/1, the mixture is lean or has excess air and this is the normal situation in gas turbines. But, if the air/fuel ratio is less than 15/1, then the mixture is rich or has excess fuel. Furthermore, the equivalence ratio ϕ is defined as the ratio of the actual fuel consumption to the theoretical stoichiometric fuel consumption for the same air supply. In air/fuel ratio it is

$$\phi = \frac{(Air/Fuel)_{stoichiometric}}{(Air/Fuel)_{flame}} \tag{65}$$

The flame temperature is strongly dependent upon the equivalence ratio ϕ [32]. An equivalence ratio of 1 corresponds to the stoichiometric ratio and is the point at which a flame burns at its highest theoretical temperature [9].

Combustion is said to be fuel-lean ($\phi < 1$) when there is excess oxygen available. Conversely, combustion is fuel-rich ($\phi > 1$) if insufficient oxygen is present to burn all of the available fuel.

In practice, it is not possible to vary the equivalence ratio arbitrarily. In fact, there exist flammability limits which define the range where flame propagation is possible. As shown in figure (3), the flammability limits [14] are :

- the lean limit, i.e. the least amount of fuel in air that will propagate a flame, and

- the rich limit, i.e. the maximum amount of fuel in air that will support a flame.
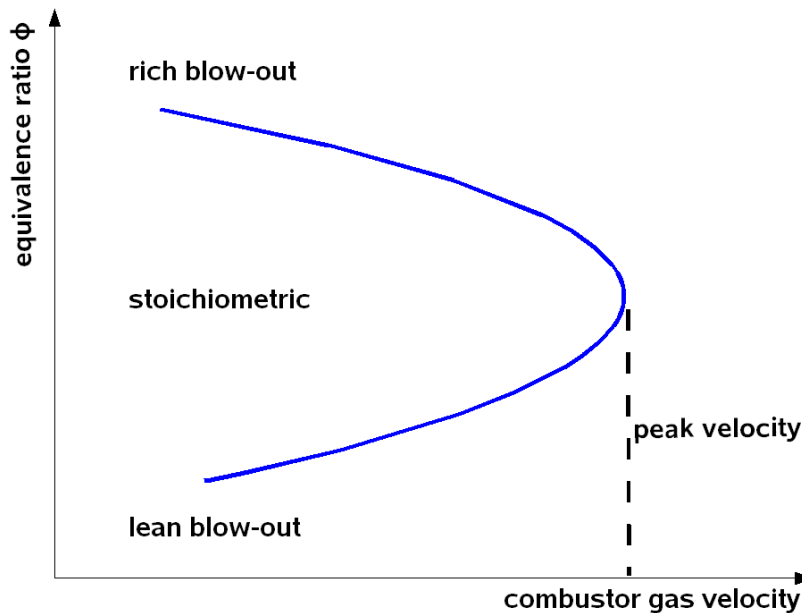
Figure 3: Range of burnable equivalence ratios versus combustor gas velocity

For flame stability, these flamability limits represent a vital information since the aim of a lean-burn well-mixed low NOx gas turbine is to burn as close to the lean flammability limit as possible [9]. All hydrocarbons are represented by the generic chemical formula CH_y with y being the hydrogen/carbon ratio. Let n be the carbon number (e.g. $n = 1$ for methane) then the generic formula is

- for alkanes $y = 2 + \frac{2}{n}$, (e.g. $y = 2.67$ for propane)

- for naphtenes $y = 2 - \frac{2}{n}$, (e.g. $y = 1$ for ethylene)

- for aromatics $y = 2 - \frac{6}{n}$, (e.g. $y = 1$ for benzene)

The simplest fire reaction is between CH_y and oxygen

$$CH_y + a \ O_2 \longrightarrow b \ CO_2 + c \ H_2O \tag{66}$$

The atom balance yields the value of the coefficients a, b and c

$$a = 1 + \frac{y}{4}, \ b = 1, \ c = \frac{y}{2} \tag{67}$$

Hence, the oxygen/fuel ratio by volume is $1 + \frac{y}{4}$ and the fuel concentration by volume is $\frac{1}{2+\frac{y}{4}}$. Using the molecular weight of C, H and O, we convert this quantity from volume to mass ratios

$$(O/F)_{mass} = (O/F)_{vol} \times \frac{2W_O}{W_C + yW_H} = \frac{32 + 8y}{12 + y} \tag{68}$$

As we are usually more interested in combustion in air, all we have to do to convert the O/F ratio to A/F ratio is use the fact that there is around 21% oxygen in air by volume, corresponding to 23% by mass. Hence for a general hydrocarbon CH_y, the air/fuel ratio is

$$(A/F)_{vol} = \frac{1}{21\%}\left(1 + \frac{y}{4}\right), \ \ (A/F)_{mass} = \frac{1}{23\%}\frac{32 + 8y}{12 + y} \tag{69}$$

A stoichiometric mixture of fuel and oxidant is one in which the amount of oxidant present is just sufficient to completely oxidise the fuel. As an example, we consider the reaction between methane and oxygen :

$$CH_4 + 2 \ O_2 \longrightarrow CO_2 + 2 \ H_2O \tag{70}$$

The stoichiometric oxygen to fuel ratio is 2 by volume and 4 by mass. Using the formula above yields the stoichiometric air to fuel ratio by volume $\frac{1}{10\%}$ and by mass $\frac{1}{6\%}$.

3.2   Chemical species equations

In reactive flows the medium consists of many chemical species which interact with one another inducing a change in the composition of the flow. As we are interested in this detailed chemical composition we need to determine the evolution of each species present in the flow [22].

We achieve this by writing the continuity equation for species X_s and taking into account the chemical reactions taking place as well as the diffusion process

$$\frac{\partial \rho_s}{\partial t} + \nabla \bullet (\rho_s \mathbf{u}) = \nabla \bullet \left(\rho \mathcal{D}_s \nabla \frac{\rho_s}{\rho} \right) + \dot{\omega}_s \qquad (71)$$

ρ_s denotes the density of species X_s, $\mathcal{D}_s$ its diffusion coefficient and $\dot{\omega}_s$ its chemical production rate. To quantify the chemical composition of the flow, we also use the mass fraction of species s given by

$$Y_s = \frac{\rho_s}{\rho} \qquad (72)$$

The total density ρ equals the sum of the partial densities ρ_i. Hence the mass fractions Y_s sum to 1 :

$$\sum_{s=1}^{N_s} Y_s = 1 \qquad (73)$$

Taking the continuity equation for the total density ρ into account

$$\frac{\partial \rho}{\partial t} + \nabla \bullet (\rho \mathbf{u}) = 0 \qquad (74)$$

we note that the conservation law for the species X_s simplifies to

$$\rho \left(\frac{\partial Y_s}{\partial t} + \mathbf{u} \bullet \nabla Y_s \right) = \nabla \bullet (\rho \mathcal{D}_s \nabla Y_s) + \dot{\omega}_s \qquad (75)$$

3.3   Balance laws

A chemical reaction involves one or more substances, called *reactants*, that react to produce other substances called *products*. As the reaction proceeds, some chemical species are depleted while others are formed. This process is governed by certain laws which can be expressed in mathematical terms [8]. One of the assumptions made in chemical kinetics is the preservation of the number of atoms, i.e. atoms are neither created nor destroyed. For example, if there are n atoms of carbon present before the reaction begins, then there will be the same number n of atoms of carbon during all stages of the reaction. To illustrate this, we take the following reactions which take place inside some automobile catalytic converters based on the oxidation reaction of CO, hydrocarbons and H_2

$$
\begin{aligned}
2\ CO + O_2 &\rightarrow 2\ CO_2 \\
2\ C_3H_6 + 9\ O_2 &\rightarrow 6\ CO_2 + 6\ H_2O \\
2\ H_2 + O_2 &\rightarrow 2\ H_2O
\end{aligned}
$$
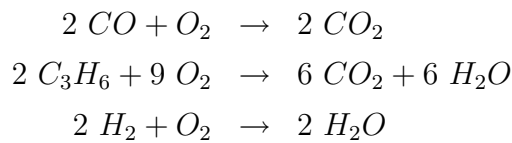
Note the conservation of the atoms of C, H and O in each of these reactions.
Suppose a moles of A react with b moles of B to produce c moles of C and d moles of D

$$aA + bB \rightarrow cC + dD$$
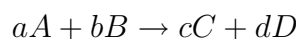
Let N_A, N_B, N_C, N_D represent the molar amounts of the chemical species in the reaction and let V be the volume occupied by the reaction mixture. Thus the *reaction rate* [25] of the species A is expressed as

$$r_A = \frac{1}{V}\frac{dN_A}{dt} = \frac{1}{V}\frac{d}{dt}([A]\cdot V) = \frac{1}{V}\left(\frac{dV}{dt}\cdot[A] + V\cdot\frac{d[A]}{dt}\right)$$

where $[A] = \frac{\rho_A}{W_A}$, ρ_A is the partial density, W_A the molecular weight of species A.

Assuming the reaction volume V does not vary in time, the rates of change of the concentrations of A and B are then given by

$$r_A = \frac{d[A]}{dt}, \ r_B = \frac{d[B]}{dt}$$

Since the number of atoms is conserved, the rates at which C and D are formed are directly related to the rates at which A and B are depleted.

Considering only the species A and C, it is true that for every a moles of A that react, c moles of C are produced. Thus the rate of change of C is c/a times the rate of change of A. Since $[A]$ decreases and $[C]$ increases, the signs are reverted and the mathematical expression reads

$$\frac{d[C]}{dt} = -\frac{c}{a}\frac{d[A]}{dt}$$

Reasoning the same way with any pair of species we conclude that

$$\boxed{-\frac{1}{a}\frac{d[A]}{dt} = -\frac{1}{b}\frac{d[B]}{dt} = \frac{1}{c}\frac{d[C]}{dt} = \frac{1}{d}\frac{d[D]}{dt}}$$

3.4 Law of mass action

Based on experimental observation, but also explained by collision theory, the *law of mass action* states that the rate of an elementary reaction (at a constant temperature) is proportional to the product of the concentrations of the reactants.

We consider the following reaction

$$X + Y \rightarrow Z$$

and introduce the reaction rate coefficient k as a constant of proportionality. Then, according to the law of mass action, the rate of change of $[X]$ is given by

$$\frac{d[X]}{dt} = -k[X][Y]$$

Applying this principle to a reaction where two molecules X combine to build X_2

$$X + X \rightarrow X_2$$
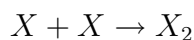
we obtain the rate of consumption of X

$$\frac{d[X]}{dt} = -k[X][X] - k[X][X] = -2k[X]^2$$

The factor 2 appears because two moles of X are consumed.
This reasoning may be extended to our first reaction

$$a\ A + b\ B \rightarrow c\ C + d\ D$$
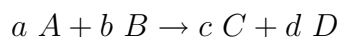
and the time rate of consumption/formation of $[A], [B], [C], [D]$ by the forward reaction are then

$$\left(\frac{d[A]}{dt}\right)_f = -a\ \ k_f[A]^a[B]^b$$

$$\left(\frac{d[B]}{dt}\right)_f = -b\ \ k_f[A]^a[B]^b$$

$$\left(\frac{d[C]}{dt}\right)_f = c\ \ \ k_f[A]^a[B]^b$$

$$\left(\frac{d[D]}{dt}\right)_f = d\ \ \ k_f[A]^a[B]^b$$

For every elementary reaction, it is in principle possible that the reaction proceeds in the backward direction as well. Assuming that C and D react to form A and B, we may write

$$aA + bB \leftarrow cC + dD$$
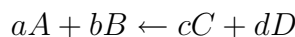
The time rate of consumption/formation of $[A], [B], [C], [D]$ by the backward reaction are then

$$\left(\frac{d[A]}{dt}\right)_b = a\ \ \ k_b[C]^c[D]^d$$

$$\left(\frac{d[B]}{dt}\right)_b = b\ \ \ k_b[C]^c[D]^d$$

$$\left(\frac{d[C]}{dt}\right)_b = -c\ \ k_b[C]^c[D]^d$$

$$\left(\frac{d[D]}{dt}\right)_b = -d\ \ k_b[C]^c[D]^d$$

The subscript b denotes here the backward reaction and k_b its rate coefficient.
So, the net rate of change is given by the sum of the forward and backward time rate

$$\frac{d[A]}{dt} = \left(\frac{d[A]}{dt}\right)_f + \left(\frac{d[A]}{dt}\right)_b = -a\ \ k_f[A]^a[B]^b + a\ k_b[C]^c[D]^d$$

$$\frac{d[B]}{dt} = \left(\frac{d[B]}{dt}\right)_f + \left(\frac{d[B]}{dt}\right)_b = -b\ \ k_f[A]^a[B]^b + b\ k_b[C]^c[D]^d$$

$$\frac{d[C]}{dt} = \left(\frac{d[C]}{dt}\right)_f + \left(\frac{d[C]}{dt}\right)_b = c\ \ \ k_f[A]^a[B]^b - c\ k_b[C]^c[D]^d$$

$$\frac{d[D]}{dt} = \left(\frac{d[D]}{dt}\right)_f + \left(\frac{d[D]}{dt}\right)_b = d\ \ \ k_f[A]^a[B]^b - d\ k_b[C]^c[D]^d$$

Written in matrix form, the reaction kinetics for the species (A, B, C, D) are

$$\frac{d}{dt}\begin{pmatrix} [A] \\ [B] \\ [C] \\ [D] \end{pmatrix} = \begin{pmatrix} a & & & \\ & b & & \\ & & c & \\ & & & d \end{pmatrix} \begin{pmatrix} -1 & 1 \\ -1 & 1 \\ 1 & -1 \\ 1 & -1 \end{pmatrix} \begin{pmatrix} k_f[A]^a[B]^b \\ k_b[C]^c[D]^d \end{pmatrix} \tag{76}$$
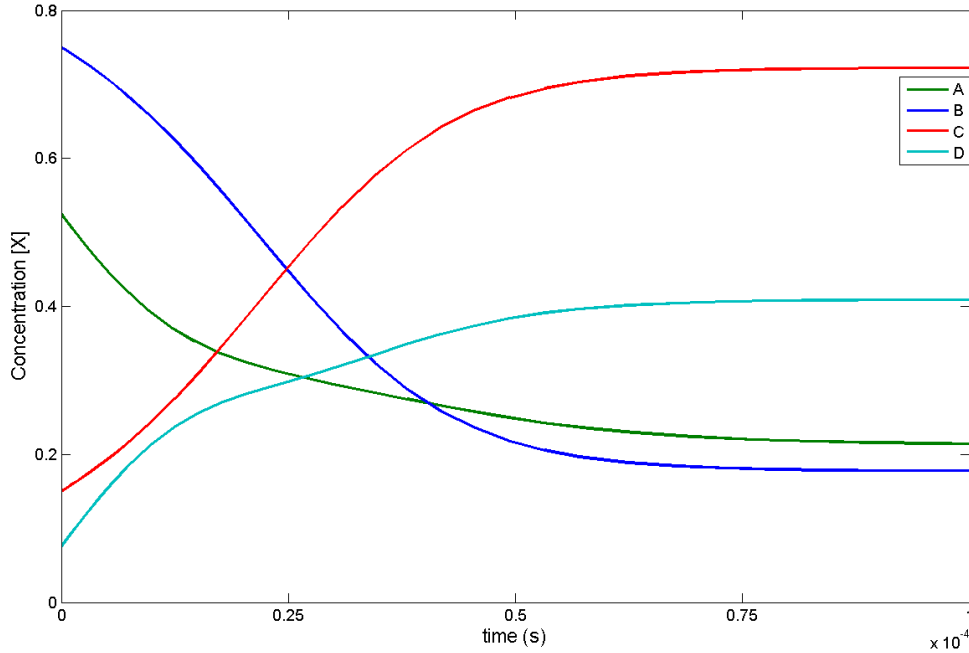
Figure 4: Time evolution of the concentration of species A, B, C, D

3.5   Reaction rate coefficients

On the basis of statistical thermodynamics [5], it can be shown that the temperature dependence of the rate coefficients follows a modified Arrhenius law

$$k_f(T) = A_f T^{n_f} exp\left(-\frac{E_f^a}{\mathcal{R}T}\right)$$

$$k_b(T) = A_b T^{n_b} exp\left(-\frac{E_b^a}{\mathcal{R}T}\right)$$

The steric factor $T^{n_{f,b}}$ is due to the fact that few collisions between reactive molecules have the correct geometry to react. $E_{f,b}^a$ represents the *activation energy*, i.e. the minimum energy needed for the reaction to occur. $A_{f,b}$ is the collision frequency, precisely the frequency of collisions between two molecules in the proper orientation for reaction to occur. The value of $A_{f,b}$ is determined by experiment and will be different for every reaction. $\mathcal{R}$ is the universal gas constant.
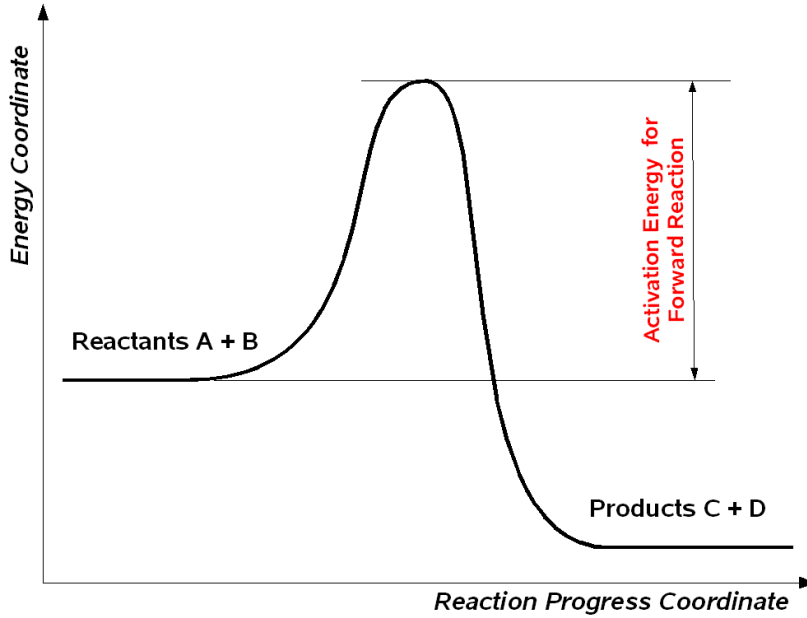
Figure 5: Barrier that must be overcome before forward reaction can proceed

Remark :   An important consequence of the temperature dependence of the reaction rate coefficients is that if the reactions taking place are not thermally neutral, and/or if the temperature is varying due to the effect of an external source, then the system (76) no longer describes the correct reaction kinetics, and needs to be extended to include an equation accounting for the change of temperature due to the endo- or exothermicity of the reaction, or due to external effects.

3.6   Chemical source terms

3.6.1   Single-step reactions

We consider an elementary reaction containing an arbitrary number N_s of reactants and products

$$\sum_{j=1}^{N_s} \nu_j^f X_j \; \rightleftharpoons \; \sum_{j=1}^{N_s} \nu_j^b X_j$$
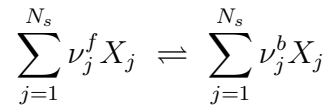
ν_j^f and ν_j^b are respectively the stoichiometric coefficient for the forward and the backward reactions of species X_j. Further we introduce $\nu_j := \nu_j^b - \nu_j^f$.
We define the reaction rate of the forward reaction, $\dot{\Omega}_f$, respectively the backward reaction, $\dot{\Omega}_b$ by

$$\dot{\Omega}_f \;\; = \;\; k_f \prod_{s=1}^{N_s} [X_s]^{\nu_j^f}$$

$$\dot{\Omega}_b \;\; = \;\; k_b \prod_{s=1}^{N_s} [X_s]^{\nu_j^b}$$

The time rate of change due to the forward and the backward reaction of any species participating in the reaction is then

$$\frac{1}{\nu_i}\left(\frac{d[X_i]}{dt}\right)_f = \frac{1}{\nu_j}\left(\frac{d[X_j]}{dt}\right)_f = \dot{\Omega}_f$$

$$\frac{1}{\nu_i}\left(\frac{d[X_i]}{dt}\right)_b = \frac{1}{\nu_j}\left(\frac{d[X_j]}{dt}\right)_b = \dot{\Omega}_b$$

Thus, the net reaction rate for the s-th species, also called *chemical production rate*, reads

$$
\begin{aligned}
\dot{\omega}_s &= W_s\nu_s(\dot{\Omega}_f - \dot{\Omega}_b)\\
&= W_s(\nu_s^b - \nu_s^f)\left[k_f(T)\prod_{j=1}^{N_s}[X_j]^{\nu_j^f} - k_b(T)\prod_{j=1}^{N_s}[X_j]^{\nu_j^b}\right]\\
&= W_s(\nu_s^b - \nu_s^f)\left[k_f(T)\prod_{j=1}^{N_s}(\frac{\rho_j}{W_j})^{\nu_j^f} - k_b(T)\prod_{j=1}^{N_s}(\frac{\rho_j}{W_j})^{\nu_j^b}\right]
\end{aligned}
\tag{77}
$$

where W_s denotes the molecular weight. Furthermore, the *chemical heat release* of the given reaction reads

$$\dot{Q}_c = -\sum_{s=1}^{N_s} h_s^0 \dot{\omega}_s \tag{78}$$

with h_s^0 the specific heat of formation of species X_s [26].

3.6.2   General reaction mechanisms

Generalizing these results to more complex reaction mechanisms is quite straightforward. In fact, a multicomponent mixture in which N_r chemical reactions take place may be written in the form

$$\sum_{s=1}^{N_s} \nu_{sr}^f X_s \;\rightleftharpoons\; \sum_{s=1}^{N_s} \nu_{sr}^b X_s, \quad r = 1, \cdots, N_r$$

where ν^f is now the matrix of the stoichiometric coefficients for the forward reactions, ν^b is the matrix of the stoichiometric coefficients for the backward reactions. N_s denotes the number of species.
The source term in the transport equation of species X_s is the chemical production rate of that species. It is obtained as a sum of the contributions of every reaction in which the species X_s is involved [26]

$$\dot{\omega}_s = W_s \sum_{r=1}^{N_r} (\nu_{sr}^b - \nu_{sr}^f)\dot{\Omega}_r \tag{79}$$

In this relation, $\dot{\Omega}_r$ denotes the rate of the r-th reaction

$$\dot{\Omega}_r = k_f^r(T)\prod_{s=1}^{N_s}[X_s]^{\nu_{sr}^f} - k_b^r(T)\prod_{s=1}^{N_s}[X_s]^{\nu_{sr}^b} \tag{80}$$

and the Arrehnius coefficient is provided for each reaction by the relation

$$k^r(T) = A_r T^{n_r} exp\left(-\frac{E_r^a}{\mathcal{R}T}\right)$$

(81)

The chemical heat release of the whole reaction mechanism reads

$$\dot{Q}_c = -\sum_{s=1}^{N_s} h_s^0 \dot{\omega}_s$$

(82)

The chemical heat release is a source term in the energy equation and couples the chemical reactions to the flow internal energy [25].

Example :   Kinetics of the Zeldovich mechanism for NO

We consider the Zeldovich mechanism which describes the formation of thermal NO. It basically consists of three reactions.

$$\begin{aligned}
\text{Reaction 1} \;:\;\; N_2 + O \;&\rightleftharpoons\; NO + N \\
\text{Reaction 2} \;:\;\; N + O_2 \;&\rightleftharpoons\; NO + O \\
\text{Reaction 3} \;:\;\; N + OH \;&\rightleftharpoons\; NO + H
\end{aligned}$$
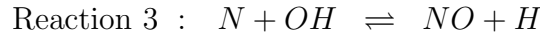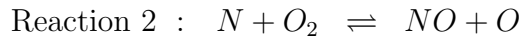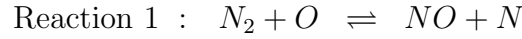
Each of these reactions has two experimentally determined rate coefficients for the forward and backward reaction. We will denote these reaction rates k_1, k_2 and k_3 and use f and b to indicate the forward, respectively the backward reaction. The formation kinetics of thermal NO is described by

$$\boxed{\frac{d[NO]}{dt} = k_1^f[O][N_2] + k_2^f[N][O_2] + k_3^f[N][OH] - k_1^b[NO][N] - k_2^b[NO][O] - k_3^b[NO][H]}$$

(83)

4   Acoustic system

4.1   Reynolds Averaging

At any point in an unsteady flow all physical variables fluctuate with time even though their average
may remain constant. A very useful approach to study this instationary system is to decompose each
flow variable $Z(x,t)$ into

- a mean part denoted $\overline{Z}$ and

- a fluctuating part $Z'(x,t)$

such that

$$\boxed{Z = \bar{Z} + Z'} \tag{84}$$

The mean value $\bar{Z}$ is obtained by an averaging procedure and can be a function of time and/or space.
In fact, we distinguish between three different forms of averaging :

- *Ensemble Averaging* :
  The average value is obtained through the mean of a sum of realizations or experiments

  $$\bar{Z}(x,t) = \lim_{N \to \infty} \frac{1}{N} \sum_{n=0}^{N} Z_n(x,t) \tag{85}$$

  The obtained average is still a function of time and space.

- *Spatial Averaging* :
  In this case, the mean variable is uniform in space but is allowed to vary in time. It is obtained
  through an averaging over the control volume V

  $$\bar{Z}(t) = \frac{1}{|V|} \int_V Z(x,t)dx \tag{86}$$

- *Time Averaging* :

  $$\bar{Z}(x) = \lim_{\Delta T \to \infty} \frac{1}{\Delta T} \int_{t_0}^{t_0 + \Delta T} Z(x,t)dt \tag{87}$$

  Since the mean value varies only in space and does not depend on time, we call it *steady state*
  or *stationary state.*
  In practice, $\Delta T \to \infty$ means that the time interval ΔT should be much larger than the typical
  time scale of the fluctuations.

Remark : In this thesis, we are primarily interested in the assessment of the thermo-acoustic insta-
bilites. As these instabilities are mainly triggered by the unsteady pressure and heat release oscillations
[2], we will restrict in the following to the *time averaging*. A common terminology used to denoted
the unsteady pressure is the *acoustic pressure.*
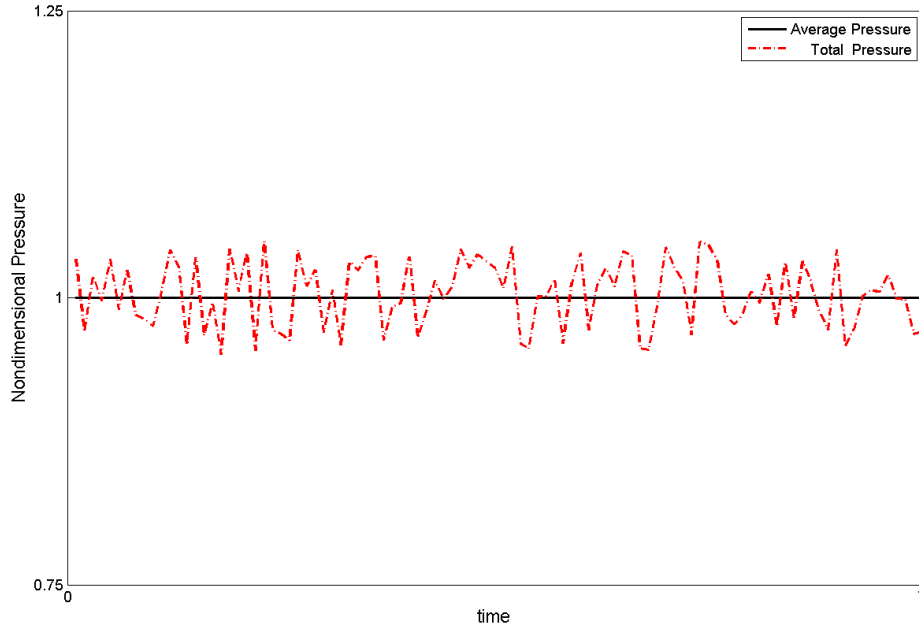
Figure 6: The acoustic pressure is the difference between total and time-averaged pressure

By definition, unsteady terms are obtained from the difference between total and mean terms

$$Z'(x,t) = Z(x,t) - \bar{Z}(x) \tag{88}$$

The following rules will be useful while deriving the Reynolds-averaged Navier-Stokes equations.
Let Y and Z be two flow variables, e.g. density ρ, velocity u or pressure p and s be one of the independent variables x, y, z or t, then the averaging rules are

$$\overline{\overline{Z}} = \overline{Z} \tag{89}$$
$$\overline{Y+Z} = \overline{Y} + \overline{Z} \tag{90}$$
$$\overline{\overline{Y}Z} = \overline{Y}\overline{Z} \tag{91}$$
$$\overline{\frac{\partial Z}{\partial s}} = \frac{\partial \overline{Z}}{\partial s} \quad s \in \{x, y, z, t\} \tag{92}$$

Also, we should note that the average of the product is generally different from the product of the averages

$$\overline{Y \cdot Z} \neq \overline{Y} \cdot \overline{Z} \tag{93}$$

Furthermore we assume that the fluctuations are much smaller than the steady-state variables

$$|Z'(x,t)| \ll |\bar{Z}(x)| \quad \forall\, x, t \tag{94}$$

The fluctuating terms Y' and Z' obtained through this averaging procedure satisfy

$$\overline{Z'} = 0, \text{ but in general } \overline{Y'Z'} \neq 0 \tag{95}$$

A further assumption is that the product of any two fluctuations is negligible. As a consequence all equations will be linear in the instationary terms.

4.2   Linearization

In the following we will use the Reynolds time averaging and split all variables appearing in the governing equations into two parts : steady-state and acoustic such that

$$
\begin{array}{l|l}
\rho(x,t) = \overline{\rho}(x) + \rho'(x,t) & \mathbf{u}(x,t) = \overline{\mathbf{u}}(x) + \mathbf{u}'(x,t) \\
p(x,t) = \overline{p}(x) + p'(x,t) & T(x,t) = \overline{T}(x) + T'(x,t) \\
Y(x,t) = \overline{Y}(x) + Y'(x,t) & \dot{\omega}(x,t) = \overline{\dot{\omega}}(x) + \dot{\omega}'(x,t)
\end{array}
\tag{96}
$$

As a consequence the governing equations will also be split into two sets :

- a set of equations for the steady-state part and

- a set of equations for the instationary acoustic terms.

To illustrate this we take the continuity equation as an example. Inserting the Reynolds-average ansatz in the continuity equation leads to

$$
\frac{\partial \rho}{\partial t} + \nabla \bullet (\rho \mathbf{u}) = 0 \Rightarrow
\begin{cases}
\text{steady} & : & \nabla \bullet (\overline{\rho}\overline{\mathbf{u}}) = 0 \\
\text{unsteady} & : & \frac{\partial \rho'}{\partial t} + \nabla \bullet (\rho'\overline{\mathbf{u}} + \overline{\rho}\mathbf{u}') = 0
\end{cases}
\tag{97}
$$

Note that the term $\nabla \bullet (\rho'\mathbf{u}')$ was neglected since it includes the product of two acoustic variables. As a second example, we consider the chemical species equation. Since we are only interested in the instationary part of the mass fraction, we insert the Reynolds average ansatz in the conservation equation of species X_s and neglect all nonlinear terms (in addition to the term $\nabla \bullet (\rho'\mathcal{D}_s \nabla \overline{Y}_s))$ [8]. We obtain the following equation for the unsteady mass fraction Y'_s

$$
\overline{\rho}\frac{\partial Y'_s}{\partial t} + \overline{\rho}\overline{\mathbf{u}} \bullet \nabla Y'_s + \overline{\rho}\mathbf{u}' \bullet \nabla \overline{Y}_s + \rho'\overline{\mathbf{u}} \bullet \nabla \overline{Y}_s \quad = \quad \nabla \bullet (\overline{\rho}\mathcal{D}_s \nabla Y'_s) + \dot{\omega}'_s
\tag{98}
$$

Since $\rho' \ll \overline{\rho}$ this equation simplifies to

$$
\frac{\partial Y'_s}{\partial t} + \overline{\mathbf{u}} \bullet \nabla Y'_s + \mathbf{u}' \bullet \nabla \overline{Y}_s \quad = \quad \frac{1}{\overline{\rho}}\nabla \bullet (\overline{\rho}\mathcal{D}_s \nabla Y'_s) + \frac{1}{\overline{\rho}}\dot{\omega}'_s
\tag{99}
$$

Inserting this ansatz in the pressure, velocity and temperature equations provides equations for the steady-state variables [24] as well as for the instationary terms.
The steady-state variables are much easier to obtain than the acoustic variables. In fact, there are many reliable experimental techniques as well as computational methods available to determine the values of the steady-state variables. In the following we assume that the steady-state variables have been obtained either from measurements or previous steady-state simulations [3]. We focus on solving the equations for the acoustic variables.
We write the linearized equations for the acoustic pressure, velocity, temperature and chemical species

$$
\frac{\partial p'}{\partial t} + \overline{\mathbf{u}} \bullet \nabla p' + \mathbf{u}' \bullet \nabla \overline{p} + \gamma(\overline{p}\nabla \bullet \mathbf{u}' + p'\nabla \bullet \overline{\mathbf{u}}) = (\gamma - 1)(m' + \nabla \bullet (\lambda \nabla T') + Q')
$$

$$\frac{\partial \mathbf{u}'}{\partial t} + (\overline{\mathbf{u}} \bullet \nabla)\mathbf{u}' + (\mathbf{u}' \bullet \nabla)\overline{\mathbf{u}} + \frac{\rho'}{\overline{\rho}}(\overline{\mathbf{u}} \bullet \nabla)\overline{\mathbf{u}} + \frac{1}{\overline{\rho}}\nabla p' = \frac{1}{\overline{\rho}}\mathbf{M}'$$

$$\frac{\partial T'}{\partial t} + \overline{\mathbf{u}} \bullet \nabla T' + \mathbf{u}' \bullet \nabla \overline{T} + \frac{\rho'}{\overline{\rho}}\overline{\mathbf{u}} \bullet \nabla \overline{T} + \frac{\gamma}{\overline{\rho}c_p}(\overline{p}\nabla \bullet \mathbf{u}' + p'\nabla \bullet \overline{\mathbf{u}}) = \frac{\gamma}{\overline{\rho}c_p}(\nabla \bullet (\lambda \nabla T') + Q' + m') - (\overline{\mathbf{u}} \bullet \mathbf{M}' + \mathbf{u}' \bullet \overline{\mathbf{M}})$$

$$\frac{\partial Y_s'}{\partial t} + \overline{\mathbf{u}} \bullet \nabla Y_s' + \mathbf{u}' \bullet \nabla \overline{Y}_s = \frac{1}{\overline{\rho}}\nabla \bullet (\overline{\rho}\mathcal{D}_s \nabla Y_s') + \frac{1}{\overline{\rho}}\dot{\omega}_s'$$

4.3   System equations

In the context of gas turbine applications it is physically well-justified for the computation of the eigenmodes to assume that :

- $\overline{\mathbf{u}} = 0$: low Mach number assumption [3]

- $\nabla \overline{p} = 0$: this is the typical case in a gas turbine combustion chamber [10]

- $M, m = 0$: we neglect the effects of dissipation in the eigenmodes [33]

Due to these three assumptions the acoustic system equations simplify to

$$\frac{\partial p'}{\partial t} + \gamma \overline{p} \nabla \bullet \mathbf{u}' = (\gamma - 1)(Q' + \nabla \bullet (\lambda \nabla T'))$$
$$\frac{\partial \mathbf{u}'}{\partial t} + \frac{1}{\overline{\rho}}\nabla p' = 0$$
$$\frac{\partial T'}{\partial t} + \mathbf{u}' \bullet \nabla \overline{T} + \frac{\gamma \overline{p}}{\overline{\rho}c_p}\nabla \bullet \mathbf{u}' = \frac{\gamma}{\overline{\rho}c_p}(Q' + \nabla \bullet (\lambda \nabla T'))$$
$$\overline{\rho}\frac{\partial Y_s'}{\partial t} + \overline{\rho}\mathbf{u}' \bullet \nabla \overline{Y}_s = \nabla \bullet (\overline{\rho}\mathcal{D}_s \nabla Y_s') + \dot{\omega}_s'$$

In the sequel the source term will be denoted with $S' := Q' + \nabla \bullet (\lambda \nabla T')$.
Since all these equations are linear we assume a harmonic behaviour of the instationary variables and separate the time dependence out as

$$\boxed{\psi(x,t) = \hat{\psi}(x)e^{-i\omega t}} \tag{100}$$

The function $\hat{\psi}(x)$ is implicitly a function of ω. Yet this is considered a parametric dependence and is suppressed. Using a Fourier-synthesis over frequency of these time-independent solutions $\hat{\psi}(x)$, it is possible to recover the full time-dependent solution $\psi(x,t)$.

For all instationary variables we consider harmonic oscillations at frequency $f := \frac{\omega}{2\pi}$

$$p'(x,t) = \Re(\hat{p}(x)e^{-i\omega t}) \tag{101}$$

$$\mathbf{u}'(x,t) = \Re(\hat{\mathbf{u}}(x)e^{-i\omega t}) \tag{102}$$

$$T'(x,t) = \Re(\hat{T}(x)e^{-i\omega t}) \tag{103}$$

$$Y'_s(x,t) = \Re(\hat{Y}_s(x)e^{-i\omega t}) \tag{104}$$

$$S'(x,t) = \Re(\hat{S}(x)e^{-i\omega t}) \tag{105}$$

Definition : We define the Fourier transform $\mathcal{F}$ of a function $y = \varphi(x,t)$ by

$$\mathcal{F}[\varphi(x,t)] = \hat{\varphi}(x,\omega) = \frac{1}{\sqrt{2\pi}} \int_{-\infty}^{\infty} \varphi(x,t)e^{i\omega t}dt \tag{106}$$

Further, the inverse transform is defined by

$$\mathcal{F}^{-1}[\hat{\varphi}(x,\omega)] = f(t) = \frac{1}{\sqrt{2\pi}} \int_{-\infty}^{\infty} \hat{\varphi}(x,\omega)e^{-i\omega t}d\omega \tag{107}$$

Then, the following rules hold for the Fourier transform

$$\mathcal{F}[a\varphi(x,t) + b\psi(x,t)] = a\mathcal{F}[\varphi(x,t)] + b\mathcal{F}[\psi(x,t)]$$

$$\mathcal{F}[\varphi^{(n)}(x,t)] = (-i\omega)^n \mathcal{F}[\varphi(x,t)] \tag{108}$$

Applying a Fourier transform is equivalent to inserting the harmonic ansatz in the acoustic system equations and it yields

$$-i\omega\hat{p} + \gamma\overline{p}\nabla \bullet \hat{\mathbf{u}} = (\gamma - 1)\hat{S}$$

$$-i\omega\hat{\mathbf{u}} + \frac{1}{\overline{\rho}}\nabla\hat{p} = 0$$

$$-i\omega\hat{T} + \hat{\mathbf{u}} \bullet \nabla\overline{T} + \frac{\gamma\overline{p}}{\overline{\rho}c_p}\nabla \bullet \hat{\mathbf{u}} = \frac{\gamma}{\overline{\rho}c_p}\hat{S}$$

$$-i\omega\overline{\rho}\hat{Y}_s + \overline{\rho}\hat{\mathbf{u}} \bullet \nabla\overline{Y}_s = \nabla \bullet (\overline{\rho}\mathcal{D}_s\nabla\hat{Y}_s) + \hat{\dot{\omega}}_s$$

Combining these partial differential equations, we obtain an explicit relation between the velocity and the gradient of pressure and eliminate the velocity mode shape from the remaining equations.

$$\boxed{\begin{aligned} \nabla \bullet (c^2\nabla\hat{p}) + \omega^2\hat{p} &= (\gamma - 1)i\omega\hat{S} \\ i\omega\overline{\rho}\hat{\mathbf{u}} &= \nabla\hat{p} \\ \omega^2\overline{\rho}c_p\hat{T} + c_p\nabla\overline{T} \bullet \nabla\hat{p} &= i\omega\hat{S} + \omega^2\hat{p} \\ \omega^2\overline{\rho}\hat{Y}_s + \nabla\overline{Y}_s \bullet \nabla\hat{p} &= i\omega\nabla \bullet (\overline{\rho}\mathcal{D}_s\nabla\hat{Y}_s) + i\omega\hat{\dot{\omega}}_s \end{aligned}}$$

These partial differential equations are given in the frequency domain and describe the coupling between acoustic pressure, velocity, temperature as well as the chemical species which account for the heat release. To complete these equations, one needs to specify the boundary conditions applied to the system. In fact these play a major role in determining the mode shapes. In the next section we present the different boundary conditions that could be applied to the system in real-world applications [2, 28].

4.4   Boundary conditions

For the boundary conditions the flow variables of interest are the acoustic pressure and the acoustic velocity. In theory it is possible to have some boundary conditions for the acoustic temperature and species which are different from the homogeneous Dirichlet conditions. However this does not appear in practical applications. Hence we focus on the four boundary conditions on acoustic pressure or velocity that are of particular interest for gas turbines.

4.4.1   Zero normal velocity

This condition is used in the case of fully rigid walls or of reflecting inlets where the velocity of the flow is imposed. Hence the outer normal component of the acoustic velocity is set to zero.

$$\boxed{\mathbf{u'} \bullet \mathbf{n} = 0} \tag{109}$$

Due to the relation,

$$\hat{\mathbf{u}} = \frac{1}{i\omega\bar{\rho}}\nabla\hat{p} \tag{110}$$

it becomes clear that expressed in the frequency domain, this condition corresponds to a Neumann boundary condition on the modes of the acoustic pressure:

$$\boxed{\nabla\hat{p} \bullet \mathbf{n} = 0} \tag{111}$$

Let Γ_N be the part of the boundary $\partial\Omega$ on which we impose this condition. Noteworthy is that there is no phase change in the pressure waves at Γ_N.

4.4.2   Imposed pressure

This condition is suited for open walls or fully reflecting outlets, i.e. outlets where the pressure is imposed to the flow. In this case, the pressure perturbations have to be zero. Therefore it corresponds to a Dirichlet boundary condition on the pressure fluctuations. Let Γ_D be the part of the boundary $\partial\Omega$ where we impose

$$\boxed{p'|_{\Gamma_D} = 0} \tag{112}$$

In the frequency domain, this boundary condition is still of Dirichlet type for the acoustic pressure modes p. In this case, the phase change in the pressure waves at the boundary is π.

4.4.3   Interface boundary condition

At an interface, a hyperplane of equation $H(\vec{\xi}) = 0$, separating two media M_1 and M_2 of different density ρ_1, ρ_2 and wave speed c_1, c_2, we impose the continuity of the pressure fluctuations as well as the continuity of the normal component of velocity

$$\begin{cases} \hat{p}(\vec{\xi}^-) &= \hat{p}(\vec{\xi}^+) \\ \hat{\mathbf{u}}(\vec{\xi}^-) \bullet \mathbf{n} &= \hat{\mathbf{u}}(\vec{\xi}^+) \bullet \mathbf{n} \end{cases} \tag{113}$$

where **n** is a normal to the interface. For a one-dimensional wave these conditions are equivalent to

$$\begin{cases} \hat{p}(\xi^-) &=& \hat{p}(\xi^+) \\ \frac{1}{\rho_1 c_1}\frac{\partial \hat{p}(\xi^-)}{\partial x} &=& \frac{1}{\rho_2 c_2}\frac{\partial \hat{p}(\xi^+)}{\partial x} \end{cases} \tag{114}$$

4.4.4   Impedance boundary condition

In acoustics the reflection and transmission properties of interfaces and walls are characterized by their impedance coefficient Z which relates the pressure to the normal velocity component in the frequency-domain

$$\boxed{Z = \frac{\hat{p}}{\hat{\mathbf{u}} \bullet \mathbf{n}}} \tag{115}$$

We interpret this condition as a linear combination of a Dirichlet and a Neumann boundary conditions. In fact the previous equation is equivalent to

$$Z(\nabla \hat{p} \bullet \mathbf{n}) - i\omega \bar{\rho}\hat{p} = 0 \tag{116}$$

Using the reduced impedance z defined by the following expression

$$z = \frac{Z}{\rho c} \tag{117}$$

we may rewrite the impedance boundary condition as

$$z(\nabla \hat{p} \bullet \mathbf{n}) - i\frac{\omega}{c}\hat{p} = 0 \tag{118}$$

There is a physical interpretation of the impedance boundary condition. In fact the impedance coefficient Z is usually a frequency-dependent complex number

$$Z(\omega) = \varrho(\omega) + i\varsigma(\omega), \ \text{with} \ \varrho, \varsigma \in \mathbb{R} \tag{119}$$

where $\varrho(\omega)$ and $\varsigma(\omega)$ denote respectively the frequency-dependent resistance and reactance.
The resistive part ϱ represents the various loss mechanisms an acoustic wave experiences. Resistive effects remove energy from the wave and convert it into other forms. This energy is then irreversibly lost from the system.
The reactive part ς represents the ability of the boundary to store the kinetic energy of the wave as potential energy. For example, air is a compressible medium and stores kinetic energy by compression and rarefaction. The electrical analogy for this is the capacitor's ability to store or release electric energy. By reactive effects, energy is not lost from the system but converted between kinetic and potential forms.

Part III

Modes of the thermo-acoustic system

5 Homogeneous Helmholtz equation

By neglecting the combustion source terms we get a purely acoustic system where the pressure mode shapes satisfy the homogeneous Helmholtz equation

$$\boxed{\nabla \bullet (c^2 \nabla \hat{p}) + \omega^2 \hat{p} = 0} \tag{120}$$

In this system the presence of the flame is still taken into account by the steady-state field of density, sound speed and temperature. However the unsteady flame interaction with the acoustic variables is not taken into account.

In this case the temperature modes are obtained by a linear combination of $\hat{p}$ and $\nabla \hat{p}$

$$\hat{T} = \frac{1}{\overline{\rho} c_p} \hat{p} - \frac{1}{\overline{\rho} \omega^2} \nabla \overline{T} \bullet \nabla \hat{p} \tag{121}$$

or equivalently a linear combination of $\hat{p}$ and $\hat{\mathbf{u}}$

$$\hat{T} = \frac{1}{\overline{\rho} c_p} \hat{p} + \frac{1}{i\omega} \nabla \overline{T} \bullet \hat{\mathbf{u}} \tag{122}$$

It is possible to further simplify the system by neglecting the presence of the flame and assuming a spatially-constant sound speed. As a consequence the pressure modes will depend only from the geometry of the combustion chamber. The elliptic operator simplifies to the Laplacian and we recover the standard form of the Helmholtz equation with the wave number $k := \frac{\omega}{c}$

$$\boxed{\Delta \hat{p} + k^2 \hat{p} = 0} \tag{123}$$

We want to compute the eigenmodes of this system by considering different combinations of boundary conditions. To simplify the notation we consider in a first step the one-dimensional case.

5.1 Eigenmodes of the 1D Helmholtz equation

We are interested in the mode shapes of a one-dimensional tube of length L denoted $\Omega = [0, L]$. The mode shapes are the solutions of the following Helmholtz equation

$$\hat{p}'' + k^2 \hat{p} = 0 \tag{124}$$

Hence the acoustic modes represent the eigenfunctions of the second-order spatial derivative ∂_{xx}^2. The analytic solution for the eigenfunctions is provided by the following ansatz

$$\hat{p}(x) = A e^{ikx} + B e^{-ikx} \tag{125}$$

Its spatial derivatives take the form

$$\hat{p}'(x) = ik(Ae^{ikx} - Be^{-ikx}) \tag{126}$$

$$\hat{p}''(x) = -k^2(Ae^{ikx} + Be^{-ikx}) = -k^2\hat{p}(x) \tag{127}$$

The solution is the triplet consisting in the wave number k and the coefficients A and B. To each wave number we find pairs of coefficients A and B which are equal up to a multiplicative constant. The solution is determined through the boundary conditions and through the geometry which is in the one-dimensional case through the length of the domain.

Example: we consider a one-dimensional tube $[0, L]$ with the following boundary conditions :

- a Neumann boundary condition at the inlet

$$\hat{p}'(0) = 0 \tag{128}$$

- a Dirichlet boundary condition at the outlet

$$\hat{p}(L) = 0 \tag{129}$$

These two requirements are equivalent to

$$A = B \ \ \& \ \ e^{i2kL} + 1 = 0 \tag{130}$$

The wave numbers k which satisfy this condition are given by

$$k = \left(j + \frac{1}{2}\right)\frac{\pi}{L}, \quad j \in \mathbb{N} \tag{131}$$

The corresponding eigenmodes are then

$$\hat{p}_j(x) = \cos\left(\left(j + \frac{1}{2}\right)\frac{\pi}{L}x\right), \quad j \in \mathbb{N} \tag{132}$$
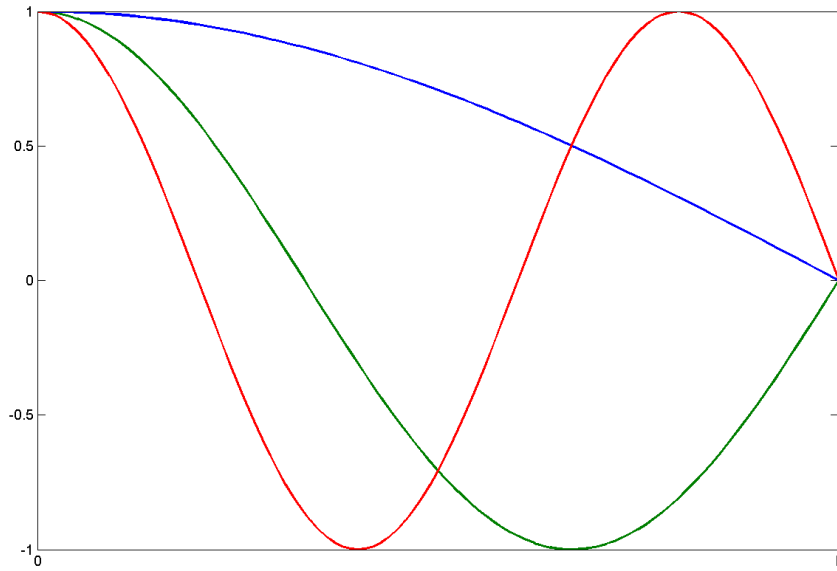
Figure 7: First three eigenmodes corresponding to $j = 0$ (blue), $j = 1$ (green), $j = 2$ (red)

The most general case is provided by impedance boundary conditions at both ends

$$z_0 \hat{p}'(0) + ik\hat{p}(0) = 0 \quad \& \quad z_L \hat{p}'(L) - ik\hat{p}(L) = 0 \tag{133}$$

To get non-trivial solutions we require that $z \neq 1$, which means that we have a domain of finite length and hence exclude transparent boundary conditions. The coefficients A and B are related through the relation

$$(A + B) + z_0(A - B) = 0 \tag{134}$$

and the wave numbers k are solutions of

$$\boxed{e^{i2kL} = \frac{1 + z_0}{1 - z_0}\frac{1 + z_L}{1 - z_L}} \tag{135}$$

5.2   Eigenmodes of the 3D Helmholtz equation

The extension of these results to the three-dimensional case is possible. The wave number $\mathbf{k}$ is in this case a vector in $\mathbb{R}^3$

$$\mathbf{k} = (k_x \quad k_y \quad k_z)^t \quad \in \mathbb{R}^3 \tag{136}$$

We make the following ansatz for the eigenmodes $\hat{p}$

$$\hat{p}(x, y, z) = \psi_x(x)\psi_y(y)\psi_z(z) \tag{137}$$

Inserting this ansatz in the Helmholtz equation

$$\Delta\hat{p} + \mathbf{k}^2\hat{p} = 0 \tag{138}$$

yields the following relation

$$\psi_x'' \psi_y \psi_z + \psi_x \psi_y'' \psi_z + \psi_x \psi_y \psi_z'' + (k_x^2 + k_y^2 + k_z^2) \psi_x \psi_y \psi_z = 0 \tag{139}$$

Dividing this equation by $\hat{p}$ yields

$$\frac{\psi_x''}{\psi_x} + \frac{\psi_y''}{\psi_y} + \frac{\psi_z''}{\psi_z} + k_x^2 + k_y^2 + k_z^2 = 0 \tag{140}$$

By splitting this relation into three equations with appropriate boundary conditions, we reduce this three dimensional problem into three independent one-dimensional problems and solve them as shown in the previous section. We illustrate the procedure through the following case.

Example : let us consider the computational domain $\Omega = [0, L_x] \times [0, L_y] \times [0, L_z]$ with

- Neumann and Dirichlet boundary conditions on the $x-$axis :

$$\left. \frac{\partial \hat{p}}{\partial x} \right|_{x=0} = 0 \ \ \& \ \ \hat{p}(L_x, y, z) = 0 \quad \forall \ y, z \tag{141}$$

- Neumann boundary conditions on the $y-$axis :

$$\left. \frac{\partial \hat{p}}{\partial y} \right|_{y=0} = 0 \ \ \& \ \ \left. \frac{\partial \hat{p}}{\partial y} \right|_{y=L_y} = 0 \tag{142}$$

- Neumann and impedance boundary conditions on the $z-$axis :

$$\left. \frac{\partial \hat{p}}{\partial z} \right|_{z=0} = 0 \ \ \& \ \ i\sqrt{\gamma \bar{p} \bar{\rho}} \left. \frac{\partial \hat{p}}{\partial z} \right|_{z=L_z} + \hat{p}(x, y, L_z) = 0 \quad \forall \ x, y \tag{143}$$

The solutions for the wave numbers k_x, k_y and k_z are

$$k_x = \left(j + \frac{1}{2} \right) \frac{\pi}{L},$$
$$k_y = j \frac{\pi}{L},$$
$$k_z = \left(j + \frac{1}{4} \right) \frac{\pi}{L}$$

The eigenfunctions corresponding to these eigenvalues have to satisfy the boundary conditions and are given by

$$\psi_x(x) = \cos\left(\left(j + \frac{1}{2} \right) \pi \frac{x}{L_x} \right)$$
$$\psi_y(y) = \cos\left(j\pi \frac{y}{L_y} \right),$$
$$\psi_z(z) = \cos\left(\left(j + \frac{1}{4} \right) \pi \frac{z}{L_z} \right)$$

Hence the eigenmodes for the three-dimensional problem read

$$\hat{p}_j(x, y, z) = \cos\left(\left(j + \frac{1}{2}\right)\pi\frac{x}{L_x}\right) \cdot \cos\left(j\pi\frac{y}{L_y}\right) \cdot \cos\left(\left(j + \frac{1}{4}\right)\pi\frac{z}{L_z}\right), \quad j \in \mathbb{N} \tag{144}$$

Since the Helmholtz equation is linear in $\hat{p}$, the full solution of is obtained by a linear combination of the functions $\hat{p}_j$.

Remark : If any or all of sides of the box tends to infinity, the eigenvalues, i.e. the wave numbers, bunch up and the eigenspectrum becomes continuous.

5.3   Orthogonality properties of the eigenmodes

Lemma : We consider the homogeneous Helmholtz equation

$$\nabla \bullet (c^2\nabla\hat{p}) + \omega^2\hat{p} = 0 \tag{145}$$

defined on Ω with the following boundary conditions on $\partial\Omega = \Gamma_D \cup \Gamma_N \cup \Gamma_F$:

$$\text{on the Dirichlet boundary } \Gamma_{\mathrm{D}} \; : \quad \hat{p} = 0 \tag{146}$$
$$\text{on the Neumann boundary } \Gamma_{\mathrm{N}} \; : \quad \nabla\hat{p} \bullet \mathbf{n} = 0 \tag{147}$$
$$\text{on the impedance boundary } \Gamma_{\mathrm{F}} \; : \quad Z(\omega)(\nabla\hat{p} \bullet \mathbf{n}) + i\omega\bar{\rho}\hat{p} = 0 \tag{148}$$

Provided that

$$\Gamma_F = \emptyset \tag{149}$$

or

$$\exists\, \mathcal{C} : \Gamma_F \to \mathbb{R} \;\; \text{such that} \;\; Z(x, \omega) = i\mathcal{C}(x)\omega \quad \forall x \in \Gamma_F \tag{150}$$

then the set of eigenmodes is orthogonal.

Proof :   Let (p_m, ω_m) and (p_n, ω_n) be two distinct eigenpairs of the Helmholtz equation defined on Ω with boundary $\partial\Omega = \Gamma_D \cup \Gamma_N \cup \Gamma_F$. Then, we have

$$
\begin{aligned}
\omega_m^2 \int_\Omega p_m p_n^* dV \;\; &= \;\; -\int_\Omega \nabla \bullet (c^2\nabla p_m)p_n^* dV \tag{151}\\
&= \;\; \int_\Omega c^2(\nabla p_m \bullet \nabla p_n^*)dV - \int_{\partial\Omega} c^2 p_n^*(\nabla p_m \bullet \mathbf{n})ds \\
&= \;\; -\int_\Omega p_m\nabla \bullet (c^2\nabla p_n^*)dV + \int_{\partial\Omega} c^2 p_m(\nabla p_n^* \bullet \mathbf{n}) - c^2 p_n^*(\nabla p_m \bullet \mathbf{n})ds \\
&= \;\; \omega_n^{*2} \int_\Omega p_m p_n^* dV + \int_{\partial\Omega} c^2 p_m(\nabla p_n^* \bullet \mathbf{n}) - c^2 p_n^*(\nabla p_m \bullet \mathbf{n})ds \tag{152}
\end{aligned}
$$

This equation is equivalent to

$$(\omega_m^2 - \omega_n^{*2})\int_\Omega p_m p_n^* dV = \int_{\partial\Omega} c^2 p_m(\nabla p_n^* \bullet \mathbf{n}) - c^2 p_n^*(\nabla p_m \bullet \mathbf{n})ds \tag{153}$$

If the boundary conditions are of homogeneous Dirichlet or Neumann type only, i.e. $\partial\Omega = \Gamma_D \cup \Gamma_N$, it is clear that the right-hand side of the previous equation is zero because

$$\text{on } \Gamma_D \cup \Gamma_N : p_i(\nabla p_j^* \bullet \mathbf{n}) = 0 \quad \text{for } \{i,j\} \subset \{m,n\} \tag{154}$$

This means that if $\partial\Omega = \Gamma_D \cup \Gamma_N$ then the eigenmodes of the Helmholtz equations are orthogonal. However, in the presence of impedance boundary conditions,

$$Z(\omega_k)(\nabla p_k \bullet \mathbf{n}) + i\omega_k \bar{\rho} p_k = 0 \tag{155}$$

the right-hand side of the previous equation is not zero anymore and takes the form

$$(\omega_m^2 - \omega_n^{*2}) \int_\Omega p_m p_n^* dV \;\; = \;\; \int_{\Gamma_F} \left(\frac{i\omega_n^*}{Z^*(\omega_n)} + \frac{i\omega_m}{Z(\omega_m)} \right) \bar{\rho} c^2 p_m p_n^* ds \tag{156}$$

In the presence of impedance boundary conditions, the eigenmodes p_m and p_n are orthogonal if

$$\frac{\omega_m}{Z(\omega_m)} + \frac{\omega_n^*}{Z^*(\omega_n)} = 0 \text{ on } \Gamma_F \tag{157}$$

The necessary condition for all eigenmodes to be orthogonal is that there exists a real-valued function $\mathcal{C} : \Gamma_F \to \mathbb{R}$ such that for all eigenfrequencies ω

$$Z(x,\omega) = i\mathcal{C}(x)\omega \quad \forall x \in \Gamma_F \tag{158}$$

∎

6 Acoustic eigenmodes in 1D

Our objective is the study of the propagation of acoustic waves in a one-dimensional domain, e.g. a tube of length L denoted $\Omega = [0, L]$. Assume that an acoustic energy source is placed at the tube inlet. The acoustic waves produced by such a source travel through the tube until they reach the other end. Depending on the outlet configuration, some part of the waves is transmitted throug the boundary while the remaining part reflects back into tho tube in form of traveling acoustic waves. These reflected waves interact with the incoming waves to produce *standing* or *stationary waves*.
To investigate this phenomenon, we will assume in a first step that the density ρ as well as the sound speed c are constant along Ω. In a second step, we consider that Ω consists of two neighboring media M_1 and M_2 having different density and sound speed.

6.1 Homogeneous medium

Without loss of generality we take as a computational domain $\Omega = [0, L]$. We assume that the domain is homogeneous and that the density ρ and the sound speed c are constant in Ω.

In the absence of source terms the acoustic pressure $p'(x,t)$ and the acoustic velocity $u'(x,t)$ satisfy

$$\frac{\partial p'}{\partial t} + \rho c^2 \frac{\partial u'}{\partial x} = 0 \tag{159}$$

$$\rho \frac{\partial u'}{\partial t} + \frac{\partial p'}{\partial x} = 0 \tag{160}$$

By combining these two equations we note that the wave equation is simultaneously verified by the acoustic pressure and velocity

$$\frac{\partial^2 p'}{\partial t^2} - c^2 \frac{\partial^2 p'}{\partial x^2} = 0 \tag{161}$$

$$\frac{\partial^2 u'}{\partial t^2} - c^2 \frac{\partial^2 u'}{\partial x^2} = 0 \tag{162}$$

To solve these equations we introduce the variables ξ and η defined by

$$\xi = x + ct, \eta = x - ct \tag{163}$$

By applying the chain rule in the acoustic pressure equation (161), we obtain

$$\frac{\partial^2 p'}{\partial \xi \partial \eta} = 0 \tag{164}$$

which means that p' is the sum of two functions f and g depending respectively from ξ and η :

$$p'(x,t) = f(\xi) + g(\eta) = f(x + ct) + g(x - ct) \tag{165}$$

The physical interpretation of this result is that the acoustic pressure is a superposition of a left- and a right-traveling wave with constant wave speed c. The same applies for the acoustic velocity u'.

Moreover, we introduce the wave number k and wave frequency ω related to the wave speed by the relation

$$c = \frac{\omega}{k} \tag{166}$$

It is then easy to show that for all eigenvalues k_j of the Helmholtz equation

$$\Delta \hat{p}_j + k_j^2 \hat{p}_j = 0 \tag{167}$$

the pressure and velocity terms, $p_j^\pm$ and $u_j^\pm$, defined by

$$p_j^\pm(x,t) = e^{i(-\omega_j t \pm k_j x)} \tag{168}$$

$$u_j^\pm(x,t) = \frac{1}{\rho c} e^{i(-\omega_j t \pm k_j x)} \tag{169}$$

are solutions of the wave equation.

Due to the linearity of the problem (161,162) the acoustic pressure p' and velocity u' take the form

$$p'(x,t) = p^+(x,t) + p^-(x,t) \tag{170}$$

$$= \sum_j A_j^+ e^{i(-\omega_j t + k_j x)} + \sum_j A_j^- e^{i(-\omega_j t - k_j x)} \tag{171}$$

$$u'(x,t) = u^+(x,t) - u^-(x,t) \tag{172}$$

$$= \frac{1}{\rho c} \sum_j A_j^+ e^{i(-\omega_j t + k_j x)} - \frac{1}{\rho c} \sum_j A_j^- e^{i(-\omega_j t - k_j x)} \tag{173}$$

where A_j^+ and A_j^- are resp. the amplitude of the right- and left-running wave with frequency ω_j.

6.2   Two neighboring media

In this section we assume that Ω consists of two neighboring media $M_1 = \{x \leq \xi\}$ and $M_2 = \{\xi < x\}$. The interface is located at $x = \xi$. Each of the media M_1 and M_2 has its own density ρ_j and wave speed c_j and hence its own acoustic impedance $Z_j = \rho_j c_j, j \in \{1, 2\}$.
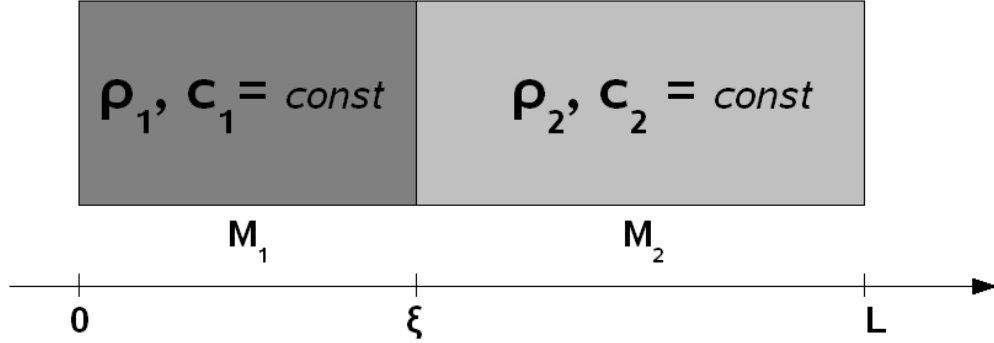
Figure 8: The domain Ω consists of two homogeneous media M_1 and M_2

We solve this problem by considering each domain apart and use the analogy of the first case. On M_j the acoustic pressure and velocity satisfy the wave equation

$$\frac{\partial^2 p'_j}{\partial t^2} - c_j^2 \frac{\partial^2 p'_j}{\partial x^2} = 0 \tag{174}$$

$$\frac{\partial^2 u'_j}{\partial t^2} - c_j^2 \frac{\partial^2 u'_j}{\partial x^2} = 0 \tag{175}$$

The continuity of the acoustic pressure and normal velocity at the interface reads

$$\begin{cases} p_1^+(\xi, t) + p_1^-(\xi, t) = p_2^+(\xi, t) + p_2^-(\xi, t) \\ \frac{1}{Z_1}\left[p_1^+(\xi, t) - p_1^-(\xi, t)\right] = \frac{1}{Z_2}\left[p_2^+(\xi, t) - p_2^-(\xi, t)\right] \end{cases} \tag{176}$$

In matrix form the interface condition is written as

$$\begin{pmatrix} 1 & -1 \\ \frac{1}{Z_1} & \frac{1}{Z_2} \end{pmatrix} \begin{pmatrix} p_1^-(\xi, t) \\ p_2^+(\xi, t) \end{pmatrix} = \begin{pmatrix} -1 & 1 \\ \frac{1}{Z_1} & \frac{1}{Z_2} \end{pmatrix} \begin{pmatrix} p_1^+(\xi, t) \\ p_2^-(\xi, t) \end{pmatrix} \tag{177}$$

Since the characteristic impedances $Z_1 = \rho_1 c_1$ and $Z_2 = \rho_2 c_2$ are strictly positive we may invert the matrix on the right-hand side and obtain the following system

$$\begin{pmatrix} p_1^-(\xi, t) \\ p_2^+(\xi, t) \end{pmatrix} = \frac{1}{Z_2 + Z_1} \begin{pmatrix} Z_2 - Z_1 & 2Z_1 \\ 2Z_2 & Z_1 - Z_2 \end{pmatrix} \begin{pmatrix} p_1^+(\xi, t) \\ p_2^-(\xi, t) \end{pmatrix} \tag{178}$$

The wave traveling from M_1 into M_2, called incident wave w^i, is not totally transmitted to the neighbor domain. In fact, depending on the reduced impedance $\frac{Z_2}{Z_1}$, a portion w^t of the incident wave

is transmitted through the interface into the second medium whereas the remaining part w^r is reflected back into the first one.
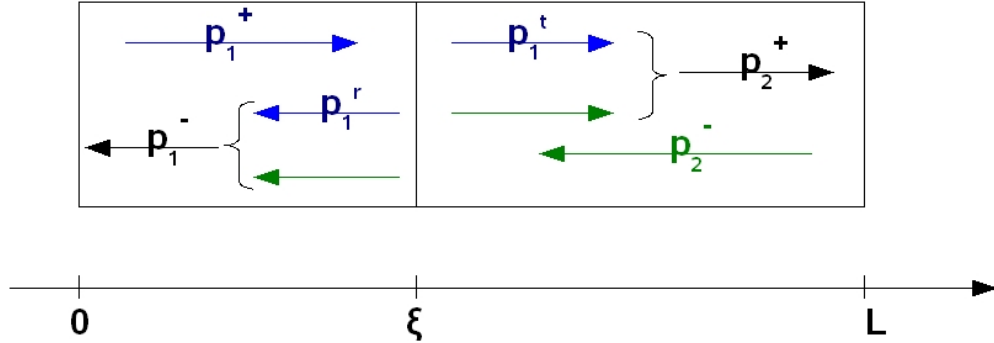
Figure 9: Reflected and transmitted wave at the interface

Hence we have at the interface $\{x = \xi\}$ between M_1 and M_2 that

$$p_1^-(\xi, t) = \underbrace{\frac{Z_2 - Z_1}{Z_2 + Z_1} p_1^+(\xi, t)}_{p_1^r(\xi, t)} + \underbrace{\frac{2Z_1}{Z_2 + Z_1} p_2^-(\xi, t)}_{p_2^t(\xi, t)} \tag{179}$$

This enables us to define the reflection factor at the interface, denoted R, which is the ratio of the amplitude of the reflected wave to the incident amplitude

$$R := \frac{p_1^r(\xi, t)}{p_1^+(\xi, t)} = \frac{Z_2 - Z_1}{Z_2 + Z_1} \tag{180}$$

Similarly we define the transmission factor T (from M_2 into M_1) which is given by the ratio of the amplitude of the transmitted wave to the amplitude of the incident one

$$T_{2 \to 1} := \frac{p_2^t(\xi, t)}{p_2^-(\xi, t)} = \frac{2Z_1}{Z_2 + Z_1} \tag{181}$$

The relations between right-running and left-running waves at the interface are summarized in the following equation

$$\begin{pmatrix} p_1^-(\xi, t) \\ p_2^+(\xi, t) \end{pmatrix} = \begin{pmatrix} R & T_{2 \to 1} \\ T_{1 \to 2} & -R \end{pmatrix} \begin{pmatrix} p_1^+(\xi, t) \\ p_2^-(\xi, t) \end{pmatrix} \tag{182}$$

Three cases are particularly noteworthy :

- in the limit case $\left| \frac{Z_2}{Z_1} \right| \to \infty$, the impedance boundary condition is equivalent to the Neumann boundary condition : the incident wave is identically reflected at the rigid wall ($R = 1$ and $T = 0$),

- whereas in the case $\frac{Z_2}{Z_1} \to 0$, the impedance boundary condition reduces to the Dirichlet boundary condition. We hence have a reflecting wall ($R = -1$ and $T = 2$) : the incident wave is fully reflected but with a sign change.

- In the case of an impedance match, i.e. $\frac{Z_2}{Z_1} = 1$, then there is no reflection ($R = 0$) and the waves are transmitted identically ($T = 1$) as it is the case for perfectly matched layers (PML).

These results are summarized in the following table

boundary condition	mathematical expression	reduced impedance $\frac{Z_2}{Z_1}$	reflection factor R	transmission factor T	Example
Dirichlet	$\hat{p} = 0$	0	-1	2	open wall
Impedance match	$\nabla \hat{p} \bullet \mathbf{n} - ik\hat{p} = 0$	1	0	1	PML
Neumann	$\nabla \hat{p} \bullet \mathbf{n} = 0$	∞	1	0	rigid wall

6.3   Case studies

6.3.1   Rigid-wall inlet and open-wall outlet

We consider a rigid wall at the inlet and an open wall at the outlet (equivalent to a fully reflecting outlet). We would like to find the pulsation number ω of the acoustic modes in this duct.
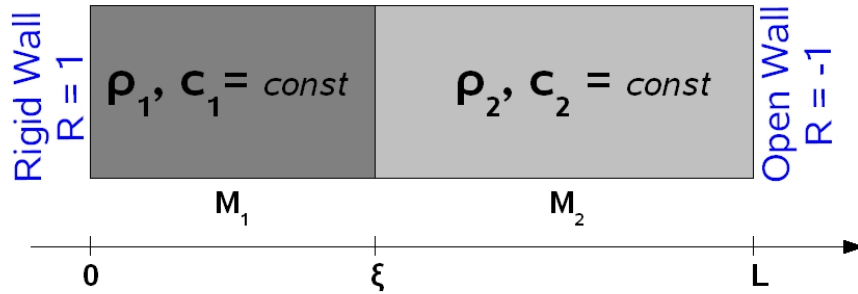
Figure 10: Rigid wall at inlet and open wall at outlet

Acoustic modes on M_1

The pressure modes of the subdomain M_1 satisfy

$$p_1'(x,t) = A_1^+ e^{i(k_1 x - \omega t)} + A_1^- e^{i(-k_1 x - \omega t)} \tag{183}$$

The **Neumann boundary condition** at the inlet is

$$\frac{\partial p_1'}{\partial n}\Big|_{x=0} = 0 \tag{184}$$

Hence the reflection factor R_1 is 1, which means that the amplitudes A_1^+ and A_1^- of the incident and reflected waves are equal. Consequently the pressure and velocity modes take the form

$$\hat{p}_1(x) \;=\; 2A_1^+ \cos(k_1 x) \tag{185}$$

$$\hat{u}_1(x) \;=\; 2i\frac{A_1^+}{\rho_1 c_1}\sin(k_1 x) \tag{186}$$

Acoustic modes on M_2
On M_2 the pressure modes are given by

$$p_2'(x,t) = A_2^+ e^{i(k_2(x-L)-\omega t)} + A_2^- e^{i(-k_2(x-L)-\omega t)} \tag{187}$$

At the outlet we have the **Dirichlet boundary condition**

$$p_2'(L,t) = 0 \tag{188}$$

which implies for the reflection factor R_2

$$\frac{A_2^-}{A_2^+} = R_2 = -1 \tag{189}$$

Then the pressure and velocity modes are

$$\hat{p}_2(x) \;=\; 2iA_2^+ \sin(k_2(x-L)) \tag{190}$$

$$\hat{u}_2(x) \;=\; 2\frac{A_2^+}{\rho_2 c_2}\cos(k_2(x-L)) \tag{191}$$

Continuity conditions and pulsation number
The continuity of the acoustic pressure and normal velocity at the interface $x = \xi$ reads

$$\begin{cases} A_1^+ \cos(\frac{\omega}{c_1}\xi) &=& iA_2^+ \sin(\frac{\omega}{c_2}(\xi - L)) \\ i\frac{A_1^+}{\rho_1 c_1}\sin(\frac{\omega}{c_1}\xi) &=& \frac{A_2^+}{\rho_2 c_2}\cos(\frac{\omega}{c_2}(\xi - L)) \end{cases} \tag{192}$$

The continuity conditions written in **matrix form** are

$$\begin{pmatrix} \cos(\frac{\omega}{c_1}\xi) & i\,\sin(\frac{\omega}{c_2}(L - \xi)) \\ \frac{i}{\rho_1 c_1}\sin(\frac{\omega}{c_1}\xi) & \frac{-1}{\rho_2 c_2}\cos(\frac{\omega}{c_2}(L - \xi)) \end{pmatrix} \begin{pmatrix} A_1^+ \\ A_2^+ \end{pmatrix} = \vec{0} \tag{193}$$

To get nontrivial solutions we require that the determinant of the matrix vanishes. Therefore we are interested in the pulsation numbers ω which make the matrix singular. The pulsation numbers are solutions of these equations

$$\boxed{sin\left(\frac{\omega}{c_2}(L - \xi)\right)\sin\left(\frac{\omega}{c_1}\xi\right) - \frac{\rho_1 c_1}{\rho_2 c_2}\cos\left(\frac{\omega}{c_1}\xi\right)\cos\left(\frac{\omega}{c_2}(L - \xi)\right) = 0} \tag{194}$$

6.3.2   Impedance wall at both ends

We consider a one-dimensional duct consisting of two parts having different density and sound speed. We assume impedance walls at left and right boundary . For the well-posedness of the problem, the domain has to be of finite dimension, which implies that we exclude the case of impedance match, i.e. $R \neq 0$ at both boundaries.
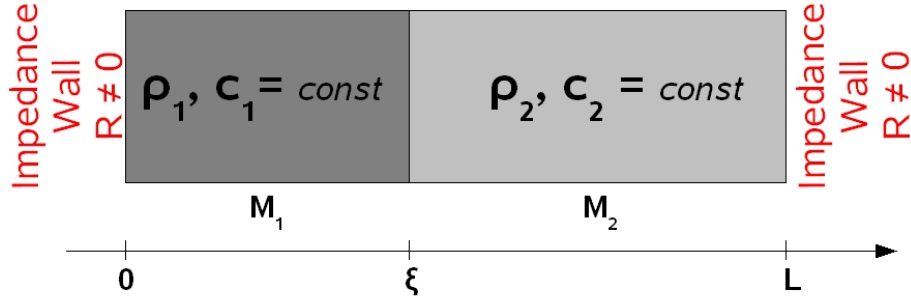
Figure 11: Impedance condition at both boundaries of Ω

Acoustic modes on M_1

The acoustic pressure is given by the general formula

$$p_1'(x,t) = A_1^+ e^{i(k_1 x - \omega t)} + A_1^- e^{i(-k_1 x - \omega t)} \tag{195}$$

At the inlet an **impedance boundary condition** is imposed

$$Z_0 \frac{\partial \hat{p}}{\partial n} |_{x=0} - i\omega \overline{\rho}_1 \hat{p}(0) = 0 \tag{196}$$

The amplitude of the reflected and the incident wave are related through the reflection factor R_0

$$\frac{A_1^+}{A_1^-} = R_0 = \frac{Z_0 - \rho_1 c_1}{Z_0 + \rho_1 c_1} \tag{197}$$

The pressure and velocity modes are then

$$\hat{p}_1(x) = A_1^- [R_0 \, e^{ik_1 x} + e^{-ik_1 x}] \tag{198}$$

$$\hat{u}_1(x) = \frac{A_1^-}{\rho_1 c_1} [R_0 \, e^{ik_1 x} - e^{-ik_1 x}] \tag{199}$$

Acoustic modes on M_2

On M_2 the acoustic pressure is given through

$$p_2'(x,t) = A_2^+ e^{i(k_2(x-L) - \omega t)} + A_2^- e^{i(-k_2(x-L) - \omega t)} \tag{200}$$

We impose an **impedance boundary condition** at the outlet

$$Z_L \frac{\partial \hat{p}}{\partial n} |_{x=L} - i\omega \overline{\rho}_2 \hat{p}(L) = 0 \tag{201}$$

The amplitude of the reflected wave is related to the incident wave through the reflection factor R_L

$$\frac{A_2^-}{A_2^+} = R_L = \frac{Z_L - \rho_2 c_2}{Z_L + \rho_2 c_2} \tag{202}$$

The pressure and velocity modes are then

$$\hat{p}_2(x) = A_2^+[e^{ik_2(x-L)} + R_L e^{-ik_2(x-L)}] \tag{203}$$

$$\hat{u}_2(x) = \frac{A_2^+}{\rho_2 c_2}[e^{ik_2(x-L)} - R_L e^{-ik_2(x-L)}] \tag{204}$$

Continuity conditions and pulsation number

Written in matrix form the continuity conditions at the interface $x = \xi$ read

$$\begin{pmatrix} R_0\,e^{ik_1\xi} + e^{-ik_1\xi} & e^{ik_2(\xi-L)} + R_L e^{-ik_2(\xi-L)} \\ \frac{1}{\rho_1 c_1}[R_0\,e^{ik_1\xi} - e^{-ik_1\xi}] & \frac{1}{\rho_2 c_2}[e^{ik_2(\xi-L)} - R_L e^{-ik_2(\xi-L)}] \end{pmatrix} \begin{pmatrix} A_1^- \\ A_2^+ \end{pmatrix} = \vec{0} \tag{205}$$

For non-trivial solutions the determinant of the matrix has to vanish. This implies the folllowing frequency equation

$$\boxed{\rho_1 c_1 (R_0\,e^{i\frac{\omega}{c_1}\xi} + e^{-i\frac{\omega}{c_1}\xi})(e^{i\frac{\omega}{c_2}(\xi-L)} - R_L\,e^{-i\frac{\omega}{c_2}(\xi-L)}) = \rho_2 c_2 (e^{i\frac{\omega}{c_2}(\xi-L)} + R_L\,e^{-i\frac{\omega}{c_2}(\xi-L)})(R_0\,e^{i\frac{\omega}{c_1}\xi} - e^{-i\frac{\omega}{c_1}\xi})}$$

6.4 General Case

In the previous subsections, we showed how to determine the eigenmodes of a duct consisting either of one homogeneous medium or of two media separated by an interface. However if we want to solve the problem of the eigenmodes for a more realistic case, we need a method to find these eigenmodes in a duct where there is an arbitrary evolution of $\rho(x), c(x)$ and $T(x)$.

The idea is to recursively divide the domain Ω into subintervals such that the flow variables can assumed to be constant in each subinterval. Hence solving the problem on Ω consists on applying the procedure described in the previous section to each pair of subintervals.

By dividing the interval Ω to N subintervals $M_1, .., M_N$, we get $2N$ wave amplitudes $\{A_i^+, A_i^-\}_{i=1,..,N}$ where A_i^+ and A_i^- are respectively the amplitudes of the right-running and left-running wave in the subinterval M_i. To obtain the acoustic modes of the system, which correspond to its standing waves, we require that all these $2N$ unknown amplitudes are different from zero.

To obtain a complete system of equations, we need to find $2N$ relations coupling these amplitudes. In the case of N subintervals there are $(N-1)$ interfaces which means $2(N-1)$ continuity conditions. The two boundary conditions, i.e. at inlet and outlet, provide the two remaining equations.

Remark : The subintervals do not need to be of the same size. Since the steady-state variables are known, the intervals can be adaptively refined or coarsened such that the evolution of the stationary flow variables is well resolved.

7 Combustion source terms

By neglecting the source terms in the previous section we reduced the complexity of the problem and could easily compute the mode shapes of the acoustic variables. However, these mode shapes are not accurate enough to yield a reliable assessment of the dynamics of the thermo-acoustic system since they do not take into account the unsteady effect of combustion [34]. For a better assessment of the dynamic behaviour of the system it is necessary to consider the coupling between unsteady flame and acoustics. In this section we will investigate the coupling between unsteady heat release and the acoustic variables [35].

7.1 Flame transfer functions

In order to eliminate the combustion oscillations, it is important to understand the fundamental mechanisms of the burner system. This guides the engineers at a very early stage on how to make a redesign of the critical components or to increase the acoustic damping at the appropriate locations, or even apply active control techniques to suppress the instability. To achieve this goal, it is necessary to identify the dynamics of the system by examination of the flame transfer function.
The analysis consists in considering the combustion chamber as a dynamical system apart, with the fluid dynamical properties of air and fuel inflow being its input variables. The output variables of interest for this dynamical system are the heat release rate, the outflow mixture fraction as well as the temperature. Generally, the system is linearized since the scope of the analysis is the determination of the growing and decaying modes when their amplitudes and rates of change are small. The analysis could be performed on discrete-time or continuous-time signals. In the last case, the flame transfer function can be described as the ratio of the Fourier transform of the output of the system, to the Fourier transform of its input variable. As an example of flame transfer function it is possible to consider the ratio of the unsteady heat release at a fixed position in the combustion chamber to the fluctuations in air inflow rate.

To determine the transfer function it is necessary to know the performance of the combustor in the time domain. By means of experiments the characteristics of several burner systems have been assessed. The response of the flames to different imposed acoustic perturbations have been measured and investigated.

Unfortunately, experimental sutdy of burner systems is not always feasible. Not only are they expensive and time-consuming but also prone to high pressure and high temperature rises which damage the hardware. Nowadays more and more studies are performed using numerical simulation and computational fluid dynamics. Simulation provides a flexible tool which is widely used to analyse the system dynamics at different operation points.
Bohn performed a numerical simulation of the burner system to determine the transfer function. After a steady-state solution is determined, the mass flow rate is changed suddenly. The frequency response to this disturbance represents the dynamic behavior of the flame. Dowling et al. [51] used

numerical simulation to calculate the unsteady flow in the combustor. Through calculations of the forced unsteady combustion resulting from the specified time-dependent variation in the fuel and air supplies, they identified the main source of the unsteady heat release. By forcing harmonically at a specified frequency, they determined the transfer function between the heat release rate and the air inflow rate. In a more recent paper, Zhu, Dowling and Bray investigated the transfer function through time-dependent simulations of the combustion process. They compared four different methods which are the use of harmonic forcing frequency, infinite impulse response, the random binary signal and the sum of sinusoidal signals. The transfer functions are determined as a function of the acoustic frequency.

In addition to numerical simulation, intensive research has been made using analytical techniques to obtain the transfer function. For Bunsen-type flames, the interaction with an acoustic field is studied analytically by Fleifil et al. in [23], where the flow field is described by a Poiseuille flow and the profile is assumed to be undistorted by the flame. The motion of the flame is determined by using the G-equation and a constant burning velocity.
Burner-stabilized flat flames have been thoroughly investigated in the works of Van Harten et al, Buckmaster and McIntosh and Clark [34]. Raun and Beckstead, McIntosh and Rylands used the flame/acoustic transfer functions to investigate Rijke tube oscillations. In [35] McIntosh studied flames that are anchored to a burner plate and pointed out that it is important to determine the the significant change in the phase of the velocity of the acoustic disturbance to identify the conditions of resonance. The change in velocity is governed by a velocity transfer function which depends on the type of flame and on the geometry used. In his study McIntosh exploits the largeness of the activation energy and the smallness of the Mach number to find an analytical expression for the transfer function. The analysis is based on the exact asymptotic solution of the governing equations with one-step chemistry and provides relations for the velocity fluctuations through the flame. Thus for any combination of flame and tube, a prediction of the change in velocity of the acoustic disturbance across the flame region can be made and an estimate given as to the growth or decay rate of a particular mode. Furthermore the developed theory might be applied to predict where the flame should sit in a constant length tube in order to cause the largest amplification of the flame noise. The obtained results indicate that the most significant growth always occurs when the flame is in the lower quadrant of the tube.

In a more recent paper, Rook and de Goey [44] studied numerically the interaction of burner-stabilized flat flame with acoustic waves. The study is restricted to the regime with low Mach numbers and relatively low frequencies. The flame model is based on flames with a rigid internal structure, in which the effect of reactions on acoustic distortions is determined by linearized quasi-steady relations. By comparing the numerical results, the authors concluded that the one-step model and the skeletal model predict a similar behavior for the acoustic response. Furthermore they pointed out that for an accurate prediction of the acoustic response of burner-stabilized flames at relatively low frequencies even a simple chemical reaction scheme is useful.

7.2 Relation between combustion and velocity

We consider a reactive gas flowing [20] across a one-dimensional duct of length L in which a flame is stabilized at $x = \xi$. The flame represents an interface between two sections M_1 and M_2.

On M_1, the part of the duct upstream the flame, the gas is cold and unburnt and has a sound speed $\bar{c}_1$, a temperature $\bar{T}_1$ and a density $\bar{\rho}_1$. Downstream the flame on M_2, the gas is hot and burnt and has a sound speed $\bar{c}_2$, a temperature $\bar{T}_2$ and a density $\bar{\rho}_2$ [19].
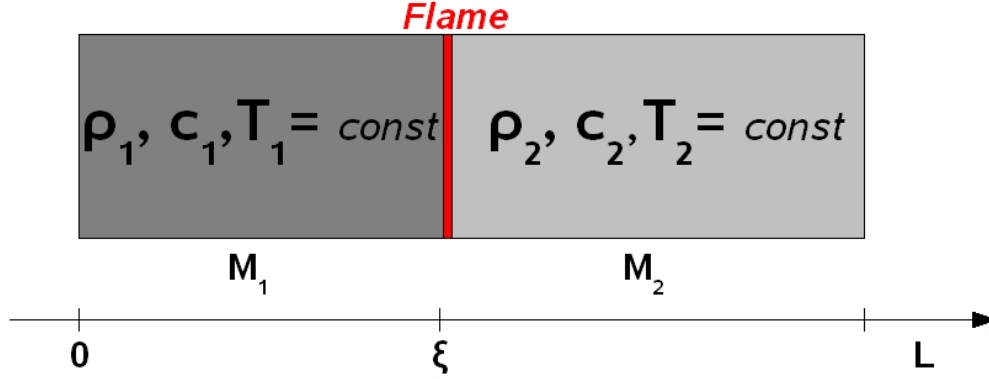
Figure 12: Flame zone represents the interface between unburnt and burnt gas

Therefore the mean variables $\bar{\rho}, \bar{c}$ and $\bar{T}$ are essentially constant along Ω except for a step change at the interface ξ. Therefore we may describe the mean variables through a Heaviside function $H(\,\cdot\,)$. In particular the mean temperature $\bar{T}$ takes the form

$$\overline{T}(x) = \overline{T}_1 + H(x - \xi)(\overline{T}_2 - \overline{T}_1) \tag{206}$$

and the continuity of steady mass flow is expressed through

$$\overline{\rho}_1 \overline{u}_1 = \overline{\rho}_2 \overline{u}_2 \tag{207}$$

Furthermore we assume the gas to be ideal and that the mean flow pressure $\bar{p}$ is constant along the duct

$$\overline{p} = \overline{\rho} \frac{\mathcal{R}}{W} \overline{T} \tag{208}$$

By combining these last two results we obtain a characteristic ratio which we denote Θ

$$\Theta := \frac{\overline{\rho}_1}{\overline{\rho}_2} = \frac{\overline{u}_2}{\overline{u}_1} = \frac{\overline{T}_2}{\overline{T}_1} > 1 \tag{209}$$

We assume the flame to be stabilized at $x = \xi$ and ignore the local boundary layer at the flame front. This means that the combustion process and the flame zone are spatially localized at the interface ξ

$$\boxed{Q'(x,t) = q'(t)\delta(x - \xi)} \tag{210}$$

where q' denotes the heat release rate per unit area and $\delta(\,\cdot\,)$ denotes the Dirac delta function. In this case the equations for unsteady density, velocity, temperature and pressure on M_j are given by

$$\frac{\partial \rho'_j}{\partial t} + \frac{\partial \overline{\rho}_j u'_j}{\partial x} = 0 \tag{211}$$

$$\overline{\rho}_j \frac{\partial u'_j}{\partial t} + \frac{\partial p'_j}{\partial x} = 0 \tag{212}$$

$$\overline{\rho}_j c_p \frac{\partial T'_j}{\partial t} + \gamma \overline{p} \frac{\partial u'_j}{\partial x} = (\gamma - 1)Q' \tag{213}$$

$$p'_j = \overline{\rho}_j c_p T'_j \tag{214}$$

To obtain the matching conditions between the two domains M_1 and M_2, we consider a small control interval which includes the flame front that we denote $I = [\xi^-, \xi^+] = [\xi - \varepsilon, \xi + \varepsilon]$, for $\varepsilon \to 0$.

The **first matching condition** is that the acoustic pressure is continuous across the flame [19]

$$\boxed{p'(\xi^-, t) = p'(\xi^+, t)} \tag{215}$$

Assuming the jump of density to occur in a very thin layer we integrate the unsteady density equation and obtain the **second matching condition**

$$\boxed{\overline{\rho}_2 u'(\xi^+, t) = \overline{\rho}_1 u'(\xi^-, t)} \tag{216}$$

The **third matching condition** relates the jump of the unsteady velocity to the heat release.
Lemma : At the interface the jump condition for the unsteady velocity reads

$$\boxed{u'(\xi^+, t) - u'(\xi^-, t) = \frac{\gamma - 1}{\gamma \overline{p}} q'(t)} \tag{217}$$

Proof : the pressure equation is given by

$$\frac{\partial p'}{\partial t} + \gamma \overline{p} \frac{\partial u'}{\partial x} = (\gamma - 1)Q'(x, t)$$

We integrate this equation over the control interval $I = [\xi^-, \xi^+]$

$$\int_{\xi^-}^{\xi^+} \left[\frac{\partial p'}{\partial t} + \gamma \overline{p} \frac{\partial u'}{\partial x} \right] dx = (\gamma - 1) \int_{\xi^-}^{\xi^+} Q'(x, t) dx$$

Since $\gamma \overline{p} = const$, we obtain for $\varepsilon \to 0$ the following jump condition of the velocity

$$u'(\xi^+, t) - u'(\xi^-, t) = \frac{\gamma - 1}{\gamma \overline{p}} q'(t)$$

$\blacksquare$

We remind the relation between mean flow variables and summarize the three matching conditions at the flame front

$$\Theta = \frac{\overline{\rho}_1}{\overline{\rho}_2} = \frac{\overline{u}_2}{\overline{u}_1} = \frac{\overline{T}_2}{\overline{T}_1} \tag{218}$$

$$p'(\xi^+, t) = p'(\xi^-, t) \tag{219}$$

$$u'(\xi^+, t) = \Theta u'(\xi^-, t) \tag{220}$$

$$u'(\xi^+, t) = u'(\xi^-, t) + \frac{\gamma - 1}{\gamma \overline{p}} q'(t) \tag{221}$$

The last two conditions describe the unsteady velocity near the flame and are equivalent to

$$u'(\xi^+, t) = \frac{\Theta}{\Theta - 1} \frac{\gamma - 1}{\gamma \overline{p}} q'(t) \tag{222}$$

$$q'(t) = \frac{\Theta - 1}{\gamma - 1} \gamma \overline{p} u'(\xi^-, t) \tag{223}$$

The last equation shows a proportionality between the heat release rate $q'(t)$ and the unsteady velocity upstream the flame $u'(\xi^-, t)$. By rearranging the proportionality factor, we are able to deduce a physical interpretation of this relation. In fact, using the definition of the heat capacity at constant pressure c_p and the upstream sound speed $\overline{c}_1^2$

$$c_p = \frac{\gamma}{\gamma - 1} \frac{\mathcal{R}}{W}, \quad \text{and} \quad \overline{c}_1^2 = \gamma \frac{\mathcal{R}}{W} \overline{T}_1 \tag{224}$$

we rewrite the expression for the coefficient Θ to get

$$\Theta = \frac{\overline{T}_2}{\overline{T}_1} \tag{225}$$

$$= 1 + \frac{\overline{T}_2 - \overline{T}_1}{\overline{T}_1} \tag{226}$$

$$= 1 + (\gamma - 1) c_p \frac{\overline{T}_2 - \overline{T}_1}{\overline{c}_1^2} \tag{227}$$

Since the upstream sound speed $\overline{c}_1$ is also given by

$$\overline{c}_1 = \sqrt{\frac{\gamma \overline{p}}{\rho_1}} \tag{228}$$

the unsteady heat release rate takes the form

$$\boxed{q'(t) = \overline{\rho}_1 c_p u'_1(\xi^-, t)(\overline{T}_2 - \overline{T}_1)} \tag{229}$$

Remark : $\overline{T}_2 - \overline{T}_1$ represents the temperature jump across the flame. Hence, the physical interpretation of this equation is that the unsteady heat release is proportional to the unsteady mass flow rate into the heating zone, i.e. $\overline{\rho}_1 u'_1(\xi^-, t)$, and to the heat input required to raise the mean temperature

from upstream temperature $\overline{T}_1$ to downstream temperature $\overline{T}_2$, i.e. $c_p(\overline{T}_2 - \overline{T}_1)$.
Written in matrix form the jump conditions for the particular case above are

$$
\begin{pmatrix}
\cos(\frac{\omega}{\overline{c}_1}\xi) & i \, \sin(\frac{\omega}{\overline{c}_2}(L-\xi)) \\
\frac{i}{\rho_1\overline{c}_1}\sin(\frac{\omega}{\overline{c}_1}\xi)\Theta & \frac{-1}{\rho_2\overline{c}_2}\cos(\frac{\omega}{\overline{c}_2}(L-\xi))
\end{pmatrix}
\begin{pmatrix}
A_1^+ \\
A_2^+
\end{pmatrix} = \vec{0}
\tag{230}
$$

The frequency equation is obtained by setting the determinant of the matrix to zero, i.e.

$$
\sqrt{\Theta} \sin(\frac{\omega}{\overline{c}_1}\xi) \sin(\frac{\omega}{\overline{c}_2}(L-\xi)) - \cos(\frac{\omega}{\overline{c}_1}\xi) \cos(\frac{\omega}{\overline{c}_2}(L-\xi)) = 0
\tag{231}
$$

Remark : If there is no combustion $(q'(t) = 0)$, hence no temperature jump $(\overline{T}_2 = \overline{T}_1)$, the parameter Θ equals 1 and we get the same equations for the pulsation ω obtained for the case without combustion.

7.3   Modeling the unsteady heat release

We want to compute the eigenmodes of the combustion chamber taking into account the effect of combustion. Since all the acoustic variables are unsteady terms, only the effect of unsteady heat release needs to be considered in the Helmholtz equation. The effect of stationary heat release is already taken into account in computing the steady state of pressure, density, sound speed and temperature fields [19].
The total heat release due to combustion is given by negative the sum over the reaction rate times the heat of formation of every species

$$
\dot{Q}_c = - \sum_{s=1}^{N_s} h_s^0 \dot{\omega}_s
\tag{232}
$$

By definition, unsteady terms are obtained from the difference between total and stationary terms. Using this property, the unsteady heat release is given by

$$
\dot{Q}'_c = \dot{Q}_c - \overline{\dot{Q}}_c = - \sum_{s=1}^{N_s} h_s^0 \dot{\omega}_s + \sum_{s=1}^{N_s} h_s^0 \overline{\dot{\omega}}_s = - \sum_{s=1}^{N_s} h_s^0 (\dot{\omega}_s - \overline{\dot{\omega}}_s)
\tag{233}
$$

The same applies to the unsteady reaction rate $\dot{\omega}'_s$

$$
\begin{aligned}
\dot{\omega}'_s &= \dot{\omega}'_s(Y'_{s=1,..,N_s}, \rho', T') \tag{234} \\
&= \dot{\omega}_s(Y_{s=1,..,N_s}, \rho, T) - \overline{\dot{\omega}}_s(\overline{Y}_{s=1,..,N_s}, \overline{\rho}, \overline{T}) \tag{235} \\
&= \dot{\omega}_s((\overline{Y}_s + Y'_s)_{s=1,..,N_s}, \overline{\rho} + \rho', \overline{T} + T') - \overline{\dot{\omega}}_s(\overline{Y}_{s=1,..,N_s}, \overline{\rho}, \overline{T}) \tag{236}
\end{aligned}
$$

The idea of the present model is to consider a Taylor series of the total reaction rate around the stationary reaction rate

$$
\begin{aligned}
\dot{\omega}_s &= \dot{\omega}_s((\overline{Y}_s + Y'_s)_{s=1,..,N_s}, \overline{\rho} + \rho', \overline{T} + T') \tag{237} \\
&= \overline{\dot{\omega}}_s(\overline{Y}_{s=1,..,N_s}, \overline{\rho}, \overline{T}) + \frac{\partial \overline{\dot{\omega}}_s}{\partial Y_1}Y'_1 + \ldots + \frac{\partial \overline{\dot{\omega}}_s}{\partial Y_{N_s}}Y'_{N_s} + \frac{\partial \overline{\dot{\omega}}_s}{\partial \rho}\rho' + \frac{\partial \overline{\dot{\omega}}_s}{\partial T}T' + \text{h.o.t.}
\end{aligned}
$$

By neglecting the high-order terms we obtain a first-order approximation of the unsteady reaction rate $\dot{\omega}'_s$

$$\dot{\omega}'_s \doteq \frac{\partial \overline{\dot{\omega}}_s}{\partial Y_1} Y'_1 + \ldots + \frac{\partial \overline{\dot{\omega}}_s}{\partial Y_{N_s}} Y'_{N_s} + \frac{\partial \overline{\dot{\omega}}_s}{\partial \rho} \rho' + \frac{\partial \overline{\dot{\omega}}_s}{\partial T} T' \tag{238}$$

To simplify the notation we define the vector $\mathbf{Y}$ which consists of all mass fractions

$$\mathbf{Y} = (Y_1 \; Y_2 \; \ldots \; Y_{N_s})^t \tag{239}$$

and rewrite the unsteady reaction rate $\dot{\omega}'_s$ in the compact form

$$\dot{\omega}'_s = \nabla_Y \overline{\dot{\omega}}_s \bullet \mathbf{Y}' + \frac{\partial \overline{\dot{\omega}}_s}{\partial \rho} \rho' + \frac{\partial \overline{\dot{\omega}}_s}{\partial T} T' \tag{240}$$

As a result we obtain the following relation for the unsteady heat release

$$\dot{Q}'_c = -\sum_{s=1}^{N_s} h_s^0 \dot{\omega}'_s = -\sum_{s=1}^{N_s} h_s^0 \left(\nabla_Y \overline{\dot{\omega}}_s \bullet \mathbf{Y}' + \frac{\partial \overline{\dot{\omega}}_s}{\partial \rho} \rho' + \frac{\partial \overline{\dot{\omega}}_s}{\partial T} T' \right) \tag{241}$$

Remark : Through this formalism, we obtained an expression for the unsteady heat release Q' as a function of the fluctuations of the mass fractions, density and temperature. It is noteworthy that quite contrary to most of the models used sofar in numerical combustion, this formulation does not involve any model parameters or empiric assumptions. It is based on a mathematical approach which linearizes the heat release around its steady state. On the basis of this relation, we will construct a flame transfer function coupling the unsteady heat release to the pressure fluctuations.

7.4   Density and chemical species equations

In addition to the mode shapes of temperature, the source term $\hat{Q}$ involves the mode shapes of density as well as the mass fractions $\{\hat{Y}_s\}_{s=1,..N_s}$. Therefore, we need to find additional equations for these new unknown quantities.

7.4.1   Equations for the density fluctuation

Assuming the flow to be isentropic it is possible to provide a relation between the acoustic pressure p' and the density fluctuation ρ'. Indeed we have for an isentropic flow the following constitutive equation

$$p = \overline{p} + p' = \overline{p} + \rho' \left[\frac{\partial p}{\partial \rho} \right]_S + \frac{1}{2}(\rho')^2 \left[\frac{\partial^2 p}{\partial \rho^2} \right]_S + .. \tag{242}$$

Neglecting the nonlinear term this equation means that the density perturbation is proportional to the pressure perturbation

$$p' = \rho' \left[\frac{\partial p}{\partial \rho} \right]_S = \rho' c^2 \tag{243}$$

which yields for the Fourier transforms

$$\hat{\rho} = \frac{1}{c^2} \hat{p} \tag{244}$$

7.4.2 Equations for the chemical species

The conservation laws of the chemical species X_s reads

$$\overline{\rho}\frac{\partial Y'_s}{\partial t} + \overline{\rho}\mathbf{u}' \bullet \nabla \overline{Y}_s = \nabla \bullet (\overline{\rho}\mathcal{D}_s \nabla Y'_s) + \dot{\omega}'_s \tag{245}$$

We take the Fourier transform of this equation and use the expression of the acoustic velocity

$$\overline{\rho}\omega^2 \hat{Y}_s + \nabla \overline{Y}_s \bullet \nabla \hat{p} = i\omega \nabla \bullet (\overline{\rho}\mathcal{D}_s \nabla Y'_s) + i\omega \hat{\dot{\omega}}_s \tag{246}$$

Inserting the first-order approximation for $\dot{\omega}_s$ yields

$$\overline{\rho}\omega^2 \hat{Y}_s + \nabla \overline{Y}_s \bullet \nabla \hat{p} = i\omega \nabla \bullet (\overline{\rho}\mathcal{D}_s \nabla \hat{Y}_s) + i\omega(\nabla_Y \overline{\dot{\omega}}_s \bullet \hat{\mathbf{Y}} + \frac{\partial \overline{\dot{\omega}}_s}{\partial \rho}\hat{\rho} + \frac{\partial \overline{\dot{\omega}}_s}{\partial T}\hat{T}) \tag{247}$$

8 Computing the eigenmodes of active combustion chambers

8.1 Combining the equations for temperature and species

At this stage we obtained the additional equations for the temperature, mass fractions and density modes. We would like to combine the temperature modes equation

$$\overline{\rho}\omega^2 \hat{T} + \nabla \overline{T} \bullet \nabla \hat{p} = \frac{1}{c_p}\omega^2 \hat{p} + \frac{1}{c_p}i\omega \nabla \bullet (\lambda \nabla \hat{T}) - \frac{1}{c_p}i\omega \sum_{s=1}^{N_s} h_s^0 \left(\nabla_Y \overline{\dot{\omega}}_s \bullet \hat{\mathbf{Y}} + \frac{\partial \overline{\dot{\omega}}_s}{\partial \rho}\hat{\rho} + \frac{\partial \overline{\dot{\omega}}_s}{\partial T}\hat{T}\right) \tag{248}$$

with the N_s chemical species equations

$$\overline{\rho}\omega^2 \hat{Y}_s + \nabla \overline{Y}_s \bullet \nabla \hat{p} = i\omega \nabla \bullet (\overline{\rho}\mathcal{D}_s \nabla \hat{Y}_s) + i\omega(\nabla_Y \overline{\dot{\omega}}_s \bullet \hat{\mathbf{Y}} + \frac{\partial \overline{\dot{\omega}}_s}{\partial \rho}\hat{\rho} + \frac{\partial \overline{\dot{\omega}}_s}{\partial T}\hat{T}), \quad s = 1, \dots, N_s \tag{249}$$

and write all these equations in matrix form as

$$i\omega \begin{pmatrix} \nabla \bullet (\overline{\rho}\mathcal{D}_1 \nabla \hat{Y}_1) \\ \vdots \\ \nabla \bullet (\overline{\rho}\mathcal{D}_{N_s} \nabla \hat{Y}_{N_s}) \\ \frac{1}{c_p}\nabla \bullet (\lambda \nabla \hat{T}) \end{pmatrix} + i\omega J \begin{pmatrix} \hat{Y}_1 \\ \vdots \\ \hat{Y}_{N_s} \\ \hat{T} \end{pmatrix} = \mathbf{b}(\hat{p}) + \mathbf{b}_\nabla(\hat{p}) \tag{250}$$

The vectors $\mathbf{b}(\hat{p})$ and $\mathbf{b}_\nabla(\hat{p})$ on the right-hand side are dependent on the acoustic pressure $\hat{p}$ and its gradient $\nabla \hat{p}$ as well as the frequency number ω. All other terms appearing in the expression of these vectors are either constants or steady-state variables.

$$\mathbf{b}(\hat{p}) = -\frac{\omega^2}{c_p} \begin{pmatrix} 0 \\ \vdots \\ 0 \\ 1 \end{pmatrix} \hat{p} - \frac{i\omega}{c^2} \begin{pmatrix} \frac{\partial \overline{\dot{\omega}}_1}{\partial \rho} \\ \vdots \\ \frac{\partial \overline{\dot{\omega}}_{N_s}}{\partial \rho} \\ -\sum_{s=1}^{N_s} \frac{h_s^0}{c_p}\frac{\partial \overline{\dot{\omega}}_s}{\partial \rho} \end{pmatrix} \hat{p}, \ \mathbf{b}_\nabla(\hat{p}) = \begin{pmatrix} \nabla \overline{Y}_1 \\ \vdots \\ \nabla \overline{Y}_{N_s} \\ \nabla \overline{T} \end{pmatrix} \bullet \nabla \hat{p}, \tag{251}$$

The matrix J is a square matrix of dimension $(N_s + 1)$ and is given by

$$J = i\omega\overline{\rho}I + \tilde{J} \tag{252}$$

where I represents the identity matrix of size $(N_s + 1)$. The matrix $\tilde{J}$ couples the temperature fluctuation to the mass fractions fluctuations and is given by

$$\tilde{J} = \begin{pmatrix} \frac{\partial\overline{\dot{\omega}}_1}{\partial Y_1} & \cdots & \frac{\partial\overline{\dot{\omega}}_1}{\partial Y_{N_s}} & \frac{\partial\overline{\dot{\omega}}_1}{\partial T} \\ \vdots & \vdots & \vdots & \vdots \\ \frac{\partial\overline{\dot{\omega}}_{N_s}}{\partial Y_1} & \cdots & \frac{\partial\overline{\dot{\omega}}_{N_s}}{\partial Y_{N_s}} & \frac{\partial\overline{\dot{\omega}}_{N_s}}{\partial T} \\ -\sum_{s=1}^{N_s}\frac{h_s^0}{c_p}\frac{\partial\overline{\dot{\omega}}_s}{\partial Y_1} & \cdots & -\sum_{s=1}^{N_s}\frac{h_s^0}{c_p}\frac{\partial\overline{\dot{\omega}}_s}{\partial Y_{N_s}} & -\sum_{s=1}^{N_s}\frac{h_s^0}{c_p}\frac{\partial\overline{\dot{\omega}}_s}{\partial T} \end{pmatrix} \tag{253}$$

Remark : it is straightforward to note that the last line of the matrix $\tilde{J}$ which corresponds to the temperature equation can be obtained by a linear combination of all previous lines. Furthermore, the conservation of mass being still valid in a reactive flow, we know that all reaction rates $\overline{\dot{\omega}}_s$ sum up to 0. Hence the sum of the first N_s lines of the matrix $\tilde{J}$ is also 0. As a result of these two observations the matrix $\tilde{J}$ of dimension $(N_s + 1)$ cannot have full rank

$$1 \leq rank(\tilde{J}) \leq N_s - 1 \tag{254}$$

8.2 Investigating the coupling matrix

We would like to develop a flame-transfer function which couples directly the heat release to the acoustic pressure. To achieve this we need to examine the properties of the matrix J and if possible find an inverse of this matrix. It is important to obtain an analytic formula for the inverse of the functional matrix J as computing the inverse numerically in every grid point would be cumbersome and infeasible in real-world applications. The only option is to investigate the coupling matrix J thoroughly and try to use the physical as well as mathematical properties of the thermo-acoustic system to obtain an analytical expression for the inverse of J.

For a multicomponent mixture in which N_r chemical reactions take place, the reaction mechanism is written as

$$\sum_{s=1}^{N_s} \nu_{sr}^f X_s \rightleftharpoons \sum_{s=1}^{N_s} \nu_{sr}^b X_s, \quad r = 1, 2, \cdots, N_r$$

ν^f and ν^b are respectively the matrices of the stoichiometric coefficients for the forward and backward reactions. $\nu = \nu^b - \nu^f$ represents the matrix of the net stoichiometric coefficients. Let $\dot{\Omega}_r$ denote the net reaction rate of the r-th reaction. Then $\dot{\Omega}_r$ has the following expression

$$\dot{\Omega}_r = k_r^f(T)\prod_{s=1}^{N_s}(\frac{\rho_s}{W_s})^{\nu_{sr}^f} - k_r^b(T)\prod_{s=1}^{N_s}(\frac{\rho_s}{W_s})^{\nu_{sr}^b} \tag{255}$$

The net reaction rate $\dot{\omega}_s$ of species X_s is obtained by summing over all N_r reactions and is given by

$$\dot{\omega}_s = \sum_{r=1}^{N_r} W_s\nu_{sr}\dot{\Omega}_r \tag{256}$$

This relation is very interesting as it allows us to understand the special structure of the matrix $\tilde{J}$ which becomes more clear by introducing the vectors $\mathbf{u}$ and $\mathbf{v}$ defined as

$$
\begin{array}{rcl}
\mathbf{u}_r &=& \left(\begin{array}{ccccccc} W_1\nu_{1r} & \ldots & W_s\nu_{sr} & \ldots & W_{N_s}\nu_{N_s r} & -\sum_{s=1}^{N_s} W_s \frac{h_s^0}{c_p}\nu_{sr} \end{array} \right)^t \\[2mm]
\mathbf{v}_r &=& \left(\begin{array}{ccccccc} \frac{\partial \dot{\Omega}_r}{\partial Y_1} & \ldots & \frac{\partial \dot{\Omega}_r}{\partial Y_s} & \ldots & \frac{\partial \dot{\Omega}_r}{\partial Y_{N_s}} & \frac{\partial \dot{\Omega}_r}{\partial T} \end{array} \right)^t
\end{array}
\tag{257}
$$

The matrix $\tilde{J}$ can be obtained by combinations of these vectors $\mathbf{u}_r$ and $\mathbf{v}_r$. More precisely the matrix $\tilde{J}$ takes the form of a sum of rank-1 updates

$$
\tilde{J} = \sum_{r=1}^{N_r} \mathbf{u}_r \mathbf{v}_r^t
\tag{258}
$$

As a direct consequence we obtain a better bound for $rank(\tilde{J})$

$$
1 \leq rank(\tilde{J}) \leq min(N_r, N_s - 1)
\tag{259}
$$

Remarks :

- Let $\mathbf{z}$ denote the vector $(h_1^0 \; h_2^0 \; \ldots \; h_{N_s}^0 \; c_p)^t$. The vector z is orthogonal to all vectors u_r for any combination of stoechiometric coefficients ν_{sr} and any molecular weights W_s.

$$
\boxed{\forall r \in 1, .., N_r \quad : \quad \mathbf{z}^t \mathbf{u}_r = 0 \Rightarrow \mathbf{z}^t \tilde{J} = 0}
\tag{260}
$$

- An important consequence of $\mathbf{z}^t \tilde{J} = 0$ is that $\mathbf{z}$ is a right eigenvector of J and the corresponding eigenvalue is $i\omega\bar{\rho}$.

- Due to equation (256) we have that

$$
\frac{\partial \overline{\dot{\omega}}_s}{\partial \rho} = \sum_{r=1}^{N_r} W_s \nu_{sr} \frac{\partial \overline{\dot{\Omega}}_r}{\partial \rho}
\tag{261}
$$

and rewrite the right-hand side vector $\mathbf{b}(\hat{p})$

$$
\mathbf{b}(\hat{p}) = -\frac{\omega^2}{c_p} \begin{pmatrix} 0 \\ \vdots \\ 0 \\ 1 \end{pmatrix} \hat{p} - \frac{i\omega}{c^2} \sum_{r=1}^{N_r} \frac{\partial \overline{\dot{\Omega}}_r}{\partial \rho} \mathbf{u}_r \hat{p}
\tag{262}
$$

8.3 Equation for the acoustic pressure modes

To get the acoustic pressure modes of the thermo-acoustic system [17] we need to solve the Helmholtz equation with the unsteady heat realease as a source term

$$
\nabla \bullet (c^2 \nabla \hat{p}) + \omega^2 \hat{p} = (\gamma - 1) i\omega \hat{Q}
\tag{263}
$$

In the previous section we derived the following equation to describe the unsteady heat release

$$\hat{Q} = -\sum_{s=1}^{N_s} h_s^0 \left(\nabla_Y \overline{\dot{\omega}}_s \bullet \hat{\mathbf{Y}} + \frac{\partial \overline{\dot{\omega}}_s}{\partial \rho} \hat{\rho} + \frac{\partial \overline{\dot{\omega}}_s}{\partial T} \hat{T} \right) \tag{264}$$

Hence the pressure modes equation involves all the unknown modes $\hat{p}$, $\hat{T}$, $\hat{\rho}$ and $\hat{\mathbf{Y}}$. As it stands it is not possible to solve this equation. We need to obtain an equation for the acoustic pressure having only the eigenpair $(\hat{p}, \omega)$ as unknown. To obtain such an equation we combined the temperature and species equation in matrix form. We are primarily interested in getting the low-frequency modes of the system which are in practice included in the set of the first thirty eigenomdes. Numerical simulation shows that diffusion effects are not significant in the low-frequency range of interest. For this reason the equations coupling temperature and chemical species become

$$i\omega J \begin{pmatrix} \hat{\mathbf{Y}} \\ \hat{T} \end{pmatrix} = \mathbf{b}(\hat{p}) + \mathbf{b}_\nabla(\hat{p}) \tag{265}$$

Assuming that the coupling matrix J is invertible -this will be shown later on- it is possible to use the previous system of equations to eliminate $\hat{Y}_s, \hat{T}$ and ρ from the pressure equation. By doing so we get an equation with only the eigenpair $(\hat{p}, \omega)$ as unknown

$$\nabla \bullet (c^2 \nabla \hat{p}) + \omega^2 \hat{p} + i\omega \frac{(\gamma-1)}{c^2} \sum_{s=1}^{N_s} h_s^0 \frac{\partial \overline{\dot{\omega}}_s}{\partial \rho} \hat{p} = -(\gamma-1) \sum_{s=1}^{N_s} h_s^0 \left(\nabla_Y \overline{\dot{\omega}}_s \frac{\partial \overline{\dot{\omega}}_s}{\partial T} \right) J^{-1}(\mathbf{b}(\hat{p}) + \mathbf{b}_\nabla(\hat{p})) \tag{266}$$

8.3.1   Computing the inverse matrix J^{-1}

The *Sherman-Morrison* formula provides a way to obtain an analytical expression for the inverse of the matrix J. In fact let A be a square matrix of size n and $\mathbf{u}$, $\mathbf{v}^t$ be vectors of length n. We consider the matrix $\hat{A}$ obtained by a rank-1 update of A

$$\hat{A} = A + \mathbf{u}\mathbf{v}^t \tag{267}$$

Lemma : If A is invertible and satisfies $\mathbf{v}^t A^{-1} \mathbf{u} \neq -1$, then $\hat{A}$ is invertible and the inverse matrix $\hat{A}^{-1}$ reads

$$\hat{A}^{-1} = (A + \mathbf{u}\mathbf{v}^t)^{-1} = A^{-1} - \frac{A^{-1}\mathbf{u}\mathbf{v}^t A^{-1}}{1 + \mathbf{v}^t A^{-1}\mathbf{u}} \tag{268}$$

As a result of this lemma it is straightforward to construct a recursive scheme [43] to obtain the inverse of the matrix J for any number of rank-1 updates N_r :

$$J = i\omega\overline{\rho}I + \sum_{r=1}^{N_r} \mathbf{u}_r \mathbf{v}_r^t \tag{269}$$

For this we need first to check that the conditions required in the lemma are satisfied by the matrix J. It is indeed the case since :

- $\omega \neq 0$ and hence the matrix $i\omega\overline{\rho}I$ is invertible

- $\frac{\mathbf{v}^t \mathbf{u}}{i\omega\overline{\rho}}$ is a complex number having a non-zero imaginary part and hence cannot be equal -1

Clearly this reasoning can be extended by induction for an arbitrary number N_r of rank-1 updates.

8.3.2 Velocity, temperature and species modes

By providing an analytical expression for the inverse of the matrix J we obtained an eigenvalue problem in $\hat{p}$. After solving for the pressure modes we use the following equation to get the acoustic velocity modes

$$\hat{\mathbf{u}} = \frac{1}{i\omega\bar{\rho}}\nabla\hat{p} \tag{270}$$

The temperature and species modes are provided through the following relation

$$\begin{pmatrix} \hat{Y}_1 \\ \vdots \\ \hat{Y}_{N_s} \\ \hat{T} \end{pmatrix} = \frac{J^{-1}}{i\omega}(\mathbf{b}(\hat{p}) + \mathbf{b}_\nabla(\hat{p})) \tag{271}$$

9 Benchmark and simulation methods

A suitable benchmark for preliminary studies is a duct, with uniform cross-sectional area, mean temperature, constant density and having no mean flow. The duct is connected to a large plenum at the inlet cross section and has a restriction at the outlet. In [6] Dowling and Stow examined a similar benchmark and performed different analysis on its dynamic behavior. Since the cross-section is constant, this benchmark can be considered as a one-dimensional case in which the planar wave hypothesis is appropriate. The variation of acoustic pressure and velocity in the duct is a function of time and abscissa x only. Furthermore the flame is supposed to be concentrated at a particular abscissa. Under the no flow hypothesis, a Dirichlet boundary condition at the inlet and a Neumann boundary condition at the outlet is assumed. Considering a quasi-one-dimensional geometry provides a more realistic approach to the combustion instabilities. The geometry consists in three co-axial cylindrical ducts modelling the diffuser, the premixer and the combustion chamber. The blockage at the premixer inlet is modelled by a Neumann boundary condition, whereas the open end at the exit of the combustor is described by a Dirichlet boundary condition. As in the one-dimensional benchmark, the flame sheet is supposed to be concentrated at the exit of the premixer, exactly at the inlet of the combustion chamber. The heat release fluctuation is then related to the fluctuations of the fuel and air inflow rates.

In this study the test case consists in a combustor through which a reactive gas is flowing and gets burnt in the flame region [34]. All external body forces such as gravity are neglected. The diameter-to-length ratio being very small, we may assume that the propagation is one-dimensional in the longitudinal direction of the combustor. Furthermore we assume that dissipation effects on the acoustic waves are negligible. Also we suppose adiabatic conditions, i.e. no heat loss to the surrounding takes place.

Taking these assumptions into account, the equations describing the reactive gas dynamics are the conservation of mass, momentum and energy.

$$\frac{\partial \rho}{\partial t} + \frac{\partial (\rho u)}{\partial x} = 0 \tag{272}$$

$$\rho \frac{\partial u}{\partial t} + \rho u \frac{\partial u}{\partial x} + \frac{\partial p}{\partial x} = 0 \tag{273}$$

$$\rho \frac{\partial e}{\partial t} + \rho u \frac{\partial e}{\partial x} = -p \frac{\partial u}{\partial x} + q \tag{274}$$

where ρ, u, p and e denote the density, velocity, pressure and specific internal energy. The variable q accounts for the heat release due to chemical reactions.

In addition to these three equations we need further equations to describe the evolution of the chemical species. These are given by

$$\frac{\partial (\rho Y_1)}{\partial t} + \frac{\partial (\rho Y_1 u)}{\partial x} = \dot{\omega}_1 \tag{275}$$

$$\frac{\partial (\rho Y_2)}{\partial t} + \frac{\partial (\rho Y_2 u)}{\partial x} = \dot{\omega}_2 \tag{276}$$

$$\vdots \tag{277}$$

$$\frac{\partial (\rho Y_{N_s})}{\partial t} + \frac{\partial (\rho Y_{N_s} u)}{\partial x} = \dot{\omega}_{N_s} \tag{278}$$

Y_s denotes the mass fraction of species X_s and $\dot{\omega}_s$ its chemical production rate. Furthermore we assume that the flow is an ideal gas and hence the pressure is related to density and temperature through the ideal gas law which states that

$$p = (\gamma - 1)\rho e = \rho \frac{\mathcal{R}}{W} T \tag{279}$$

where $\mathcal{R}$ is the universal gas constant and W the molecular weight of the mixture.

Combining the mass conservation, the energy conservation and the ideal gas law, we obtain an equation describing the evolution of the pressure field

$$\frac{\partial p}{\partial t} + u \frac{\partial p}{\partial x} + \gamma p \frac{\partial u}{\partial x} = (\gamma - 1)q \tag{280}$$

Finally the assumptions are summarized as :

- one-dimensional ideal gas flow in the longitudinal direction of the combustor [20]

- negligible dissipation on the acoustic waves [21]

- negligible thermal conductivity to the surrounding domain

9.1   Analytical model for steady-state variables

We propose the following model to describe the mean variables in the case of steady combustion.
Let $\Omega = [0, L]$ be the one-dimensional combustor in which the reactive gas is flowing and let $b \in (0, L)$ denote the location of the flame in its steady state. Without loss of generality we may suppose that $b = \frac{L}{2}$ meaning that the flame front is located in the middle of the combustor.
The computational grid has to be defined in such a way that it resolves the flame front as well as the boundary conditions accurately. To achieve this we require the grid to be very fine at both boundaries and near the flame zone and to be coarser elsewhere.

Parameters :
h_{min} : minimum step size of grid,
$\bar{h}$: typical step size of grid,
n_0, n_b, n_L : control parameters for grid size distribution

Algorithm :
$i = 0, x_i = 0$
while $(x_i < L)$
$h_i \;\; = h_{min} + \bar{h} \left(\frac{x_i}{L}\right)^{n_0} \left|\frac{x_i}{b} - 1\right|^{n_b} \left(1 - \frac{x_i}{L}\right)^{n_L}$,
$x_{i+1} \;\; = x_i + h_i$,
$i \;\; = i + 1$,
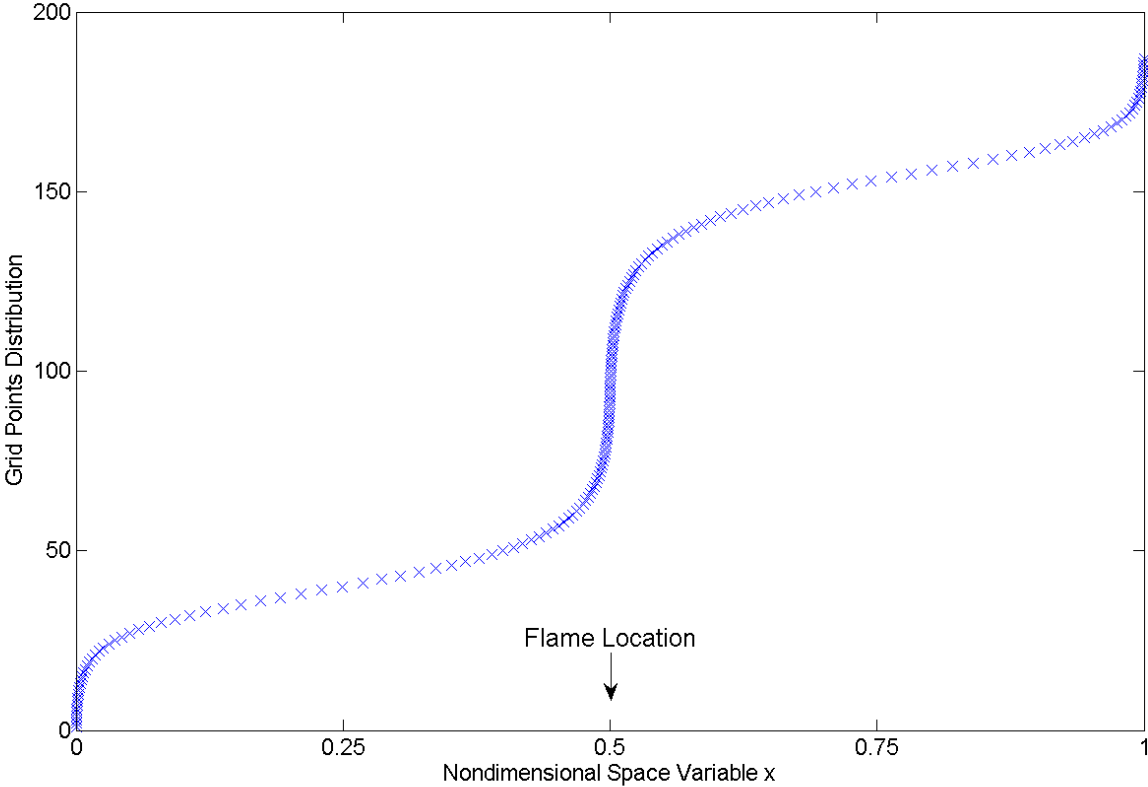**end**
$x_i = L$,
$h_{i-1} = L - x_{i-1}$

Figure 13: Grid points distribution obtained by the adaptive mesh size algorithm

In order to capture the very steep gradients of temperature and mass fractions at the flame front it is very useful to introduce the stretched variable $\hat{x}$ defined by

$$\hat{x} = \frac{\frac{x}{b} - 1}{\varepsilon} \tag{281}$$

where ε is a typical flame thickness ($e.g. 10^{-3}$ m). The choice of $\hat{x}$ is such that it has its origin exactly at the stationary position of the flame and takes very large values at both boundaries. Furthermore we introduce the variable χ which describes a profile showing two almost constant states and a sudden jump in between

$$\chi = \frac{tanh(\hat{x}) + 1}{2} = \frac{1}{1 + e^{-2\hat{x}}} \tag{282}$$

The following table summarizes the space variables used in the grid generation and their values at the cold boundary in the preheat zone, at the flame and at the hot boundary in the equilibrium zone.

Variable values at	cold boundary	flame zone	hot boundary
x	0	b	L
$\hat{x}$	$-\varepsilon^{-1}$	0	ε^{-1}
χ	0	$\frac{1}{2}$	1

For all steady-state variables representing the density, the temperature, the sound speed or the mass fractions of the chemical species we expect a very slow variation at both the preheat and the equilibrium zone and a rapid change across the flame. For this reason we choose the following model to describe all these variables

$$\bar{\rho}(x) = (1 - \chi)\bar{\rho}_0 + \chi\bar{\rho}_1 \tag{283}$$
$$\overline{T}(x) = (1 - \chi)\overline{T}_0 + \chi\overline{T}_1 \tag{284}$$
$$c^2(x) = (1 - \chi)c_0^2 + \chi c_1^2 \tag{285}$$
$$\overline{Y}_s(x) = (1 - \chi)\overline{Y}_{s,0} + \chi\overline{Y}_{s,1} \tag{286}$$

where v_0 and v_1 represent respectively the value of the variable v upstream and downstream the flame. **Remarks :** the values of these variables upstream and downstream the flame cannot be chosen at will. In fact these quantities are coupled [26]. As already shown in (209) we require that

$$\Theta = \frac{\bar{\rho}_0}{\bar{\rho}_1} = \frac{\bar{u}_1}{\bar{u}_0} = \frac{\overline{T}_1}{\overline{T}_0} > 1 \tag{287}$$

Also since the sound speed is given by

$$c^2 = \frac{\gamma\bar{p}}{\bar{\rho}} = \gamma\frac{\mathcal{R}}{W}\bar{T} \tag{288}$$

then as a consequence we have that

$$\frac{\bar{c}_1}{\bar{c}_0} = \sqrt{\Theta} > 1 \tag{289}$$
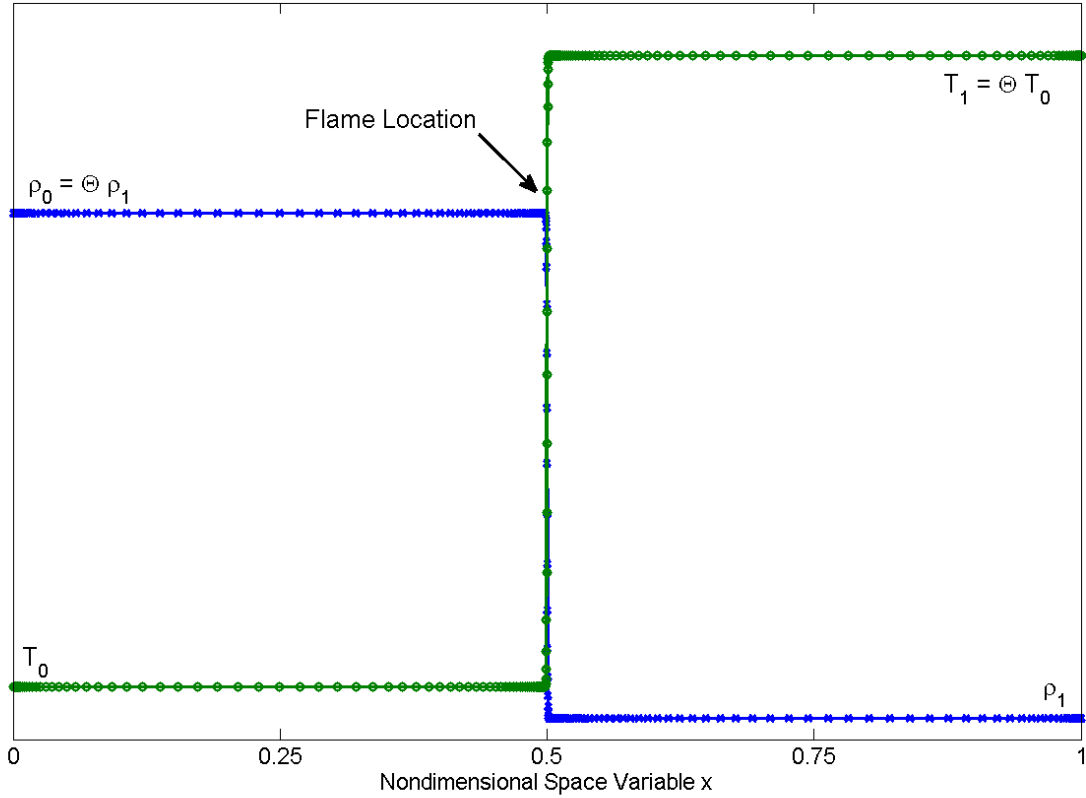
Figure 14: Evolution of steady-state profiles of density and temperature

Furthermore the temperature values upstream and downstream the flame are directly linked to the mass fractions values [26]. This is shown by considering the steady-state equations for the mass fractions and the temperature

$$\overline{\rho u}\frac{d\overline{Y}_s}{dx} = \overline{\dot{\omega}}_s$$
$$\overline{\rho}c_p\overline{u}\frac{d\overline{T}}{dx} = \overline{Q} = -\sum_{s=1}^{N_s} h_s^0 \overline{\dot{\omega}}_s \tag{290}$$

Combining these two equations and integrating over the whole domain we obtain an equation describing the conversion of chemical energy into heat

$$\bar{T}_1 - \bar{T}_0 = -\sum_{s=1}^{N_s} \frac{h_s^0}{c_p}(\bar{Y}_{s,1} - \bar{Y}_{s,0}) \tag{291}$$

The coupling of the upstream and downstream variables is summarized in the following equation

$$\boxed{\Theta = \frac{\overline{\rho}_0}{\overline{\rho}_1} = \frac{\overline{u}_1}{\overline{u}_0} = \frac{\overline{T}_1}{\overline{T}_0} = \frac{\bar{c}_1^2}{\bar{c}_0^2} = 1 - \sum_{s=1}^{N_s} \frac{h_s^0}{c_p\bar{T}_0}(\bar{Y}_{s,1} - \bar{Y}_{s,0}) > 1} \tag{292}$$

9.2   Chemical reaction rates and their derivatives

For a given reaction mechanism [49, 50] involving N_s species undergoing N_r reactions the chemical reaction rate of the r-th reaction denoted $\dot{\Omega}_r$ can be modeled by

$$\dot{\Omega}_r \;=\; k_f^r(T)\prod_{s=1}^{N_s}[X_s]^{\nu_{sr}^f} - k_b^r(T)\prod_{s=1}^{N_s}[X_s]^{\nu_{sr}^b} \tag{293}$$

$$=\; k_f^r(T)\prod_{s=1}^{N_s}\left(\frac{\rho Y_s}{W_s}\right)^{\nu_{sr}^f} - k_b^r(T)\prod_{s=1}^{N_s}\left(\frac{\rho Y_s}{W_s}\right)^{\nu_{sr}^b} \tag{294}$$

with the Arrehnius rate coefficients k_f, k_b for the forward and backward reactions

$$k(T) = AT^\mu exp(-\frac{E^a}{\mathcal{R}T}) \tag{295}$$

For the combustion model developed in this thesis we need to know the derivatives of the chemical reaction rates with respect to the mass fractions Y_s, the density ρ and the temperature T. These are given through the following equations

$$\frac{\partial\dot{\Omega}_r}{\partial Y_i} \;=\; \nu_{ir}^f k_f^r(T)\frac{\rho}{W_i}\left(\frac{\rho Y_i}{W_i}\right)^{\nu_{ir}^f-1}\prod_{s=1,s\neq i}^{N_s}\left(\frac{\rho Y_s}{W_s}\right)^{\nu_{sr}^f} - \nu_{ir}^b k_b^r(T)\frac{\rho}{W_i}\left(\frac{\rho Y_i}{W_i}\right)^{\nu_{ir}^b-1}\prod_{s=1,s\neq i}^{N_s}\left(\frac{\rho Y_s}{W_s}\right)^{\nu_{sr}^b} \tag{296}$$

$$\frac{\partial\dot{\Omega}_r}{\partial\rho} \;=\; \frac{\sum_{s=1}^{N_s}\nu_{sr}^f}{\rho}k_f^r(T)\prod_{s=1}^{N_s}\left(\frac{\rho Y_s}{W_s}\right)^{\nu_{sr}^f} - \frac{\sum_{s=1}^{N_s}\nu_{sr}^b}{\rho}k_b^r(T)\prod_{s=1}^{N_s}\left(\frac{\rho Y_s}{W_s}\right)^{\nu_{sr}^b} \tag{297}$$

$$\frac{\partial\dot{\Omega}_r}{\partial T} = \frac{dk_f^r(T)}{dT}\prod_{s=1}^{N_s}\left(\frac{\rho Y_s}{W_s}\right)^{\nu_{sr}^f} - \frac{dk_b^r(T)}{dT}\prod_{s=1}^{N_s}\left(\frac{\rho Y_s}{W_s}\right)^{\nu_{sr}^b} \tag{298}$$

with

$$\frac{dk(T)}{dT} = \frac{E^a + \mu\mathcal{R}T}{\mathcal{R}T^2}k(T) \tag{299}$$

Alternatively it is possible to give a mathematical model for the chemical production rate ω_s of each species X_s. We know that the chemical properties of combustion are such that the reaction terms are zero at both ends and have their maximum around the flame position. Hence we suggest the following model function

$$\overline{\omega}_s(\hat{x}) = \frac{\alpha}{(e^{\hat{x}} + e^{-\hat{x}})^2}, \quad \alpha \in \mathbb{R} \tag{300}$$

According to the chemical species equation the stationary reaction rate $\overline{\overline{\omega}}_s$ of species X_s satisfies

$$\int_0^L \overline{\omega}_s(x)dx \;=\; \int_{\overline{Y_s}^0}^{\overline{Y_s}^1}\overline{\rho}\overline{u}dY \tag{301}$$

$$=\; [\overline{\rho}\overline{u}\overline{Y_s}]_0^1 = \overline{\rho}_1\overline{u}_1(\overline{Y_s}^1 - \overline{Y_s}^0) \tag{302}$$

As a consequnce the constant α is provided by the following equation

$$\alpha = \frac{\int_0^L \overline{\overline{\omega}}_s(x)dx}{\int_{-\infty}^{+\infty} \frac{d\hat{x}}{(e^{\hat{x}}+e^{-\hat{x}})^2}} \tag{303}$$

$$= \frac{2(\overline{\rho}_1\overline{u}_1\overline{Y}_s^1 - \overline{\rho}_0\overline{u}_0\overline{Y}_s^0)}{\int_0^1 d\chi} = \frac{2\overline{\rho}_1\overline{u}_1(\overline{Y}_s^1 - \overline{Y}_s^0)}{\int_0^1 d\chi} \tag{304}$$

Hence we model the stationary reaction rate $\overline{\overline{\omega}}_s$ by

$$\overline{\overline{\omega}}_s(\hat{x}) = \frac{2\overline{\rho}\overline{u}[\overline{Y}_s]_0^1}{(e^{\hat{x}} + e^{-\hat{x}})^2} \tag{305}$$

Through this model it is possible to obtain the derivative of $\overline{\overline{\omega}}_s$ with respect to any of the steady-state variables $\overline{\rho}, \overline{T}$ and $\overline{Y}_s$. Let v be one of these steady-state variables, then we have

$$\frac{\partial \overline{\overline{\omega}}_s}{\partial v} = \frac{d\overline{\overline{\omega}}_s}{d\hat{x}} \frac{d\hat{x}}{d\chi} \left(\frac{dv}{d\chi}\right)^{-1} \tag{306}$$

$$= -2[\overline{\rho}\overline{u}\overline{Y}_s]_0^1 \frac{2(e^{\hat{x}} - e^{-\hat{x}})}{(e^{\hat{x}} + e^{-\hat{x}})^3} \frac{(e^{\hat{x}} + e^{-\hat{x}})^2}{2} \frac{1}{[v]_0^1} \tag{307}$$

$$= -\frac{2\overline{\rho}\overline{u}[\overline{Y}_s]_0^1}{[v]_0^1} \frac{e^{\hat{x}} - e^{-\hat{x}}}{e^{\hat{x}} + e^{-\hat{x}}} \tag{308}$$

$$= -\frac{2\overline{\rho}\overline{u}[\overline{Y}_s]_0^1}{[v]_0^1} tanh(\hat{x}) \tag{309}$$

where $[v]_0^1$ represents the jump in the value of v downstream (subscript 1) and upstream (subscript 0) the flame. For example the derivative of $\overline{\overline{\omega}}_s$ with respect to temperature is given by

$$\frac{\partial \overline{\overline{\omega}}_s}{\partial T} = -\frac{[\overline{\rho}\overline{u}[\overline{Y}_s]_0^1}{[T]_0^1} tanh(\hat{x}) \tag{310}$$

9.3   Oxydant-fuel combustion reaction

For the computation of the eigenmodes of the gas turbine, we have extended the acoustic pressure equation in order to take the combustion processes into account. In the following we assume that the combustion process is triggered by one dominant reaction as it is the case for most hydrocarbon fuels.

$$C_nH_m + \frac{4n + m}{4}O_2 \rightarrow nCO_2 + \frac{m}{2}H_2O \tag{311}$$
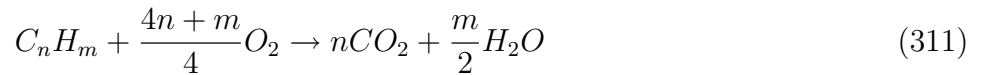
For example the combustion reaction of propane $(n = 3, m = 8)$ is given by

$$C_3H_8 + 5O_2 \rightarrow 3CO_2 + 4H_2O \tag{312}$$

As a generalisation we consider a reaction of the form

$$\nu_F^f F + \nu_O^f O \rightarrow P \tag{313}$$

where O denotes the oxydant, F the fuel and P the combustion products. Let $[X]$ denote the concentration of species X then the combustion reaction rate $\dot{\Omega}$ is given by

$$\dot{\Omega} = k(T)[O]^{\nu_O^f}[F]^{\nu_F^f} \tag{314}$$

and the reaction rates for the fuel and the oxydant are then

$$\dot{\omega}_O = \nu_O W_O \dot{\Omega} \tag{315}$$
$$\dot{\omega}_F = \nu_F W_F \dot{\Omega} \tag{316}$$

Note that $\nu_O = -\nu_O^f$ and $\nu_F = -\nu_F^f$.

As derived in the previous section we combine the equation for temperature and chemical species and obtain an equation describing the coupling between these quantities and the acoustic pressure

$$i\omega J \begin{pmatrix} \hat{Y}_O \\ \hat{Y}_F \\ \hat{T} \end{pmatrix} = \mathbf{b}(\hat{p}) + \mathbf{b}_\nabla(\hat{p}) \tag{317}$$

The coupling matrix J for the fuel-oxydant combustion reaction takes the form

$$J = i\omega\bar{\rho}I + \begin{pmatrix} \frac{\partial\bar{\omega}_O}{\partial Y_O} & \frac{\partial\bar{\omega}_O}{\partial Y_F} & \frac{\partial\bar{\omega}_O}{\partial T} \\ \frac{\partial\bar{\omega}_F}{\partial Y_O} & \frac{\partial\bar{\omega}_F}{\partial Y_F} & \frac{\partial\bar{\omega}_F}{\partial T} \\ -\sum_{s=O,F}\frac{h_s^0}{c_p}\frac{\partial\bar{\omega}_s}{\partial Y_O} & -\sum_{s=O,F}\frac{h_s^0}{c_p}\frac{\partial\bar{\omega}_s}{\partial Y_F} & -\sum_{s=O,F}\frac{h_s^0}{c_p}\frac{\partial\bar{\omega}_s}{\partial T} \end{pmatrix} \tag{318}$$

The terms on the right-hand side $\mathbf{b}(\hat{p})$ and $\mathbf{b}_\nabla(\hat{p})$ are given by

$$\mathbf{b}(\hat{p}) = -\frac{i\omega}{c^2}\begin{pmatrix} \frac{\partial\bar{\omega}_O}{\partial\rho} \\ \frac{\partial\bar{\omega}_F}{\partial\rho} \\ -\frac{i\omega c^2}{c_p} - \sum_{s=O,F}\frac{h_s^0}{c_p}\frac{\partial\bar{\omega}_s}{\partial\rho} \end{pmatrix}\hat{p}, \ \mathbf{b}_\nabla(\hat{p}) = \begin{pmatrix} \nabla\bar{Y}_O \\ \nabla\bar{Y}_F \\ \nabla\bar{T} \end{pmatrix}\bullet\nabla\hat{p} \tag{319}$$

We define the variable $\mathcal{H}$ as a global enthalpy of the combustion reaction

$$\mathcal{H} := \sum_{s=O,F} h_s^0\nu_s W_s \tag{320}$$

By introducing the vectors

$$\mathbf{u} = \begin{pmatrix} \nu_O W_O \\ \nu_F W_F \\ -\frac{\mathcal{H}}{c_p} \end{pmatrix}, \quad \mathbf{v} = \begin{pmatrix} \frac{\partial\bar{\dot{\Omega}}}{\partial Y_O} \\ \frac{\partial\bar{\dot{\Omega}}}{\partial Y_F} \\ \frac{\partial\bar{\dot{\Omega}}}{\partial T} \end{pmatrix} \tag{321}$$

we write the matrix J as rank-1 update of the diagonal matrix $i\omega\bar{\rho}I$ of dimension 3

$$J = i\omega\bar{\rho}I + \mathbf{u}\mathbf{v}^t \tag{322}$$

According to the Shermann-Morrison formula the inverse of the matrix J is given by

$$J^{-1} = \frac{I}{i\omega\bar{\rho}} - \frac{\mathbf{u}\mathbf{v}^t}{i\omega\bar{\rho}(i\omega\bar{\rho} + \mathbf{v}^t\mathbf{u})} \tag{323}$$

Also we rewrite the right-hand side vector $\mathbf{b}(\hat{p})$ as

$$\mathbf{b}(\hat{p}) = -\frac{i\omega}{c^2} \begin{pmatrix} \nu_O W_O \frac{\partial \overline{\dot{\Omega}}}{\partial \rho} \\ \nu_F W_F \frac{\partial \overline{\dot{\Omega}}}{\partial \rho} \\ -\frac{i\omega c^2}{c_p} - \frac{\mathcal{H}}{c_p}\frac{\partial \overline{\dot{\Omega}}}{\partial \rho} \end{pmatrix} \hat{p} \tag{324}$$

At this stage we remind the equation for the pressure modes

$$\nabla \bullet (c^2 \nabla \hat{p}) + \omega^2 \hat{p} = (\gamma - 1)i\omega \hat{Q}$$

$$\text{with} \quad \hat{Q} = -\sum_{s=1}^{N_s} h_s^0 \left(\nabla_Y \overline{\dot{\omega}}_s \bullet \hat{\mathbf{Y}} + \frac{\partial \overline{\dot{\omega}}_s}{\partial \rho}\hat{\rho} + \frac{\partial \overline{\dot{\omega}}_s}{\partial T}\hat{T} \right)$$

We used the additional equations to eliminate $\hat{Y}_s, \hat{T}$ and $\hat{\rho}$ from the pressure equation by inverting the coupling matrix J

$$\nabla \bullet (c^2 \nabla \hat{p}) + \omega^2 \hat{p} \quad + \quad i\omega \frac{(\gamma - 1)}{c^2}\sum_{s=1}^{N_s} h_s^0 \frac{\partial \overline{\dot{\omega}}_s}{\partial \rho}\hat{p} \tag{325}$$

$$= \quad -(\gamma - 1)\sum_{s=1}^{N_s} h_s^0 \left(\nabla_Y \overline{\dot{\omega}}_s \frac{\partial \overline{\dot{\omega}}_s}{\partial T} \right) J^{-1}(\mathbf{b}(\hat{p}) + \mathbf{b}_\nabla(\hat{p}))$$

Using the analytical expression for the inverse of J we obtain an equation with just two unknowns, namely the eigenpair $(\hat{p}, \omega)$.

$$i\omega^3 \overline{\rho}\hat{p} + \omega^2 \left(\nu_O W_O \frac{\partial \overline{\dot{\Omega}}}{\partial Y_O} + \nu_F W_F \frac{\partial \overline{\dot{\Omega}}}{\partial Y_F} - \frac{\mathcal{H}}{c_v}\frac{\partial \overline{\dot{\Omega}}}{\partial T} - \frac{\overline{\rho}\mathcal{H}}{c_p\overline{T}}\frac{\partial \overline{\dot{\Omega}}}{\partial \rho} \right) \hat{p} \tag{326}$$

$$+ \left(i\omega\overline{\rho} + \nu_O W_O \frac{\partial \overline{\dot{\Omega}}}{\partial Y_O} + \nu_F W_F \frac{\partial \overline{\dot{\Omega}}}{\partial Y_F} - \frac{\mathcal{H}}{c_p}\frac{\partial \overline{\dot{\Omega}}}{\partial T} \right) \nabla \bullet (c^2 \nabla \hat{p})$$

$$+ (\gamma - 1)\mathcal{H} \left(\frac{\partial \overline{\dot{\Omega}}}{\partial Y_O}\nabla \overline{Y_O} + \frac{\partial \overline{\dot{\Omega}}}{\partial Y_F}\nabla \overline{Y_F} + \frac{\partial \overline{\dot{\Omega}}}{\partial T}\nabla \overline{T} \right) \bullet \nabla \hat{p} = 0$$

Using the formula of the combustion reaction rate $\dot{\Omega}$ of the combustion we will provide the exact expression of the different steady-state terms appearing in the eigenvalue problem. To simplify notation let us introduce the three variables A, B and C defined as

$$A \quad := \quad \nu_O W_O \frac{\partial \overline{\dot{\Omega}}}{\partial Y_O} + \nu_F W_F \frac{\partial \overline{\dot{\Omega}}}{\partial Y_F} - \frac{\mathcal{H}}{c_v}\frac{\partial \overline{\dot{\Omega}}}{\partial T} - \frac{\overline{\rho}\mathcal{H}}{c_p\overline{T}}\frac{\partial \overline{\dot{\Omega}}}{\partial \rho} \tag{327}$$

$$B \quad := \quad \nu_O W_O \frac{\partial \overline{\dot{\Omega}}}{\partial Y_O} + \nu_F W_F \frac{\partial \overline{\dot{\Omega}}}{\partial Y_F} - \frac{\mathcal{H}}{c_p}\frac{\partial \overline{\dot{\Omega}}}{\partial T} \tag{328}$$

$$C \quad := \quad (\gamma - 1)\mathcal{H} \left(\frac{\partial \overline{\dot{\Omega}}}{\partial Y_O}\nabla \overline{Y_O} + \frac{\partial \overline{\dot{\Omega}}}{\partial Y_F}\nabla \overline{Y_F} + \frac{\partial \overline{\dot{\Omega}}}{\partial T}\nabla \overline{T} \right) \tag{329}$$

Using the total derivative of $\overline{\dot{\Omega}}$ we obtain an alternative expression for C which reads

$$C = (\gamma - 1)\mathcal{H}\left(\nabla\overline{\dot{\Omega}} - \frac{\partial\overline{\dot{\Omega}}}{\partial\rho}\nabla\overline{\rho}\right) \tag{330}$$

With the new variables A, B and C the cubic eigenvalue problem takes the form

$$\boxed{i\omega^3\overline{\rho}\hat{p} + \omega^2 A\hat{p} + (i\omega\overline{\rho} + B)\nabla \bullet (c^2\nabla\hat{p}) + C \bullet \nabla\hat{p} = 0} \tag{331}$$

The combustion reaction rate is given by

$$\dot{\Omega} = k(T)[O]^{-\nu_O}[F]^{-\nu_F} = k(T)\left(\frac{\rho Y_O}{W_O}\right)^{-\nu_O}\left(\frac{\rho Y_F}{W_F}\right)^{-\nu_F} \tag{332}$$

with the Arrehnius coefficient $k(T)$ being a temperature-dependent function

$$k(T) = A_0 T^\mu exp(-\frac{E^a}{\mathcal{R}T}) \tag{333}$$

Hence the derivatives of $\dot{\Omega}$ with respect to fuel and oxydant mass fractions Y_F, Y_O, to temperature T and density ρ are

$$\frac{\partial\dot{\Omega}}{\partial Y_F} = -\frac{\nu_F}{Y_F}\dot{\Omega} \tag{334}$$

$$\frac{\partial\dot{\Omega}}{\partial Y_O} = -\frac{\nu_O}{Y_O}\dot{\Omega} \tag{335}$$

$$\frac{\partial\dot{\Omega}}{\partial T} = \frac{E^a + \mu\mathcal{R}T}{\mathcal{R}T^2}\dot{\Omega} \tag{336}$$

$$\frac{\partial\dot{\Omega}}{\partial\rho} = -\frac{\nu_F + \nu_O}{\rho}\dot{\Omega} \tag{337}$$

With these analytical expressions for the derivatives we obtain for the three variables A, B and C

$$A = \left(-\frac{\nu_O^2 W_O}{Y_O} - \frac{\nu_F^2 W_F}{Y_F} - \frac{\mathcal{H}}{c_v}\frac{E^a + \mu\mathcal{R}\overline{T}}{\mathcal{R}\overline{T}^2} + \frac{(\nu_F + \nu_O)\mathcal{H}}{c_p\overline{T}}\right)\overline{\dot{\Omega}} \tag{338}$$

$$B = \left(-\frac{\nu_O^2 W_O}{Y_O} - \frac{\nu_F^2 W_F}{Y_F} - \frac{\mathcal{H}}{c_p}\frac{E^a + \mu\mathcal{R}\overline{T}}{\mathcal{R}\overline{T}^2}\right)\overline{\dot{\Omega}} \tag{339}$$

$$C = (\gamma - 1)\mathcal{H}\left(-\frac{\nu_O}{Y_O}\nabla\overline{Y_O} - \frac{\nu_F}{Y_F}\nabla\overline{Y_F} + \frac{E^a + \mu\mathcal{R}\overline{T}}{\mathcal{R}\overline{T}^2}\nabla\overline{T}\right)\overline{\dot{\Omega}} \tag{340}$$

or alternatively for C

$$C = (\gamma - 1)\mathcal{H}\left(\nabla\overline{\dot{\Omega}} + \frac{\nu_F + \nu_O}{\rho}\dot{\Omega}\nabla\overline{\rho}\right) \tag{341}$$

Remarks :

- We should note that the expressions for the derivatives of $\dot{\Omega}$ with respect to the mass fractions Y_F and Y_O are only valid for $\dot{\Omega} \neq 0$, i.e. $Y_F \neq 0$ and $Y_O \neq 0$. If any of the mass fractions is zero, then clearly $\dot{\Omega} = 0$ and the derivatives $\frac{\partial \dot{\Omega}}{\partial Y}$ are set to be zero as well.

$$\frac{\partial \dot{\Omega}}{\partial Y} = \begin{cases} 0 & \text{if } Y, \dot{\Omega} = 0 \\ -\frac{\nu}{Y}\dot{\Omega} & \text{else} \end{cases} \tag{342}$$

- Assuming that there is no combustion reaction, i.e. $\dot{\Omega} = 0$, then the three variables A, B and C vanish and the eigenvalue problem takes the form

$$i\omega(\nabla \bullet (c^2 \nabla \hat{p}) + \omega^2 \hat{p}) = 0 \tag{343}$$

Since the frequency number ω cannot be zero we recover the original Helmholtz equation.

- If we assume that the reaction is active but thermally neutral, i.e. no heat release ($\mathcal{H} = 0$), then only the variable C vanishes whereas the variables A and B become equal

$$A = B = -\left(\frac{\nu_O^2 W_O}{Y_O} + \frac{\nu_F^2 W_F}{Y_F}\right)\overline{\dot{\Omega}} \tag{344}$$

and the cubic eigenvalue problem takes the form

$$(i\omega\overline{\rho} + A)(\nabla \bullet (c^2 \nabla \hat{p}) + \omega^2 \hat{p}) = 0 \tag{345}$$

The complex number $i\omega\overline{\rho} + A$ corresponds exactly to the term $i\omega\overline{\rho} + \mathbf{v}^t\mathbf{u}$ and is a factor appearing in the determinant of the matrix J which is for the special case of a single-step reaction mechanism

$$det(J) = i\omega\overline{\rho}(i\omega\overline{\rho} + \mathbf{v}^t\mathbf{u}) \tag{346}$$

As already shown the matrix J is invertible and the complex number $i\omega\overline{\rho} + A$ is nonzero. Hence in the absence of heat release, i.e. $\mathcal{H} = 0$, we recover the original Helmholtz equation without source terms as expected

$$\nabla \bullet (c^2 \nabla \hat{p}) + \omega^2 \hat{p} = 0 \tag{347}$$

Once we solved the eigenvalue problem for the pressure modes it is possible to obtain the modeshapes of the velocity and of the density

$$\hat{\mathbf{u}} = \frac{1}{i\omega\overline{\rho}}\nabla\hat{p}, \quad \hat{\rho} = \frac{1}{c^2}\hat{p} \tag{348}$$

The modeshapes of the chemical species and of the temperature are obtained using

$$\begin{pmatrix} \hat{Y}_O \\ \hat{Y}_F \\ \hat{T} \end{pmatrix} = \frac{J^{-1}}{i\omega}(\mathbf{b}(\hat{p}) + \mathbf{b}_\nabla(\hat{p})) \tag{349}$$

By inserting the expression of the inverse matrix we obtain

$$
\begin{pmatrix} \hat{Y}_O \\ \hat{Y}_F \\ \hat{T} \end{pmatrix} = -\frac{1}{\overline{\rho}\omega^2} \left(I - \frac{\mathbf{u}\mathbf{v}^t}{i\omega\overline{\rho} + \mathbf{v}^t\mathbf{u}} \right) (\mathbf{b}(\hat{p}) + \mathbf{b}_\nabla(\hat{p}))
$$
(350)

which is equivalent to

$$
\begin{pmatrix} \hat{Y}_O \\ \hat{Y}_F \\ \hat{T} \end{pmatrix} = \frac{1}{i\omega\overline{\rho}c^2} \left[\frac{-\frac{i\omega c^2}{c_p}\frac{\partial\overline{\dot{\Omega}}}{\partial T} + \mathbf{v}^t\mathbf{u}\frac{\partial\overline{\dot{\Omega}}}{\partial\rho}}{i\omega\overline{\rho} + \mathbf{v}^t\mathbf{u}} \begin{pmatrix} \nu_O W_O \\ \nu_F W_F \\ -\frac{\mathcal{H}}{c_p} \end{pmatrix} - \begin{pmatrix} \nu_O W_O \frac{\partial\overline{\dot{\Omega}}}{\partial\rho} \\ \nu_F W_F \frac{\partial\overline{\dot{\Omega}}}{\partial\rho} \\ -\frac{i\omega c^2}{c_p} - \frac{\mathcal{H}}{c_p}\frac{\partial\overline{\dot{\Omega}}}{\partial\rho} \end{pmatrix} \right] \hat{p}
$$
(351)

$$
+ \frac{1}{i\omega} \left[\left(\begin{pmatrix} \nabla\overline{Y}_O \\ \nabla\overline{Y}_F \\ \nabla\overline{T} \end{pmatrix} - \frac{\frac{\partial\overline{\dot{\Omega}}}{\partial Y_O}\nabla\overline{Y}_O + \frac{\partial\overline{\dot{\Omega}}}{\partial Y_F}\nabla\overline{Y}_F + \frac{\partial\overline{\dot{\Omega}}}{\partial T}\nabla\overline{T}}{i\omega\overline{\rho} + \mathbf{v}^t\mathbf{u}} \begin{pmatrix} \nu_O W_O \\ \nu_F W_F \\ -\frac{\mathcal{H}}{c_p} \end{pmatrix} \right) \bullet \hat{\mathbf{u}} \right]
$$
(352)

By simplifying these equations we get the modeshapes of species and temperature

$$
\begin{pmatrix} \hat{Y}_O \\ \hat{Y}_F \\ \hat{T} \end{pmatrix} = \frac{1}{i\omega\overline{\rho} + \mathbf{v}^t\mathbf{u}} \begin{pmatrix} -\nu_O W_O \left(\frac{1}{\overline{\rho}c_p}\frac{\partial\overline{\dot{\Omega}}}{\partial T} + \frac{1}{c^2}\frac{\partial\overline{\dot{\Omega}}}{\partial\rho} \right) \\ -\nu_F W_F \left(\frac{1}{\overline{\rho}c_p}\frac{\partial\overline{\dot{\Omega}}}{\partial T} + \frac{1}{c^2}\frac{\partial\overline{\dot{\Omega}}}{\partial\rho} \right) \\ \frac{1}{c_p} \left(i\omega + \frac{\nu_O W_O}{\overline{\rho}}\frac{\partial\overline{\dot{\Omega}}}{\partial Y_O} + \frac{\nu_F W_F}{\overline{\rho}}\frac{\partial\overline{\dot{\Omega}}}{\partial Y_F} + \frac{\mathcal{H}}{c^2}\frac{\partial\overline{\dot{\Omega}}}{\partial\rho} \right) \end{pmatrix} \hat{p}
$$
(353)

$$
+ \frac{1}{i\omega} \left[\left(\begin{pmatrix} \nabla\overline{Y}_O \\ \nabla\overline{Y}_F \\ \nabla\overline{T} \end{pmatrix} - \frac{\frac{\partial\overline{\dot{\Omega}}}{\partial Y_O}\nabla\overline{Y}_O + \frac{\partial\overline{\dot{\Omega}}}{\partial Y_F}\nabla\overline{Y}_F + \frac{\partial\overline{\dot{\Omega}}}{\partial T}\nabla\overline{T}}{i\omega\overline{\rho} + \mathbf{v}^t\mathbf{u}} \begin{pmatrix} \nu_O W_O \\ \nu_F W_F \\ -\frac{\mathcal{H}}{c_p} \end{pmatrix} \right) \bullet \hat{\mathbf{u}} \right]
$$
(354)

9.4   Test case

The scope of this test case is to validate the model equations and to compare the eigenmodes of a tube obtained by taking into account a chemical reaction with the eigenmodes of the same tube but neglecting the reaction effects, i.e. without source terms.

For an easy comparison we choose the undergoing reaction to be **weakly exothermic**. For example we might take the parameter Θ defined in (209) to be $\Theta = 1.1$.

With the benchmark assumptions defined in the previous section, we consider a reactive fluid flowing through a tube. The boundary conditions imposed are of Dirichlet at the inlet and of Neumann at the outlet. Therefore the pressure modes are sucht that

$$
\hat{p}|_{inlet} = 0, \quad \left.\frac{\partial\hat{p}}{\partial n}\right|_{outlet} = 0
$$
(355)

By taking the chemical source terms into account the eigenvalue problem is cubic

$$
i\omega^3\overline{\rho}\hat{p} + \omega^2 A\hat{p} + (i\omega\overline{\rho} + B)\frac{\partial}{\partial x}\left(c^2\frac{\partial\hat{p}}{\partial x} \right) + C\frac{\partial\hat{p}}{\partial x} = 0
$$
(356)

whereas in the homogeneous case it is linear

$$\frac{\partial}{\partial x}\left(c^2\frac{\partial\hat{p}}{\partial x}\right) + \omega^2\hat{p} = 0 \tag{357}$$

Using the finite element method [1] described in the appendix we discretize the eigenvalue problem in both cases and solve for the eigenpair $(\hat{p}, \omega)$. By using an adaptive meshing algorithm we are able to accurately resolve the reaction front and have a coarser mesh in the regions of small gradients. This makes the number of grid points needed reasonable and the solution procedure quite fast.

First of all we would like to compare the eigenspectrum in both cases. As expected the eigenvalues $\lambda = -i\omega$ obtained for the homogeneous Helmholtz equation are pure imaginary numbers, i.e. the eigenmodes do not show any growth or decay. For the cubic eigenvalue problem the obtained eigenvalues λ appear always in pairs as complex conjugate eigenvalues. This means that depending on the sign of $\Re(\lambda)$ the eigenmodes will be growing or decaying or eventually remain unchanged if λ is pure imaginary. The following figure shows the eigenspectrum of both cases.
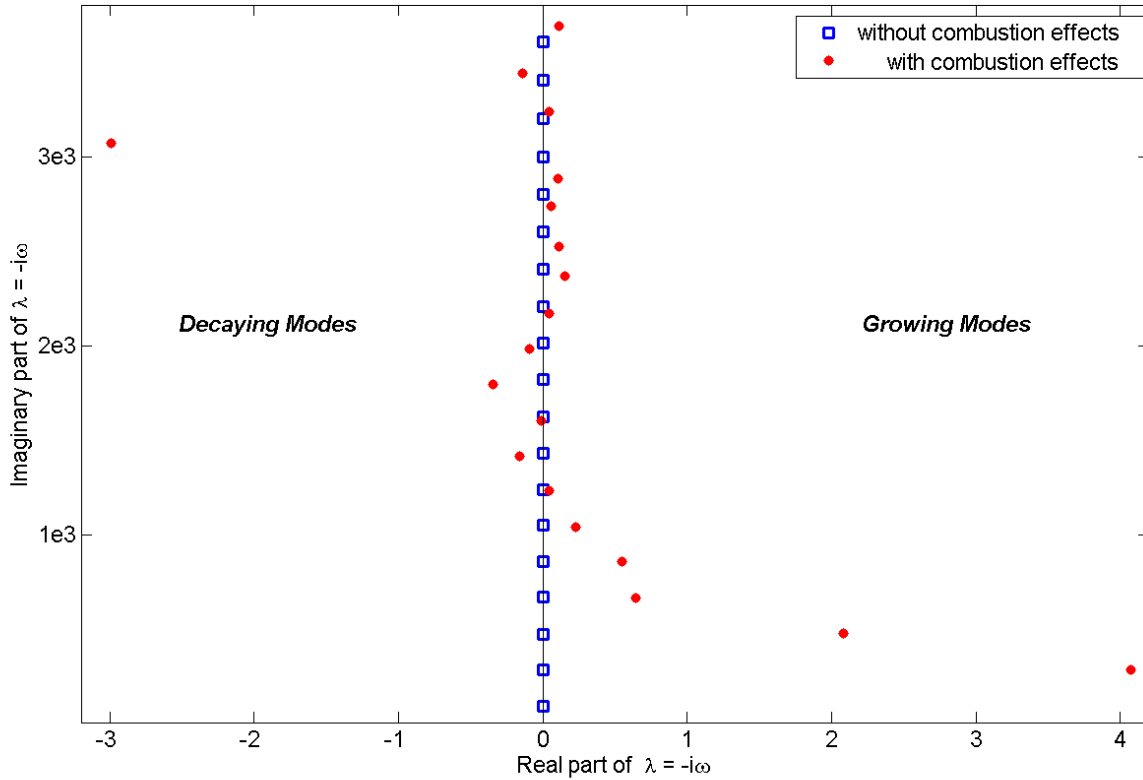

Figure 15: Imaginary part vs. Real part of eigenvalue $\lambda = -i\omega$ with and without combustion effects

We note that taking combustion effects into accounts not only alters the real part of the eigenvalue to become either positive (i.e. growing mode) or negative (decaying mode) but it also shifts the frequency

of the mode. As shown in figure (15) there is no global trend which applies to all modes. We note that some modes get a higher frequency and become decaying while others decrease their frequency and grow in time. This confirms that the effect of the combustion on the eigenmodes and on their stability is quite complex and should not be neglected.
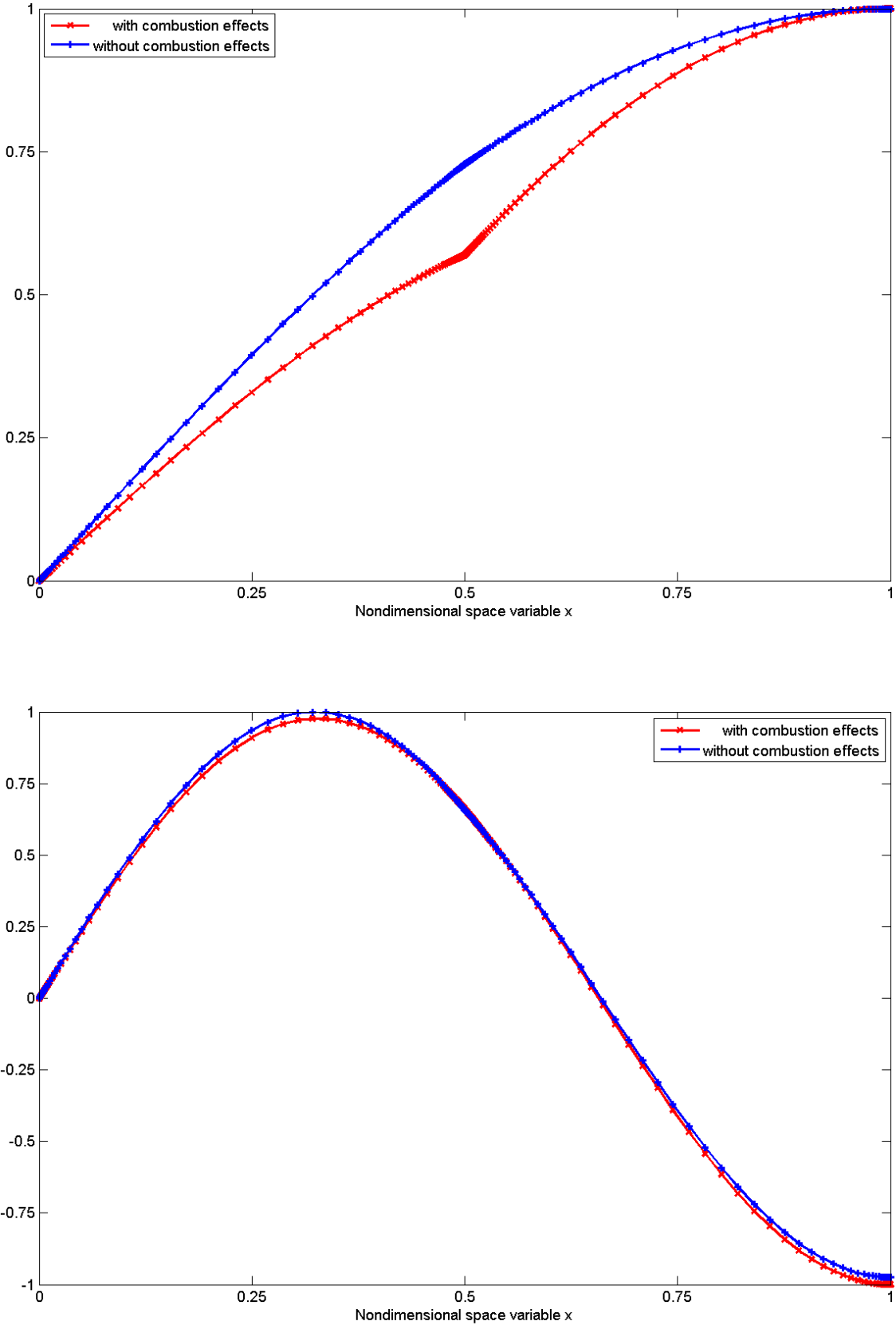
Figure 16: First (upper figure) and second pressure eigenmodes

10   Conclusion

The subject of this thesis is the study of thermo-acoustic instabilities appearing in ultra-low emission gas turbines. The enorm potential of lean premixed combustion in reducing the NOx emissions can be widely used only if the thermo-acoustic instabilities inherent to this combustion regime are eliminated. Hence these instabilities represent one of the major obstacles towards cleaner gas turbines.

In this thesis we derived the mathematical equations describing the reactive flows inside the combustion chambers of gas turbines. The Navier-Stokes equations have been extended to include the effects of chemical reactions. Of particular interest is the equation relating the pressure field to the heat release. To describe the instationary properties of the combustion system we derived the equations of the unsteady variables of interest such as the pressure, the temperature and the chemical composition of the flow. As our primary scope is finding the eigenmodes and assessing their stability, we transformed the unsteady reactive Navier-Stokes equations in the frequency domain and obtained a system of coupled eigenvalue problems. This system shows the interaction between the pressure fluctuations, the unsteady heat release and the chemical components. Such a system can only be solved if an additional equation, called flame transfer function, is provided. This function describes the unsteady heat release as a function of the pressure and velocity fluctuations. In this thesis a novel model has been developed. The flame transfer function developed in this thesis does not involve any model parameters or empiric assumptions. To the author's knowledge such a model is developed for the first time. Since it does not include any parameters it can be used in many applications. It is based on an approach which takes advantage of the physical as well as mathematical properties of the system to find a closed-form expression for the unsteady heat release. The developed model does not link the unsteady heat release directly to the pressure and velocity fluctations. It accurately describes how the fluctuations in temperature, density and chemical components affect the heat release cycle. In a further step we derive partial differential equations which couple these influence factors to the pressure and velocity fluctuations through an operator $\mathcal{J}$. We investigate this mathematical operator and show that it is invertible for any reaction mechanism. By inverting the operator $\mathcal{J}$ we obtain the equation of the unsteady heat release as a direct function of the pressure and velocity fluctuations without any empirical assumptions or model parameters. With this result it is possible to study the dynamics the thermo-acoustic system in the frequency domain as presented in this thesis or in the time-domain as presented in a report to be submitted for publication.

Using the model of the unsteady heat release we derived an eigenvalue problem with only the pressure modes as unknown. We showed that the cubic eigenvalue problem obtained is an extension of the homogeneous Helmholtz equation. Using adaptive mesh generation and finite element discretization we solved both eigenvalue problems with high accuracy. The comparison of the pressure eigenmodes obtained in both cases shows that the combustion effects are complex. In fact it does not only affect the stability of the system but also shifts its eigenfrequencies. The mode shapes are also altered particularly at the flame zone. At the present stage no clear trend could be identified on how combustion makes some modes go unstable while it dissipates other. This represents a very interesting problem. Answers could be provided through a sensitivity analysis of the eigenfrequencies to combustion parameters.

References

References

[1]   G. Allaire : Numerical Analysis and Optimization, Oxford 2007

[2]   K. Arens, S. Bethke, U. Wever : Numerical simulation and modeling of 3D nonlinear thermoacoustics in gasturbines. Eccomas Conference on Computational Combustion Lissabon (2005)

[3]   T. Arima : Numerical methods for chemically reacting fluid flow computation under low-Mach number approximation, Tokyo J. Math. Vol 29, 1, 2006

[4]   N. Sharduldeo, F. Culick : Reduced order modeling and dynamics of nonlinear acoustic waves in a combustion chamber, Combust. Sci. and Tech., 177: 221247, 2005

[5]   K. Annamalai, I. Puri : Advanced Thermodynamics Engineering, CRC Press 2001

[6]   C. Baukal : Heat Transfer in Industrial Combustion, CRC Press 2000

[7]   C. Baukal : Industria1 Combustion Pollution and Control, Dekker 2004

[8]   L. Belfiore : Transport phenomena for chemical reactor design, Wiley 2003

[9]   R. Borghi, M. Champion : Modelisation et theorie des flammes, Editions Technip 2000

[10]   M. Boyce : Gas Turbine Engineering Handbook, second edition, Gulf Professional Publishing 2001

[11]   M. Bruneau : Fundamentals of Acoustics, Societe Francaise d'Acoustique 2006

[12]   H. Chiu, M. Summerfield : Theory of combustion noise, Acta Astronautica. Vol. 1, pp. 967-984, 1974

[13]   R. Courant, K. Friedrichs, H. Lewy : Über die partiellen Differentialgleichungen der mathematischen Physik, Math. Annalen 1928

[14]   H. Coward, G. Jones : Limits of flammability of gases and vapours, Technical Report 503, U. S. Bureau of Mines, 1952

[15]   L. Crocco : Aspects of combustion instability in liquid solid propellant rocket motors, Part 1. J. American Rocket Society (1951) 21

[16]   L. Crocco : Aspects of combustion instability in liquid solid propellant rocket motors, Part 2. J. American Rocket Society (1952) 22

[17]   F. Culick, Some recent results for nonlinear acoustic in combustion chambers, AIAA Journal 1994. 32(1) : p. 146-169

[18]   S. Dixon : Fluid Mechanics, Thermodynamics of Turbomachinery, 5th Edition, Elsevier 2005

[19]   F. El-Mahallawy, S. El-Din Habik : Fundamentals and technology of combustion, Elsevier 2002

[20]   G. Engl, P. Rentrop : Gas flow in a single cylinder internal combustion engine: a model and its numerical treatment. Int. J. Num. Meth. Heat Fluid Flow 2 (1992) 63-78

[21]   S. Evesque : Adaptive Control of Combustion Oscillations, Ph.D. thesis, University of Cambridge 2000

[22]   B. Finlayson : Introduction to Chemical Engineering Computing, Wiley 2006

[23]   M. Fleifil, A. Annaswamy, Z. Ghoniem, A. Ghoniem : Response of a laminar premixed flame to flow oscillations: A kinematic model and thermoacoustic instability result Combustion and Flame,vol.106, pp.487510, 1996

[24]   P. Flohr, C. Paschereit, and V. Bellucci : Steady CFD Analysis for Gas Turbine Burner Transfer Functions. in 41st AIAA Aerospace Sciences Meeting 2003

[25]   A. Hmaidi : Mathematical modeling and numerical simulation of reactive 1-D Euler gas equations. Bachelor's thesis, Munich University of Technology 2005

[26]   A. Hmaidi, A. McIntosh, J. Brindley : A mathematical model of hotspot condensed phase ignition in the presence of a competitive endothermic reaction, Combustion Theory and Modeling, in review

[27]   A. Hmaidi, P. Rentrop : Differential DAE Index for Reactive Euler Equations, Numerical Mathematics and Advanced Applications Proceedings of ENUMATH 2007

[28]   W. Krebs, G. Walz, and S. Hoffmann. Thermoacoustic analysis of annular combustor. in 5th AIAA Aeroacoustics Conference. 1999

[29]   F. Kreith, R. Boehm, et. al. : Heat and Mass Transfer, Mechanical Engineering Handbook, CRC Press 1999

[30]   K. Leung, R. Lindstedt and W. Jones : Reduced Kinetic Mechanisms for Applications in Combustion Systems, Springer 1993

[31]   R. J. LeVeque : Numerical methods for conservation laws, Birkhäuser Verlag 1992

[32]   T. Lieuwen and B. Zinn : The Role of Equivalence Ratio Oscillations In Driving Combustion Instabilities In Low NOx Gas Turbines, Proc. of the Combustion Institute, 1998. 27 : p. 1809-1816

[33]   A. Linan, F. Williams : Fundamental Aspects of Combustion, Oxford University Press 1993

[34]   A. McIntosh : The interaction of acoustics and compressible combustion fronts - application to flames in tubes, 17th Colloquium on the dynamics of explosions and reactive systems 1999

[35]   A. McIntosh : Flame Resonance in Tubes, Combustion Science and Technology 1990, 69

[36]   G. Merker, C. Schwarz, G. Stiesch, F. Otto : Simulating Combustion, Springer 2006

[37]   R. Missen et al : Introduction to chemical reaction engineering and kinetics, Wiley 1999

[38]   E.S. Oran, J.P. Boris : Numerical Simulation of Reacting Flows, Elsevier 1987

[39]   N. Peters : Turbulent combustion, Cambridge University Press 2000.

[40]   T. Poinsot, D. Veynante : Combustion, in Encyclopedia of Computational Mechanics, Wiley 2004

[41]   T. Poinsot, D. Veynante : Theoretical and numerical combustion, 2nd edition, Edwards 2005

[42]   R. Raun, M. Beckstead, J. Finlinson, K. Brooks : Review of Rijke Tubes, Rijke Burners and Related Devices, Energy Combustion Science 1993, 19

[43]   L. Rayleigh : The explanation of certain acoustic phenomena. Nature (1971), 319321

[44]   R. Rook, L. de Goey : Response of Burner-stabilized Flat Flames to Acoustic Perturbations, Combustion Theory and Modeling 2002, 6

[45]   R. Saigal : On the inverse of a matrix with several rank one updates, technical report 93-41, University of Michigan 1993

[46]   K. Schreel, L. de Goey, D. Roekaerts : Course on Combustion, J.M. Burgerscentrum, TU Eindhoven 2005

[47]   S. Turns : Introduction to Combustion : Concepts and Applications, 2nd edition, McGraw-Hill 2000

[48]   US Environmental Protection Agency : NOx Emissions from Stationary Gas Turbines, Report 1993

[49]   J. Warnatz, U. Maas, R.W. Dibble : Verbrennung : Physikalisch-Chemische Grundlagen, Modellierung und Simulation, Experimente, Schadstoffentstehung, Springer 2001

[50]   Y. Zeldovich, D. Frank-Kamenetzki. Theorie thermischer Flammenausbreitung. Zh. Fiz. Khim., 12:100, 1938

[51]   M. Zhu, A. Dowling, K. Bray : Transfer function calculations for aeroengine combustion oscillations, ASME Transactions, Engineering for Gas Turbines and Power 2005, 127 (1)

[52]   JANAF Thermochemical Tables, 3rd edition, Journal of Physical and Chemical Reference Data 14(1985) Supplement 1, http://www.galcit.caltech.edu/EDL/public/thermo.html

[53]   NIST scientific databases : NIST Chemistry WebBook - NIST Standard Reference Database Number 69, June 2005 Release http://webbook.nist.gov/chemistry/

Appendix

Rayleigh criterion

The Rayleigh criterion says basically that an acoustic wave will amplify if its pressure and heat release are in phase. The mathematical formulation of this criterion is that instability will occur if the integral over a cycle of the product of the pressure and the unsteady heat release is larger than the energy dissipation :

$$\int_0^{T_{osc}} \int_{V_f} \left[p'(x,t)\dot{Q}'(x,t) - \phi(x,t) \right] dxdt > 0 \Rightarrow \text{Instability} \tag{1}$$

$p'(x,t)$ represents the acoustic pressure and $\dot{Q}'(x,t)$ the unsteady heat release. $\phi(x,t)$ denotes the wave energy dissipation which will be neglected in the following.
The acoustic energy density e' is the sum of the kinetic acoustic energy and the potential kinetic energy. In a one-dimensional flow it takes the form

$$e' = \frac{\overline{\rho}u'^2}{2} + \frac{p'2}{2\overline{\rho}c^2} \tag{2}$$

Assuming that the mean flow velocity $\overline{u}$ as well as the steady pressure gradient $\frac{\partial \overline{p}}{\partial x}$ are negligible, the acoustic pressure and velocity equations take the form

$$\frac{\partial p'}{\partial t} + \gamma\overline{p}\frac{\partial u'}{\partial x} = (\gamma - 1)\dot{Q}' \tag{3}$$

$$\frac{\partial u'}{\partial t} + \frac{1}{\overline{\rho}}\frac{\partial p'}{\partial x} = 0 \tag{4}$$

Using the definition of the acoustic energy and of the sound speed $c^2 = \frac{\gamma\overline{p}}{\rho}$, it is possible to combine the last two equations to obtain an equation describing the evolution of the acoustic energy

$$\frac{\partial e'}{\partial t} + \frac{\partial(p'u')}{\partial x} = \frac{\gamma - 1}{\gamma\overline{p}}p'\dot{Q}' \tag{5}$$

Let L be the length of the combustor and T_{osc} be the period of acoustic oscillation. Integrating this equation temporally over the period of oscillation and spatially over the length of the combustor yields

$$\int_0^L [e'(x,t)]_0^{T_{osc}} dx = -\int_0^{T_{osc}} [p'(x,t)u'(x,t)]_0^L dt + \frac{\gamma - 1}{\gamma\overline{p}} \int_0^{T_{osc}} \int_0^L p'\dot{Q}' dxdt \tag{6}$$

The left-hand side of this equation represents the change in the acoustic energy along the combustor during an oscillation period. The first term on the right-hand side denotes the acoustic energy flux across the boundary and is typically small or inexistent. Assuming no energy flux across the control surface, i.e. $[p'(x,t)u'(x,t)]_0^L = 0$, we get the following relation

$$\int_0^L [e'(x,t)]_0^{T_{osc}} dx = \frac{\gamma - 1}{\gamma\overline{p}} \int_0^{T_{osc}} \int_0^L p'\dot{Q}' dxdt \tag{7}$$

It becomes clear that if the Rayleigh criterion is satisfied, i.e. the acoustic pressure and heat release are in phase, then there will be an increase in the acoustic energy in the combustion system and instabilities are encouraged.

$$\boxed{\int_0^{T_{osc}} \int_0^L p'(x,t)\dot{Q}'(x,t)dxdt > 0 \Rightarrow \quad \text{Instability}} \tag{8}$$

The difficulty of this criterion is that the heat release is part of the solution and not known a priori.

Linearized reactive Navier-Stokes equations

Let $Y_i = \frac{\rho_i}{\rho}$, ω_i denote the mass fraction, the production rate of species i

Continuity Equation

$$\frac{\partial \rho}{\partial t} + \frac{\partial (\rho u_j)}{\partial x_j} = 0 \tag{9}$$

Conservation of mass of species i

$$\frac{\partial \rho_i}{\partial t} + \frac{\partial (\rho_i u_j)}{\partial x_j} = \frac{\partial}{\partial x_j}(\rho \mathcal{D}_i \frac{\partial}{\partial x_j}(\frac{\rho_i}{\rho})) + \omega_i \tag{10}$$

We may write the lhs of this equation as

$$
\begin{aligned}
\frac{\partial \rho_i}{\partial t} + \frac{\partial (\rho_i u_j)}{\partial x_j} &= \frac{\partial \rho Y_i}{\partial t} + \frac{\partial (\rho Y_i u_j)}{\partial x_j} \\
&= \rho \frac{\partial Y_i}{\partial t} + Y_i(\frac{\partial \rho}{\partial t} + \frac{\partial (\rho u_j)}{\partial x_j}) + \rho u_j \frac{\partial Y_i}{\partial x_j} \\
&= \rho(\frac{\partial Y_i}{\partial t} + u_j \frac{\partial Y_i}{\partial x_j})
\end{aligned}
\tag{11}
$$

Hence we get the following 1-D equation :

$$\rho(\frac{\partial Y_i}{\partial t} + u \frac{\partial Y_i}{\partial x}) = \frac{\partial}{\partial x}(\rho \mathcal{D}_i \frac{\partial Y_i}{\partial x}) + \omega_i \tag{12}$$

and 3-D equation :

$$\rho(\frac{\partial Y_i}{\partial t} + \mathbf{u} \bullet \nabla Y_i) = \nabla \bullet (\rho \mathcal{D}_i \nabla Y_i) + \omega_i \tag{13}$$

Reynolds Average Ansatz :

$$\rho = \bar{\rho} + \rho' \ , u = \bar{u} + u' \ , Y = \bar{Y} + Y' \ , \omega = \bar{\omega} + \omega' \tag{14}$$

The steady-state variables satisfy :

$$\bar{\rho} \bar{u}_j \frac{\partial \bar{Y}_i}{\partial x_j} = \frac{\partial}{\partial x_j}(\bar{\rho} \mathcal{D}_i \frac{\partial \bar{Y}_i}{\partial x_j}) + \bar{\omega}_i \tag{15}$$

The equation for the fluctuations in the conservation equation of species i

$$(1 + \frac{\rho'}{\bar{\rho}})(\frac{\partial Y_i'}{\partial t} + \bar{u}_j \frac{\partial Y_i'}{\partial x_j} + u_j' \frac{\partial \bar{Y}_i}{\partial x_j} + u_j' \frac{\partial Y_i'}{\partial x_j}) + \frac{\rho'}{\bar{\rho}} \bar{u}_j \frac{\partial \bar{Y}_i}{\partial x_j} = \frac{1}{\bar{\rho}} \frac{\partial}{\partial x_j}(\rho' \mathcal{D}_i \frac{\partial \bar{Y}_i}{\partial x_j} + (\bar{\rho} + \rho')\mathcal{D}_i \frac{\partial Y_i'}{\partial x_j}) + \frac{1}{\bar{\rho}} \omega_i' \tag{16}$$

Neglecting the nonlinearities, this equation simplifies to

$$\frac{\partial Y_i'}{\partial t} + \bar{u}_j \frac{\partial Y_i'}{\partial x_j} + u_j' \frac{\partial \bar{Y}_i}{\partial x_j} + \frac{\rho'}{\bar{\rho}} \bar{u}_j \frac{\partial \bar{Y}_i}{\partial x_j} = \frac{1}{\bar{\rho}} \frac{\partial}{\partial x_j}(\rho' \mathcal{D}_i \frac{\partial \bar{Y}_i}{\partial x_j}) + \frac{1}{\bar{\rho}} \frac{\partial}{\partial x_j}(\bar{\rho} \mathcal{D}_i \frac{\partial Y_i'}{\partial x_j}) + \frac{1}{\bar{\rho}} \omega_i' \tag{17}$$

which yields in 1-D

$$
\begin{aligned}
\bar{\rho} \bar{u} \frac{\partial \bar{Y}_i}{\partial x} &= \frac{\partial}{\partial x}(\bar{\rho} \mathcal{D}_i \frac{\partial \bar{Y}_i}{\partial x}) + \bar{\omega}_i \\
\frac{\partial Y_i'}{\partial t} + \bar{u} \frac{\partial Y_i'}{\partial x} + u' \frac{\partial \bar{Y}_i}{\partial x} + \frac{\rho'}{\bar{\rho}} \bar{u} \frac{\partial \bar{Y}_i}{\partial x} &= \frac{1}{\bar{\rho}} \frac{\partial}{\partial x}(\rho' \mathcal{D}_i \frac{\partial \bar{Y}_i}{\partial x}) + \frac{1}{\bar{\rho}} \frac{\partial}{\partial x}(\bar{\rho} \mathcal{D}_i \frac{\partial Y_i'}{\partial x}) + \frac{1}{\bar{\rho}} \omega_i'
\end{aligned}
$$

and in 3-D

$$
\begin{aligned}
\bar{\rho} \bar{\mathbf{u}} \bullet \nabla \bar{Y}_i &= \nabla \bullet (\bar{\rho} \mathcal{D}_i \nabla \bar{Y}_i) + \bar{\omega}_i \\
\frac{\partial Y_i'}{\partial t} + \bar{\mathbf{u}} \bullet \nabla Y_i' + \mathbf{u}' \bullet \nabla \bar{Y}_i + \frac{\rho'}{\bar{\rho}} \bar{\mathbf{u}} \bullet \nabla \bar{Y}_i &= \frac{1}{\bar{\rho}} \nabla \bullet (\rho' \mathcal{D}_i \nabla \bar{Y}_i) + \frac{1}{\bar{\rho}} \nabla \bullet (\bar{\rho} \mathcal{D}_i \nabla Y_i') + \frac{1}{\bar{\rho}} \omega_i'
\end{aligned}
$$

Matrix Notation :

$$
\begin{pmatrix} Y'_1 \\ \vdots \\ Y'_i \\ \vdots \\ Y'_N \end{pmatrix}_t
+
\begin{pmatrix} \bar{u} & 0 & 0 & 0 & 0 \\ 0 & \ddots & 0 & 0 & 0 \\ 0 & 0 & \bar{u} & 0 & 0 \\ 0 & 0 & 0 & \ddots & 0 \\ 0 & 0 & 0 & 0 & \bar{u} \end{pmatrix}
\begin{pmatrix} Y'_1 \\ \vdots \\ Y'_i \\ \vdots \\ Y'_N \end{pmatrix}_x
+
\begin{pmatrix} \bar{v} & 0 & 0 & 0 & 0 \\ 0 & \ddots & 0 & 0 & 0 \\ 0 & 0 & \bar{v} & 0 & 0 \\ 0 & 0 & 0 & \ddots & 0 \\ 0 & 0 & 0 & 0 & \bar{v} \end{pmatrix}
\begin{pmatrix} Y'_1 \\ \vdots \\ Y'_i \\ \vdots \\ Y'_N \end{pmatrix}_y
$$

$$
+
\begin{pmatrix} \bar{w} & 0 & 0 & 0 & 0 \\ 0 & \ddots & 0 & 0 & 0 \\ 0 & 0 & \bar{w} & 0 & 0 \\ 0 & 0 & 0 & \ddots & 0 \\ 0 & 0 & 0 & 0 & \bar{w} \end{pmatrix}
\begin{pmatrix} Y'_1 \\ \vdots \\ Y'_i \\ \vdots \\ Y'_N \end{pmatrix}_z
+
\begin{pmatrix} (\frac{\rho'}{\bar{\rho}}\bar{\mathbf{u}} + \mathbf{u}') \bullet \nabla \bar{Y}_1 \\ \vdots \\ (\frac{\rho'}{\bar{\rho}}\bar{\mathbf{u}} + \mathbf{u}') \bullet \nabla \bar{Y}_i \\ \vdots \\ (\frac{\rho'}{\bar{\rho}}\bar{\mathbf{u}} + \mathbf{u}') \bullet \nabla \bar{Y}_N \end{pmatrix}
$$

$$
=
\begin{pmatrix} \frac{1}{\bar{\rho}}\nabla \bullet (\rho' \mathcal{D}_1 \nabla \bar{Y}_1) + \frac{1}{\bar{\rho}}\nabla \bullet (\bar{\rho}\mathcal{D}_1 \nabla Y'_1) \\ \vdots \\ \frac{1}{\bar{\rho}}\nabla \bullet (\rho' \mathcal{D}_i \nabla \bar{Y}_i) + \frac{1}{\bar{\rho}}\nabla \bullet (\bar{\rho}\mathcal{D}_i \nabla Y'_i) \\ \vdots \\ \frac{1}{\bar{\rho}}\nabla \bullet (\rho' \mathcal{D}_N \nabla \bar{Y}_N) + \frac{1}{\bar{\rho}}\nabla \bullet (\bar{\rho}\mathcal{D}_N \nabla Y'_N) \end{pmatrix}
+
\begin{pmatrix} \frac{1}{\bar{\rho}}\omega'_1 \\ \vdots \\ \frac{1}{\bar{\rho}}\omega'_i \\ \vdots \\ \frac{1}{\bar{\rho}}\omega'_N \end{pmatrix}
$$

Finite element method for steady-state chemistry

In order to find the steady-state chemical composition of the fluid, we consider the following convection-diffusion-reaction equations

$$\rho\mathbf{u} \bullet \nabla Y_k = \nabla \bullet (\rho\mathcal{D}_k \nabla Y_k) + F_k(Y_1, .., Y_k, .., Y_N, T) \tag{18}$$

We introduce a "non-physical" relaxation $\frac{\partial Y_k}{\partial t}$ (physical : $\rho\frac{\partial Y_k}{\partial t}$) and solve the following equation instead

$$\frac{\partial Y_k}{\partial t} + \rho\mathbf{u} \bullet \nabla Y_k = \nabla \bullet (\rho\mathcal{D}_k \nabla Y_k) + F_k(Y_1, .., Y_k, .., Y_N, T) \tag{19}$$

These equations build a nonlinear system of N equations

Shorthand Notation :

$$F_k(Y_1, .., Y_k, .., Y_N, T) = F_k(Y_{1,..,N}, T) := \omega_k(Y_1, .., Y_k, .., Y_N, T)$$

Weak Formulation : Test functions ψ_i, domain Ω

$$\int_\Omega \frac{\partial Y_k}{\partial t}\psi_i dx + \int_\Omega \rho\mathbf{u} \bullet \nabla Y_k \psi_i dx = \int_\Omega \nabla \bullet (\rho\mathcal{D}_k \nabla Y_k)\psi_i dx + \int_\Omega F_k(Y_{1,..,N}, T)\psi_i dx$$

Partial integration of convective and diffusive terms :

$$
\begin{aligned}
\int_\Omega \rho\mathbf{u} \bullet \nabla Y_k \psi_i dx &= \int_{\partial\Omega} \rho Y_k \psi_i(\mathbf{u} \bullet \mathbf{n})ds - \int_\Omega Y_k \nabla \bullet (\rho\psi_i\mathbf{u})dx \\
&= \int_{\partial\Omega} \rho Y_k \psi_i(\mathbf{u} \bullet \mathbf{n})ds - \int_\Omega \rho Y_k \mathbf{u} \bullet \nabla\psi_i dx - \int_\Omega \nabla \bullet (\rho\mathbf{u})Y_k\psi_i dx \\
\int_\Omega \nabla \bullet (\rho\mathcal{D}_k \nabla Y_k)\psi_i dx &= \int_{\partial\Omega} \rho\mathcal{D}_k\psi_i(\nabla Y_k \bullet \mathbf{n})ds - \int_\Omega \rho\mathcal{D}_k \nabla Y_k \bullet \nabla\psi_i dx
\end{aligned}
$$

This yields the following equation

$$
\begin{aligned}
\int_\Omega \frac{\partial Y_k}{\partial t}\psi_i dx &= \int_\Omega \nabla \bullet (\rho\mathbf{u})Y_k\psi_i dx + \int_\Omega \rho(Y_k\mathbf{u} - \mathcal{D}_k\nabla Y_k) \bullet \nabla\psi_i dx \\
&+ \int_{\partial\Omega} \rho\psi_i(\mathcal{D}_k\nabla Y_k - Y_k\mathbf{u}) \bullet \mathbf{n}ds + \int_\Omega F_k(Y_{1,..,N}, T)\psi_i dx
\end{aligned}
$$

Assuming $\psi_i = 0$ on $\partial\Omega$ we get

$$\int_\Omega \frac{\partial Y_k}{\partial t}\psi_i dx = \int_\Omega \nabla \bullet (\rho\mathbf{u})Y_k\psi_i dx + \int_\Omega \rho(Y_k\mathbf{u} - \mathcal{D}_k\nabla Y_k) \bullet \nabla\psi_i dx + \int_\Omega F_k(Y_{1,..,N}, T)\psi_i dx \tag{20}$$

We make the following Galerkin Ansatz and split time and space

$$Y_k(x,t) = \sum_j y_j^k(t)\varphi_j(x) \tag{21}$$

This ansatz yields

$$\int_\Omega \sum_j \dot{y}_j^k \varphi_j \psi_i dx = \int_\Omega \sum_j \nabla \bullet (\rho\mathbf{u})y_j^k\varphi_j\psi_i + \rho(y_j^k\varphi_j\mathbf{u} - \mathcal{D}_k y_j^k\nabla\varphi_j) \bullet \nabla\psi_i dx + \int_\Omega F_k(Y_{1,..,N}, T)\psi_i dx$$

$$\sum_j(\int_\Omega \varphi_j\psi_i dx)\dot{y}_j^k = \sum_j(\int_\Omega \nabla \bullet (\rho\mathbf{u})\varphi_j\psi_i dx + \rho(\varphi_j\mathbf{u} - \mathcal{D}_k\nabla\varphi_j) \bullet \nabla\psi_i)y_j^k + \int_\Omega F_k(Y_{1,..,N}, T)\psi_i dx$$

This is equivalent to

$$M\dot{\mathbf{Y}}_k = A_k\mathbf{Y}_k + \mathbf{r}_k \tag{22}$$

where

$$
\begin{aligned}
(\mathbf{Y}_k)_j &= y_j^k, \\
M_{ij} &= \int_\Omega \varphi_j\psi_i dx, \\
(A_k)_{ij} = C_{ij} - \mathcal{D}_k D_{ij} &= \int_\Omega \nabla \bullet (\rho\mathbf{u})\varphi_j\psi_i + \rho\varphi_j\mathbf{u} \bullet \nabla\psi_i dx - \mathcal{D}_k \int_\Omega \rho\nabla\varphi_j \bullet \nabla\psi_i dx, \\
(\mathbf{r}_k)_i = \int_\Omega F_k(Y_{1,..,N}, T)\psi_i dx &= \int_\Omega F_k(\sum_j y_j^1\varphi_j, .., \sum_j y_j^k\varphi_j, .., \sum_j y_j^N\varphi_j, T)\psi_i dx
\end{aligned}
$$

Hence the nonlinear system for the N species is

$$\begin{pmatrix} M & & & & \\ & \ddots & & & \\ & & M & & \\ & & & \ddots & \\ & & & & M \end{pmatrix} \begin{pmatrix} \dot{\mathbf{Y}}_1 \\ \vdots \\ \dot{\mathbf{Y}}_k \\ \vdots \\ \dot{\mathbf{Y}}_N \end{pmatrix} = \begin{pmatrix} A_1 & & & & \\ & \ddots & & & \\ & & A_k & & \\ & & & \ddots & \\ & & & & A_N \end{pmatrix} \begin{pmatrix} \mathbf{Y}_1 \\ \vdots \\ \mathbf{Y}_k \\ \vdots \\ \mathbf{Y}_N \end{pmatrix} + \begin{pmatrix} \mathbf{r}_1 \\ \vdots \\ \mathbf{r}_k \\ \vdots \\ \mathbf{r}_N \end{pmatrix} \tag{23}$$

SUPG ansatz for test functions ψ_i :

$$\psi_i = \varphi_i + \tau_i \mathbf{u} \bullet \nabla \varphi_i = \varphi_i + \tau_i u_k \frac{\partial \varphi_i}{\partial x_k} \tag{24}$$

$$\begin{aligned} \mathbf{u} \bullet \nabla \psi_i &= u_j \frac{\partial \psi_i}{\partial x_j} \\ &= u_j \frac{\partial \varphi_i}{\partial x_j} + \tau_i u_j \frac{\partial u_k}{\partial x_j} \frac{\partial \varphi_i}{\partial x_k} + \tau_i u_j u_k \frac{\partial^2 \varphi_i}{\partial x_k \partial x_j} \\ &= \mathbf{u} \bullet \nabla \varphi_i + \tau_i (\ (\mathbf{u} \bullet \nabla) \mathbf{u} \bullet \nabla \varphi_i + \mathbf{u}^T \nabla^2 \varphi_i \mathbf{u}) \end{aligned} \tag{25}$$

$$\begin{aligned} \nabla \varphi \bullet \nabla \psi_i &= \frac{\partial \varphi}{\partial x_j} \frac{\partial \psi_i}{\partial x_j} \\ &= \frac{\partial \varphi}{\partial x_j} \left(\frac{\partial \varphi_i}{\partial x_j} + \tau_i \frac{\partial u_k}{\partial x_j} \frac{\partial \varphi_i}{\partial x_k} + \tau_i u_k \frac{\partial^2 \varphi_i}{\partial x_j \partial x_k} \right) \\ &= \frac{\partial \varphi}{\partial x_j} \frac{\partial \varphi_i}{\partial x_j} + \tau_i \frac{\partial \varphi}{\partial x_j} \frac{\partial u_k}{\partial x_j} \frac{\partial \varphi_i}{\partial x_k} + \tau_i \frac{\partial \varphi}{\partial x_j} u_k \frac{\partial^2 \varphi_i}{\partial x_j \partial x_k} \\ &= \nabla \varphi \bullet \nabla \varphi_i + \tau_i \nabla \varphi \bullet (\nabla \mathbf{u} \nabla \varphi_i + \nabla^2 \varphi_i \mathbf{u}) \end{aligned}$$

In that case

$$\begin{aligned} M_{ij} &= \int_\Omega \varphi_j \psi_i dx \\ &= \int_\Omega \varphi_j \varphi_i dx + \tau_i \int_\Omega \varphi_j \mathbf{u} \bullet \nabla \varphi_i dx \\ &:= \bar{M}_{ij} + \tau_i \tilde{M}_{ij} \end{aligned} \tag{26}$$

$$\begin{aligned} C_{ij} &= \int_\Omega \nabla \bullet (\rho \mathbf{u}) \varphi_j \psi_i dx + \int_\Omega \rho \varphi_j \mathbf{u} \bullet \nabla \psi_i dx \\ &= \int_\Omega \nabla \bullet (\rho \mathbf{u}) \varphi_j \varphi_i dx + \tau_i \int_\Omega \nabla \bullet (\rho \mathbf{u}) \varphi_j \mathbf{u} \bullet \nabla \varphi_i dx \\ &+ \int_\Omega \rho \varphi_j \mathbf{u} \bullet \nabla \varphi_i dx + \tau_i \int_\Omega \rho \varphi_j (\ (\mathbf{u} \bullet \nabla) \mathbf{u} \bullet \nabla \varphi_i + \mathbf{u}^T \nabla^2 \varphi_i \mathbf{u}) dx \\ &:= \bar{C}_{ij} + \tau_i \tilde{C}_{ij} \end{aligned} \tag{27}$$

$$\begin{aligned} D_{ij} &= \int_\Omega \rho \nabla \varphi_j \bullet \nabla \psi_i dx \\ &= \int_\Omega \rho \nabla \varphi_j \bullet \nabla \varphi_i + \tau_i \int_\Omega \rho \nabla \varphi_j \bullet (\nabla \mathbf{u} \nabla \varphi_i + \nabla^2 \varphi_i \mathbf{u}) dx \\ &:= \bar{D}_{ij} + \tau_i \tilde{D}_{ij} \end{aligned} \tag{28}$$

Since we are looking for the stationary chemical composition of the flow, we know that density and velocity are also steady-state variables

$$\frac{\partial \rho}{\partial t} = 0, \ \frac{\partial \mathbf{u}}{\partial t} = 0, \tag{29}$$

Because of the continuity equation, the term $\nabla \bullet (\rho \mathbf{u})$ is zero and the matrix C becomes much easier to compute.

Example : 1D case with linear shape functions

In this example we will be assuming $\rho, \mathbf{u}$ piecewise constant.

For a quantity X, let $X_{i+\frac{1}{2}}$ denote $\frac{X_i + X_{i+1}}{2}$.

On $[x_{i-1}, x_i]$

$$\varphi_{i-1}(t) = \frac{x_i - t}{x_i - x_{i-1}}, \varphi_i(t) = \frac{t - x_{i-1}}{x_i - x_{i-1}}, t \in [x_{i-1}, xi], \text{else } \varphi = 0 \tag{30}$$

On $[x_i, x_{i+1}]$

$$\varphi_i(t) = \frac{x_{i+1} - t}{x_{i+1} - x_i}, \varphi_{i+1}(t) = \frac{t - x_i}{x_{i+1} - x_i}, t \in [x_i, x_{i+1}], \text{else } \varphi = 0 \tag{31}$$

$$M_{i,i-1} = \int_{x_{i-1}}^{x_i} \varphi_i(t)\varphi_{i-1}(t)dt = \frac{x_i - x_{i-1}}{6} \tag{32}$$

$$M_{i,i} = \int_{x_{i-1}}^{x_{i+1}} \varphi_i(t)\varphi_i(t)dt = \frac{x_i - x_{i-1}}{3} + \frac{x_{i+1} - x_i}{3} = \frac{x_{i+1} - x_{i-1}}{3} \tag{33}$$

$$M_{i,i+1} = \int_{x_i}^{x_{i+1}} \varphi_i(t)\varphi_{i+1}(t)dt = \frac{x_{i+1} - x_i}{6} \tag{34}$$

$$C_{i,i-1} = \int_{x_{i-1}}^{x_i} \varphi_i'(t)\varphi_{i-1}(t)dt = \frac{1}{2}\rho_{i-\frac{1}{2}}u_{i-\frac{1}{2}} \tag{35}$$

$$C_{i,i} = \int_{x_{i-1}}^{x_{i+1}} \varphi_i'(t)\varphi_i(t)dt = \frac{1}{2}\rho_{i-\frac{1}{2}}u_{i-\frac{1}{2}} - \frac{1}{2}\rho_{i+\frac{1}{2}}u_{i+\frac{1}{2}} \tag{36}$$

$$C_{i,i+1} = \int_{x_i}^{x_{i+1}} \varphi_i'(t)\varphi_{i+1}(t)dt = -\frac{1}{2}\rho_{i+\frac{1}{2}}u_{i+\frac{1}{2}} \tag{37}$$

$$D_{i,i-1} = \int_{x_{i-1}}^{x_i} \varphi_i'(t)\varphi_{i-1}'(t)dt = -\frac{1}{x_i - x_{i-1}} \tag{38}$$

$$D_{i,i} = \int_{x_{i-1}}^{x_{i+1}} \varphi_i'(t)\varphi_i'(t)dt = \frac{1}{x_i - x_{i-1}} + \frac{1}{x_{i+1} - x_i} \tag{39}$$

$$D_{i,i+1} = \int_{x_i}^{x_{i+1}} \varphi_i'(t)\varphi_{i+1}'(t)dt = -\frac{1}{x_{i+1} - x_i} \tag{40}$$

Proof of the Sherman-Morrison Formula

Let A be a square matrix of size n and u, v be vectors of length n. We consider the matrix $\hat{A}$ obtained by a rank-1 update of A

$$\hat{A} = A + uv^t \tag{41}$$

Lemma : If A is invertible and satisfies $v^t A^{-1} u \neq -1$, then $\hat{A}$ is invertible and the inverse matrix $\hat{A}^{-1}$ reads

$$\hat{A}^{-1} = (A + uv^t)^{-1} = A^{-1} - \frac{A^{-1}uv^t A^{-1}}{1 + v^t A^{-1} u} \tag{42}$$

This formula is called the *Sherman-Morrison* formula.

Proof : Let I be the identity matrix of appropriate size. Since $det(I + uv^t) = 1 + v^t u$, it follows that if A is invertible, then the determinant of $\hat{A}$ is related to the determinant of A by the relation

$$det(\hat{A}) = det(A + uv^t) = det(A(I + A^{-1}uv^t)) = det(A)(1 + v^t A^{-1} u) \tag{43}$$

This means that

$$\hat{A} \text{ is regular} \Leftrightarrow A \text{ is regular and } 1 + v^t A^{-1} u \neq 0 \tag{44}$$

In this case, it is possible to compute the inverse of $\hat{A}$ in a relatively cheap way by updating the inverse of A. In fact, the inverse of $\hat{A}$ is obtained by an update of the inverse of A

$$\hat{A}^{-1} = (A + uv^t)^{-1} = A^{-1} - \frac{A^{-1}u(A^{-t}v)^t}{1 + v^t A^{-1} u} \tag{45}$$

$$= A^{-1} - \frac{A^{-1}uv^t A^{-1}}{1 + v^t A^{-1} u} \tag{46}$$

To verify this assertion, we multiply both matrices

$$(A + uv^t)\left(A^{-1} - \frac{A^{-1}uv^t A^{-1}}{1 + v^t A^{-1} u}\right) = AA^{-1} + uv^t A^{-1} - \frac{AA^{-1}uv^t A^{-1} + uv^t A^{-1}uv^t A^{-1}}{1 + v^t A^{-1} u} \tag{47}$$

$$= I + uv^t A^{-1} - \frac{uv^t A^{-1} + uv^t A^{-1}uv^t A^{-1}}{1 + v^t A^{-1} u} \tag{48}$$

$$= I + uv^t A^{-1} - \frac{(1 + v^t A^{-1} u)uv^t A^{-1}}{1 + v^t A^{-1} u} \tag{49}$$

$$= I + uv^t A^{-1} - uv^t A^{-1} \tag{50}$$

$$= I \tag{51}$$

$\blacksquare$

Finite element method for the Helmholtz equation

In the case of a cube, a parallelepiped or a cylinder it is possible to provide analytic solutions for the eigenmodes. However, in the general case and for complicated geometries, we have to use numerical methods to compute the eigenmodes. We use the finite element method to discretize the Helmholtz equation

$$\nabla \bullet (c^2 \nabla \hat{p}) + \omega^2 \hat{p} = 0 \tag{52}$$

taking into account the following boundary conditions

Type of boundary	abbr.	boundary condition
Dirichlet	Γ_D	$p' = 0$, $\Psi_j = 0$
Neumann	Γ_N	$\mathbf{u}' \bullet \mathbf{n} = 0$, $\frac{1}{i\omega_j \bar{\rho}} \nabla \Psi_j \bullet \mathbf{n} = 0$
Impedance	Γ_F	$p' = \frac{1}{i\omega \bar{\rho}} \mathcal{Z}(\nabla \mathbf{p}' \bullet \mathbf{n})$, $\Psi_j = \frac{1}{i\omega_j \bar{\rho}} Z_j (\nabla \Psi_j \bullet \mathbf{n})$

The variational form of the Helmholtz equation is

$$\int_\Omega \varphi_i \nabla \bullet (c^2 \nabla \hat{p}) dV + \int_\Omega \varphi_i \omega^2 \hat{p} dV = 0 \tag{53}$$

Partial integration of the first term yields

$$\int_\Gamma c^2 \varphi_i (\nabla \hat{p} \bullet \mathbf{n}) ds - \int_\Omega c^2 (\nabla \varphi_i \bullet \nabla \hat{p}) dV + \int_\Omega \varphi_i \omega^2 \hat{p} dV = 0 \tag{54}$$

Hence, we may write the boundary integral as

$$\int_\Gamma c^2 \varphi_i (\nabla \hat{p} \bullet \mathbf{n}) ds = \int_{\Gamma_F} \bar{\rho} c^2 \frac{i\omega}{Z} \varphi_i \hat{p} ds = \int_{\Gamma_F} \gamma \bar{p} \frac{i\omega}{Z} \varphi_i \hat{p} ds \tag{55}$$

leading to

$$\int_\Omega c^2 (\nabla \varphi_i \bullet \nabla \hat{p}) dV = \int_{\Gamma_F} \bar{\rho} c^2 \frac{i\omega}{Z} \varphi_i \hat{p} ds + \omega^2 \int_\Omega \varphi_i \hat{p} dV \tag{56}$$

By inserting the finite element ansatz for the pressure modes $\hat{p}$

$$\hat{p}(x) = \sum_{j=1}^{N_p} p_j \psi_j(x) \tag{57}$$

in the previous relation, we obtain

$$\sum_{j=1}^{N_p} \left(\int_\Omega c^2 (\nabla \varphi_i \bullet \nabla \psi_j) dV \right) p_j = \sum_{j=1}^{N_p} \left(\int_{\Gamma_F} \bar{\rho} c^2 \frac{i\omega}{Z} \varphi_i \psi_j ds + \omega^2 \int_\Omega \varphi_i \psi_j dV \right) p_j$$

which is equivalent to the system

$$HP = (Z(\omega) + \omega^2 E) P \tag{58}$$

where

$$P_j = p_j, \quad H_{ij} = \int_\Omega c^2 (\nabla \varphi_i \bullet \nabla \psi_j) dV, \quad E_{ij} = \int_\Omega \varphi_i \psi_j dV, \quad Z_{ij} = \int_{\Gamma_F} \bar{\rho} c^2 \frac{i\omega}{Z} \varphi_i \psi_j ds \tag{59}$$

Finite element method for the convected Helmholtz equation

The variational form of the convected Helmholtz equation is

$$\int_{\Omega} \varphi_i \nabla \bullet (c^2 \nabla \hat{p})dV + \int_{\Omega} \varphi_i \mathbf{g} \bullet \nabla \hat{p}dV + \int_{\Omega} \varphi_i f \hat{p}dV + \int_{\Omega} \varphi_i \omega^2 \hat{p}dV = 0 \tag{60}$$

Partial integration of the first term yields

$$\int_{\Gamma} c^2 \varphi_i (\nabla \hat{p} \bullet \mathbf{n})ds - \int_{\Omega} c^2 (\nabla \varphi_i \bullet \nabla \hat{p})dV + \int_{\Omega} \varphi_i \mathbf{g} \bullet \nabla \hat{p}dV + \int_{\Omega} \varphi_i f \hat{p}dV + \int_{\Omega} \varphi_i \omega^2 \hat{p}dV = 0 \tag{61}$$

The pressure modes satisfy the following boundary conditions

Type of boundary	abbr.	boundary condition
Dirichlet	Γ_D	$\bar{p} = 0$, $p' = 0$, $\Psi_j = 0$
Neumann	Γ_N	$\bar{\mathbf{u}} \bullet \mathbf{n} = 0$, $\mathbf{u}' \bullet \mathbf{n} = 0$, $\frac{1}{i\omega_j \bar{\rho}} \nabla \Psi_j \bullet \mathbf{n} = 0$
Impedance	Γ_F	$p' = \frac{1}{i\omega \bar{\rho}} \mathcal{Z}(\nabla \mathbf{p}' \bullet \mathbf{n})$, $\Psi_j = \frac{1}{i\omega_j \bar{\rho}} Z_j (\nabla \Psi_j \bullet \mathbf{n})$

Hence, we may write the boundary integral as

$$\int_{\Gamma} c^2 \varphi_i (\nabla \hat{p} \bullet \mathbf{n})ds = \int_{\Gamma_F} \bar{\rho} c^2 \frac{i\omega}{Z} \varphi_i \hat{p}ds = \int_{\Gamma_F} \gamma \bar{p} \frac{i\omega}{Z} \varphi_i \hat{p}ds \tag{62}$$

leading to

$$\int_{\Omega} c^2 (\nabla \varphi_i \bullet \nabla \hat{p})dV = \int_{\Gamma_F} \bar{\rho} c^2 \frac{i\omega}{Z} \varphi_i \hat{p}ds + \int_{\Omega} \varphi_i \mathbf{g} \bullet \nabla \hat{p}dV + \int_{\Omega} \varphi_i f \hat{p}dV + \omega^2 \int_{\Omega} \varphi_i \hat{p}dV \tag{63}$$

Using the following ansatz for the pressure modes $\hat{p}$

$$\hat{p}(x) = \sum_{j=1}^{N_p} p_j \psi_j(x) = p_j \psi_j(x) \tag{64}$$

we get

$$\sum_{j=1}^{N_p} \left(\int_{\Omega} c^2 (\nabla \varphi_i \bullet \nabla \psi_j)dV \right) p_j$$
$$= \tag{65}$$
$$\sum_{j=1}^{N_p} \left(\int_{\Gamma_F} \bar{\rho} c^2 \frac{i\omega}{Z} \varphi_i \psi_j ds + \int_{\Omega} \varphi_i \mathbf{g} \bullet \nabla \psi_j dV + \int_{\Omega} f \varphi_i \psi_j dV + \omega^2 \int_{\Omega} \varphi_i \psi_j dV \right) p_j$$

which is equivalent to the system

$$HP = (Z(\omega) + G(\omega) + F(\omega) + \omega^2 E)P \tag{66}$$

where

$$P_j = p_j \tag{67}$$

$$H_{ij} = \int_{\Omega} c^2 (\nabla \varphi_i \bullet \nabla \psi_j)dV \tag{68}$$

$$G_{ij} = \int_{\Omega} \varphi_i \mathbf{g} \bullet \nabla \psi_j dV \tag{69}$$

$$F_{ij} = \int_{\Omega} f \varphi_i \psi_j dV \tag{70}$$

$$E_{ij} = \int_{\Omega} \varphi_i \psi_j dV \tag{71}$$

$$Z_{ij} = \int_{\Gamma_F} \bar{\rho} c^2 \frac{i\omega}{Z} \varphi_i \psi_j ds \tag{72}$$

Linear shape functions as finite elements

For a quantity X, let $X_{i+\frac{1}{2}}$ denote $\frac{X_i + X_{i+1}}{2}$.

On $[x_{i-1}, x_i]$

$$\varphi_{i-1}(t) = \frac{x_i - t}{x_i - x_{i-1}}, \tag{73}$$

$$\varphi_i(t) = \frac{t - x_{i-1}}{x_i - x_{i-1}}, \quad t \in [x_{i-1}, x_i], \tag{74}$$

$$\varphi_j(t) = 0, \quad \text{else} \tag{75}$$

On $[x_i, x_{i+1}]$

$$\varphi_i(t) = \frac{x_{i+1} - t}{x_{i+1} - x_i}, \tag{76}$$

$$\varphi_{i+1}(t) = \frac{t - x_i}{x_{i+1} - x_i}, t \in [x_i, x_{i+1}], \tag{77}$$

$$\varphi_j(t) = 0, \quad \text{else} \tag{78}$$

$$E_{i,i-1} = \int_{x_{i-1}}^{x_i} \varphi_i(t)\varphi_{i-1}(t)dt = \frac{x_i - x_{i-1}}{6} \tag{79}$$

$$E_{i,i} = \int_{x_{i-1}}^{x_{i+1}} \varphi_i(t)\varphi_i(t)dt = \frac{x_i - x_{i-1}}{3} + \frac{x_{i+1} - x_i}{3} \tag{80}$$

$$E_{i,i+1} = \int_{x_i}^{x_{i+1}} \varphi_i(t)\varphi_{i+1}(t)dt = \frac{x_{i+1} - x_i}{6} \tag{81}$$

$$F_{i,i-1} = \int_{x_{i-1}}^{x_i} f\varphi_i(t)\varphi_{i-1}(t)dt = f_{i-\frac{1}{2}}\frac{x_i - x_{i-1}}{6} \tag{82}$$

$$F_{i,i} = \int_{x_{i-1}}^{x_{i+1}} f\varphi_i(t)\varphi_i(t)dt = f_{i-\frac{1}{2}}\frac{x_i - x_{i-1}}{3} + f_{i+\frac{1}{2}}\frac{x_{i+1} - x_i}{3} \tag{83}$$

$$F_{i,i+1} = \int_{x_i}^{x_{i+1}} f\varphi_i(t)\varphi_{i+1}(t)dt = f_{i+\frac{1}{2}}\frac{x_{i+1} - x_i}{6} \tag{84}$$

$$G_{i,i-1} = \int_{x_{i-1}}^{x_i} g\varphi_i(t)\varphi'_{i-1}(t)dt = \frac{1}{2}g_{i-\frac{1}{2}} \tag{85}$$

$$G_{i,i} = \int_{x_{i-1}}^{x_{i+1}} g\varphi_i(t)\varphi'_i(t)dt = \frac{1}{2}g_{i-\frac{1}{2}} - \frac{1}{2}g_{i+\frac{1}{2}} \tag{86}$$

$$G_{i,i+1} = \int_{x_i}^{x_{i+1}} g\varphi_i(t)\varphi'_{i+1}(t)dt = \frac{1}{2}g_{i+\frac{1}{2}} \tag{87}$$

$$H_{i,i-1} = \int_{x_{i-1}}^{x_i} c^2\varphi'_i(t)\varphi'_{i-1}(t)dt = -\frac{1}{x_i - x_{i-1}}c^2_{i-\frac{1}{2}} \tag{88}$$

$$H_{i,i} = \int_{x_{i-1}}^{x_{i+1}} c^2\varphi'_i(t)\varphi'_i(t)dt = \frac{1}{x_i - x_{i-1}}c^2_{i-\frac{1}{2}} + \frac{1}{x_{i+1} - x_i}c^2_{i+\frac{1}{2}} \tag{89}$$

$$H_{i,i+1} = \int_{x_i}^{x_{i+1}} c^2\varphi'_i(t)\varphi'_{i+1}(t)dt = -\frac{1}{x_{i+1} - x_i}c^2_{i+\frac{1}{2}} \tag{90}$$

Formulation as a quadratic eigenvalue problem

We obtain an equivalent equation for the pressure modes by using the species equation. In fact, if we sum over all the equations for the species, we may write the unsteady heat release

$$\hat{Q} = -\sum_{s=1}^{N_s} h_s \hat{\omega}_s = -\frac{1}{i\omega} \sum_{s=1}^{N_s} h_s(\bar{\rho}\omega^2 \hat{Y}_s + \nabla\overline{Y}_s \bullet \nabla\hat{p}) \tag{91}$$

and the pressure equation takes the form

$$\nabla \bullet (c^2\nabla\hat{p}) + (\gamma-1)\sum_{s=1}^{N_s} h_s\nabla\overline{Y}_s \bullet \nabla\hat{p} + \omega^2\hat{p} = -(\gamma-1)\omega^2\bar{\rho}\sum_{s=1}^{N_s} h_s\hat{Y}_s \tag{92}$$

Moreover we use the temperature equation to rewrite the pressure equation as

$$\nabla \bullet (c^2\nabla\hat{p}) - (\gamma-1)c_p\nabla\overline{T} \bullet \nabla\hat{p} + \gamma\omega^2\hat{p} = (\gamma-1)\omega^2\bar{\rho}c_p\hat{T} \tag{93}$$

Remark: Using the two last equations we get a relation between the pressure, temperature and species modes

$$\omega^2\hat{p} - (c_p\nabla\overline{T} + \sum_{s=1}^{N_s} h_s\nabla\overline{Y}_s) \bullet \nabla\hat{p} = \omega^2\bar{\rho}(c_p\hat{T} + \sum_{s=1}^{N_s} h_s\hat{Y}_s) \tag{94}$$

We will use the last equation for the pressure modes in addition to the temperature equation

$$\bar{\rho}c_p\omega^2\hat{T} + c_p\nabla\overline{T} \bullet \nabla\hat{p} - \omega^2\hat{p} = i\omega\sum_{s=1}^{N_s} h_s(\nabla_Y\overline{\omega}_s \bullet \hat{Y} + \frac{\partial\overline{\omega}_s}{\partial p}\hat{p} + \frac{\partial\overline{\omega}_s}{\partial T}\hat{T}) \tag{95}$$

and the chemical species equations

$$\bar{\rho}\omega^2\hat{Y}_s + \nabla\overline{Y}_s \bullet \nabla\hat{p} = i\omega\nabla \bullet (\bar{\rho}\mathcal{D}_s\nabla\hat{Y}_s) + i\omega(\nabla_Y\overline{\omega}_s \bullet \hat{Y} + \frac{\partial\overline{\omega}_s}{\partial p}\hat{p} + \frac{\partial\overline{\omega}_s}{\partial T}\hat{T}) \tag{96}$$

We combine these relations to get the following equations
for the pressure $\hat{p}$

$$\nabla \bullet (c^2\nabla\hat{p}) - (\gamma-1)c_p\nabla\overline{T} \bullet \nabla\hat{p} + \gamma\omega^2\hat{p} = (\gamma-1)\omega^2\bar{\rho}c_p\hat{T} \tag{97}$$

for the temperature $\hat{T}$

$$\nabla \bullet (c^2\nabla\hat{p}) + (c_p\nabla\overline{T} + \gamma\sum_{s=1}^{N_s} h_s\nabla\overline{Y}_s) \bullet \nabla\hat{p} + \omega^2\bar{\rho}(c_p\hat{T} + \gamma\sum_{s=1}^{N_s} h_s\hat{Y}_s) = 0 \tag{98}$$

for the species $\hat{Y}_s$

$$\nabla\overline{Y}_s \bullet \nabla\hat{p} + \omega^2\bar{\rho}\hat{Y}_s = i\omega(\nabla_Y\overline{\omega}_s \bullet \hat{Y} + \frac{\partial\overline{\omega}_s}{\partial\rho}\hat{p} + \frac{\partial\overline{\omega}_s}{\partial T}\hat{T}) \tag{99}$$

For the density $\hat{\rho}$ we use the following relation

$$\hat{\rho} = \frac{1}{c^2}\hat{p} \tag{100}$$

A finite element discretization of these equations yields a quadratic eigenvalue problem

$$(\lambda^2 M + \lambda C + K)X = 0, \quad \text{where } \lambda = i\omega \tag{101}$$

Let N be the number of nodes in the finite element discretization, then the dimension of this problem is $d = (N_s + 2) * N$.
The eigenvector X consists of the eigenmodes of pressure, temperature and species

$$X = (P\ T\ Y_1\ \dots\ Y_{N_s}\ )^t \tag{102}$$

The stiffness matrix K is singular and has rank $\leq N$ since it has the following stucture

$$K = \begin{pmatrix} * & & & \\ * & & & \\ * & & & \\ \vdots & & & \\ * & & & \end{pmatrix} \tag{103}$$

The damping matrix C is also rank-defficient with the following structure

$$C = \begin{pmatrix} & & & & \\ * & * & \cdots & * & * \\ \vdots & \vdots & \vdots & \vdots & \vdots \\ * & * & \cdots & * & * \end{pmatrix} \tag{104}$$

The mass matrix M is upper triangular and has full rank

$$M = \begin{pmatrix} * & * & & & \\ & * & * & \cdots & * \\ & & * & & \\ & & & \ddots & \\ & & & & * \end{pmatrix} \tag{105}$$

Since the matrix M is nonsingular, this problem has $2*d$ finite eigenvalues.

Furthermore, the matrices M, C and K being real, the eigenvalues $\lambda = i\omega$ are either real or appear in conjugate pairs $(\lambda, \bar{\lambda})$.

Iterative resolution of the eigenvalue problem

The FEM formulation of the Helmholtz equation yields the equation

$$AP + F(\lambda)P = 0 \tag{106}$$

where $\lambda = -i\omega$. Considering that the eigenmode (P_0, λ_0) of the cold chamber is a good start guess, we want to solve this equation for the eigenpair (P, λ) in an iterative way. To do this, we need a further equation to have a complete system. We may use the following requirement

$$||P||_2^2 = 1 \Leftrightarrow P^t P = 1 \tag{107}$$

Hence we want to solve the system for $X = (P, \lambda)^t$

$$\mathcal{F}(X) = \left(\begin{array}{c} AP + F(\lambda)P \\ P^t P - 1 \end{array} \right) = 0 \tag{108}$$

Introducing the matrices $\mathcal{B}$ and $\mathcal{D}$

$$\mathcal{B}^i = A + F(\lambda^i), \quad \mathcal{D}^i = \left. \frac{\partial F}{\partial \lambda} \right|^i \tag{109}$$

the Jacobian $D\mathcal{F}$ at X^i is given by

$$D\mathcal{F}(X^i) = \left(\begin{array}{cc} \mathcal{B}^i & \mathcal{D}^i P^i \\ (P^i)^t & 0 \end{array} \right) \tag{110}$$

To solve the equation $\mathcal{F}(X) = 0$, we may linearize $\mathcal{F}$

$$0 = \mathcal{F}(X^*) = \mathcal{F}(X) + D\mathcal{F}(X)(X^* - X) + O(||X^* - X||^2) \tag{111}$$

and proceed as follows

$$\text{for } i = 1, 2, \ldots \tag{112}$$
$$D\mathcal{F}(X^i)\Delta X^{i+1} = -\mathcal{F}(X^i) \tag{113}$$
$$X^{i+1} = X^i + \gamma \Delta X^{i+1} \tag{114}$$

Reduced reaction mechanism

Combustion involves many physical and chemical processes with very complex dynamics. In practical combustion systems, reaction mechanisms are in the order of thousands of elementary reactions or more and a large number of reactive intermediates. For example, hydrocarbon combustion involves around 100 species with 10.000 reactions. A simulation of such a reaction mechanism could be possible in spatially homogenous reaction systems, such as perfectly-stirred tank reactors. However, in the simulation of real systems with spatial dependency such as combustion chambers of gas turbines, one can not afford to include all species and reactions. In fact, the spatially inhomogeneous nature of reactive flows and the large number of changing concentrations leads to extremely high computational costs in the simulation of practical systems. For a three-dimensional complex geometry as it is the case in the combustion chamber of a gas turbine, numerical procedures based on discretization techniques (such as finite difference, finite element or finite volume methods) typically involve a few million unknowns. Besides the prohibitive amount of involved variables, the underlying nonlinearities that describe the chemical kinetics bring additional complexities and make the computation significantly harder. All this represents a major obstacle to the use of detailed reaction mechanisms. The level of fundamental sophistication that can be realistically included is limited. Therefore, it is highly desirable to use simplified chemical kinetics schemes which describe the reactions in terms of only a small number of species without significant loss of detailed information and accuracy. In the last years, many algorithms have been developed to automatically produce reduced chemical kinetic mechanisms starting with a detailed mechanism and a set of input problems representing the operating conditions. The major advantage of introducing reduced reaction mechanism is making combustion models applicable as design tools for realistic industrial applications. Since computation times are reduced significantly, the models can be implemented in CFD codes to describe combustion in complex geometries for practical cases. Such systematically reduced reaction mechanisms have been successfully applied to a range of hydrogen and hydrocarbon flames in arbitrary geometries.

Basically, there are four steps in the formulation of a reduced chemical kinetic mechanism:

1. Identification of a short or skeletal mechanism containing only the most essential species and reaction steps of the detailed mechanism.

2. Identification of appropriate quasi-steady-state approximations (QSSA).

3. Elimination of reactions using the algebraic relations obtained in the previous step.

4. Solution of the coupled and nonlinear set of algebraic equations obtained in the previous steps to find the QSS species concentrations reaction rates of the non-QSS species.